Cliff Erosion of salt marshes

Experimental evaluation of the effect of vegetation characteristics and sediment properties on erodibility

UNIVERSITY OF TWENTE.

NIOZ Royal Netherlands Institute for Sea Research

Azrin Rahman

21/08/2015

Cliff Erosion of salt marshes

Experimental evaluation of the effect of vegetation characteristics and sediment properties on erodibility

Master's thesis of:
Azrin Rahman
Water Engineering & Management
University of Twente
Enschede, The Netherlands
August, 2015

Supervisors:

UNIVERSITY OF TWENTE.

Dr. Ir. C. M. Dohmen-Janssen,
Associate Professor, Water Engineering & Management
University of Twente, The Netherlands

Dr. Ir. D. C. M. Augustijn,
Assistant professor, Water Engineering & Management
University of Twente, The Netherlands

Dr. Ir. Erik M. Horstman
Water Engineering and Management
University of Twente, The Netherlands

Dr. Tjeerd Bouma
Senior Scientist, Yerseke Spatial Ecology (YRE)
Royal Netherlands Institute for Sea Research (NIOZ), The Netherlands

NIOZ Royal Netherlands Institute for Sea Research

Summary

Salt marshes are the typical types of coastal wetlands found in the high latitude areas (i.e. the temperate climatic region). These wetlands are subjected to hydrodynamic forces and inundation by saline water during flood tides. Hence, salt marsh ecosystems are home to distinctive plant species that are resistant to these conditions. These salt marsh wetlands are of engineering significance acting as natural defence against storm surges and waves. In addition, they have great ecological value providing food and sheltered nesting places for birds and animals.

Hydrodynamics and sediment dynamics are important to the development of these salt marshes. The salt marsh plants increase the drag forces on tidal currents and wave actions. This way, salt marsh vegetation directly impacts the hydrodynamics and subsequently the sediment dynamics within the salt marsh wetlands. The sediment dynamics in the salt marshes help its lateral and vertical extension. Due to the continuous sediment deposition within the salt marsh vegetation, elevation gradients can be developed between the mudflat area at the seaward side and the elevated salt marshes at the landward side. This increasing gradient positively affects the growth of salt marshes as salt stresses and tidal currents are reduced in the higher elevated parts of the marsh. With the continuous accumulation of sediments in this elevated area, the slope at the edge of the salt marsh vegetation becomes increasingly steep, prone to the wave action. High energy waves, created by storms, can induce (substantial) erosion at the salt marsh edge, resulting in the formation of a cliff.

The erosive processes within the salt marsh environment are important to understand, as they determine whether a salt marsh will develop or decline. Two types of erosion processes can be distinguished: top soil erosion and cliff erosion. Topsoil erosion occurs all over the marsh surface and this process is determined by the bed shear stresses. The cliff erosion refers to the lateral erosion of the salt marsh cliff and is rather important in the gradual loss of the salt marshes. Knowledge about the cliff erosion process and the relevant parameters is still limited. Therefore, this study is dedicated to the quantification of cliff erosion rates, focusing on the impacts of sediment properties and vegetation characteristics on these rates while considering a wide range of field conditions. With this research, knowledge will be obtained about how the cliff erosion varies depending on the salt marsh vegetation species, their density and the amount of aboveground and belowground biomass. Additionally, this research will also consider the impact of the sediment grain sizes and organic carbon content on the cliff erosion.

Laboratory experiments were carried out to quantify the cliff erosion of salt marsh substrates. Samples were collected from five field sites covering three vegetation species: *Spartina anglica, Scirpus maritimus* and *Phragmites australis*. Moreover, within each site, samples were collected from three density zones: the densely vegetated zone, the sparsely vegetated zone and the mudflat (un-vegetated) zone. For all study sites, sediment sizes and organic carbon content were analysed and vegetation properties were quantified. Cliff like marsh edges were reconstructed in the experimental wave tanks. The generated wave conditions in the wave tank were representative for potential field conditions. The collected samples were placed in the wave tanks and at intervals pictures were taken of the eroded sediment samples to record the erosion of the sediments from time to time due to the wave action. Obtained pictures were processed with a 3D image analysis method using Visual SFM and Meshlab. This procedure resolved the sediment volumes that were eroded from the samples during every time interval.

The cliff erosion in this study was quantified using two characteristic coefficients: 'erosion maximum' and 'erosion rate'. The erosion maximum resembles the maximum amount of sediments that would be eroded from a sample if it would be exposed to the simulated wave actions for an infinite period of time. Erosion rate is a rate coefficient and measures the speed by which it approaches to erosion maximum.

The results of our research show clear differences in the maximum amount of sediment loss depending upon the salt marsh plant species, their density and the amount of aboveground and belowground biomass. Among the three species studied, the smaller erosion maxima were obtained for *Spartina anglica* with a 0.01-0.02

volume fraction of the sample. The erosion maxima for the other two species, *Scirpus maritimus* and *Phragmites australis*, were around in same order of magnitude, 0.02-0.11 volume fraction. The presence of vegetation clearly caused the erosion maximum to reduce, with obtained erosion maxima for the densely vegetated zones in the range of 0.01-0.11, whereas the erosion maxima of the samples for the un-vegetated mudflat zone were 0.55-1.0 of the total sample volume. The erosion maxima of the salt marsh cliffs showed a clear relation with the vegetation species, the vegetation density, and the amount of dry belowground biomass present in the salt marsh substrates. The best relation was found for the amount of dry belowground biomass and the erosion maxima showing an exponential decrease with an increase of the amount of dry belowground biomass. Besides, the vegetation density also showed this type of exponential relation with erosion maximum. The grain sizes and the organic carbon content of the substrate showed linear relation with the erosion maxima only for the mudflat zones.

No significant relation was found between the erosion rates and different vegetation characteristics (i.e. vegetation species, vegetation density and the amount of aboveground and belowground biomass). Additional, no relation could be found between the erosion rates and median grain size or the organic carbon content of the salt marsh substrates. However, we found that the median grain size and organic carbon content are the best predictors of erosion rates for the mudflat sediments.

Overall, the erosion maxima of the salt marsh substrates are found to be significantly reduced by the presence of plants and their characteristics. Both erosion maxima and erosion rates, are influenced by median grain size and organic carbon content for mudflat locations, but similar relations could not be found for the vegetated areas because the effect of plants was dominated in these areas.

Cliff erosion of salt marshes is an intrinsic natural phenomenon in coastal wetlands. Cliff erosion is important to determine whether a salt marsh will extent laterally or retreat. The results of this study show how the cliff erosion relates to the presence of vegetation and its characteristics. Among the three species used for this research, *Spartina anglica* induced the slowest and least severe cliff erosion, meaning a more active contribution to coastal protection. Our results show that sediment properties such as grain size and organic carbon content do not affect cliff erosion from salt marsh substrates. Nevertheless, these properties are found to be important factors for the cliff erosion in mudflat areas. Un-vegetated sediments from the mudflat with smaller median grain size and larger amounts of organic carbon content are less prone to cliff erosion. The results were compared to the available results of Feagin et al., (2009). Feagin et al., (2009) found that the presence of salt marsh plants does not significantly reduce the cliff erosion, instead it improves the soil properties that reduces the cliff erosion. Our results hardly support the findings of Feagin et al., (2009). However, the output of this research still supports the concept that the presence of salt marsh plants help to reduce erosion by binding the soil and impart in the coastal management issues.

Preface

My utmost gratitude goes to ALLAH, the Almighty, without whose mercy and blessing, my research work would not have been possible. This document is the final report of my MSc thesis, which was focused on the cliff erosion of the salt marshes and the positive effect of the vegetation to the reduction of the erosion. At the end of the course work, I was searching for an appropriate MSc thesis topic and found myself interested on the mechanisms occurred within the coastal wetlands. Later, I found the internship opportunity focusing on salt marshes at NIOZ-Yerseke. During my internship period at NIOZ, I had opportunity to work in internationalized friendly working environment with well-equipped modern laboratory facilities. I also experienced several field works at different places along the Westernscheldt estuary. Nice weather in Yerseke, wonderful views and fresh fried fishes made my internship period unforgettable experience in my life. I would like to thank senior scientist 'Dr. Tjeerd Bouma', for his direct supervision that helped me to develop clear thinking ability and to work independently and confidently. I also want to give thanks to the laboratory assistances, Jeroen and Lennart and my colleagues to help in my research by their valuable advices. I also want to thank 'Isabella Kratzer'for helping me at early stage of my research during the collection of field samples and laboratory experiments. I want to thank 'Jim Van Belzen', the person who developed the method I used in my research and in later stage, evaluation of the results. I also want to thank the people in 'De Keete', where I lived during that time and enjoyed lots of delicious dinner as well as experiencing cultural diversity.

I am really grateful to 'Dr. Erik Horstman', who helped me to find out this internship opportunity at NIOZ-Yerseke. I would like to thank him for the continuous support from very first till the finishing of this thesis. If anything did not work well in any stages of my research, he always took effort for solution, which definitely helped me to finish this thesis in time. He is the person, I always bothered for the correction of my report. His suggestions, comments helped me to keep on track. I want to say 'Erik, you are one of the great teachers'.

I would like to thank my daily Supervisor 'Dr. Augustijn', for his time-to-time guidelines and directions that helped me to complete the report. I would never forget his help for moving my stuff from Enschede to Yerseke, which is really unusual at any case. I would also like to thank my Supervisor, 'Dr. Marjolein', for her valuable comments and advices, which helped me to think more critically, in depth and improve the personal skills.

I want to thank my parents and other family members for their support. Specially my mother, her mental support made me stronger and not to fear any work in life. I also want to thank my Bangladeshi friends in Netherlands, Mr. Siraj Zubair, Mr. Sarwar Morshed and his family for their suggestions and advices to take right decision. Finally, I want to thank my Husband, Jakir, who always tried to make me happy at the hard time of my thesis and helped me to take all difficulties positively. I always felt relief after complaining all the situations, when things were not in my control during this research work. Without his support, probably I could not carry out higher study in overseas.

Enjoy reading!

Azrin Rahman
Enschede. The Netherlands

TABLE OF CONTENTS

Chapter 1

1. Introduction

Recently, the integration of coastal protection and coastal wetlands has gained a lot of attention. In the past, the analysis and design of coastal protection structures focused on 'hard' solutions and has ignored the positive contribution of vegetation. It is a matter of great concern that in the near future, due to sea level rise and the increasing frequency of extreme events, the demand for coastal protection will increase. It is also acknowledged in previous studies that vegetation plays a role in energy reduction by imposing an additional friction term. The function and importance of coastal wetlands as a natural defence system against storm waves has been described by several authors (Costanza et al., 2008; Dixon et al., 1998; Gedan et al., 2011; Lopez, 2009). Therefore, coastal vegetation is of significance for engineering shoreline protection (Jadav et al., 2013). Besides, these coastal wetlands provide food, water, raw materials and other resources to the coastal population as well as environmental benefits such as air and water quality regulation. Recently, it has been recognized that vegetated coastal features have great value in economic sense if we transform its benefits to monetary units (De Groot et al., 2012). In several regions of the world, utilization of coastal wetlands has already been implemented to enhance structural measures for mitigation of coastal flooding due to storm surges and waves (Borsje et al., 2011).

Coastal wetlands provide a natural buffer zone between the coast and the ocean. They can extend their own environment by actively trapping sediments (Furukawa & Wolnaski, 1996). Both mangroves, intertidal wetland forests in the tropics, and salt marshes, found in the intertidal environments grown in temperate areas, show this property and they act as Ecosystem Engineers (Jones et al., 1994). These intertidal wetlands can withstand salt water and thrive well in sheltered coastal environments. Coastal vegetation, like salt marshes can strongly attenuate hydrodynamic energy from waves and tidal current (Bouma et al., 2005, 2007). The attenuation of the hydrodynamics above marsh surfaces will enhance sedimentation and induce self-organizing activities due to the feedback between the plant growth and the sediment accumulation. These self-organizing activities significantly reduce the erosional loss. As a consequence of these self-organizing activities, coastal wetland marshes approach a critical state as the edge of the marsh adjacent to the intertidal flat becomes increasingly steep and vulnerable to wave attack (Van de Koppel et al., 2005). With the exposure to high levels of hydrodynamic energy, for instance due to big storms, erosion of the cliff edge can lead to severe loss of the salt marsh vegetation. On the long term, this cliff erosion will cause lateral erosion of the marsh surfaces and, consequently, a loss of wetland areas (Van Belzen et al., 2015). Therefore, a fundamental understanding of the mechanisms relevant to the erosion of salt marsh cliffs is required to improve the protection of these highly dynamic environments. This study will focus on enhancing our understanding of the detailed mechanisms of cliff erosion in salt marshes.

In this introductory chapter, at first, the definition and the classification of coastal wetlands are presented, including the variations of the vegetation types found in specific marsh areas. After that, focus will be given to the salt marshes, including the bio-geomorphology of salt marshes and their bio-geomorphic succession. Next, short introductions to hydrodynamics and sediment dynamics in salt marshes will be given. Regarding the sediment dynamics, we will focus on cliff erosion at the salt marsh edges. From the available literature describing the salt marsh cliff erosion process, a knowledge gap in this field of study will be identified. The knowledge gap will lead to the identification of the aim of this study, the set-up of specific research questions and finally the structure of the remainder of this report will be introduced.

1.1 Coastal wetlands

A wetland is a land area that is saturated with water, either permanently or seasonally, such that it takes on the characteristics of a distinct ecosystem (Figure 1). The factor that distinguishes wetlands from other land forms are the characteristic vegetation types (Butler, 2010). Wetlands play important roles in the environment, for example in relation to water purification, flood control and shoreline stability. In wetlands, biologically diverse ecosystems including plants and animals can be found.

Figure 1: Tidal wetland, salt marshes on the pioneer- mudflat zone (Van Belzen et al., 2015).

The physical geography of a wetland, which explains the formation of the natural environment, the role of water therein and the landform of a specific area, affects the types of plants growing in a specific wetland. The variation of vegetation in the marshes found in various wetland areas depends largely upon the salinity gradient (King, 1995). Bulger et al. (1993) found that the organisms in coastal wetlands are affected by spatial and temporal dynamics of salinity. The low diversity in species can be found for high salinity areas, whereas the diversity of the species increases in the fresh water areas (Hampel, 2002). The wetlands in the temperate and high latitude areas can be classified in the following categories:

- Coastal (tidal) wetlands: Tidal wetlands are those wetland areas along the coastline that are influenced by tides. These **salt marshes** are the prevalent types of tidal wetlands. Vegetation species diversities in the salt marsh wetlands are relatively low, as the vegetation in this area must be salt tolerant. In the tide dominated salt marshes, smooth cord grasses such as *Spartina alterniflora* and *Spartina anglica* (Figure 2a) are common species. These are the first species to grow on the mudflat. Once the pioneer vegetation starts growing, plants such as *Limonium* species and *Scirpus* species will start to grow (Mayer, 2003).

Figure 2a: Spartina anglica, common salt marsh vegetation in the tidal wetland pioneer zone

Figure 2b: Scirpus maritimus in brackish water wetlands.

Figure 2c: Phragmites species in fresh water wetlands

- Tidal brackish water wetlands: These areas are in the transitional areas between the tidal wetlands and fresh water wetlands. Because these wetlands are less saline than the tidal wetlands, they allow for more diversity of marsh vegetation including *Scirpus* (Figure 2b) and *Phragmites* species (Figure 2c) (Bakker, 2014).

- Fresh water wetlands: These areas are dominated by herbaceous plants, commonly found along the banks of rivers and streams. Marshes found in this area have a variety of species because of the available fresh water. In these fresh water marshes, species such as *Phragmites* (Figure 2c), *Sparganium* and *Carex* can be found (Magee, 1981).

All these marsh species develop small stems, roots and rhizomes as shown in Figure 3a. By creating rhizomes, these marsh species spread horizontally, as shown in Figure 3b.

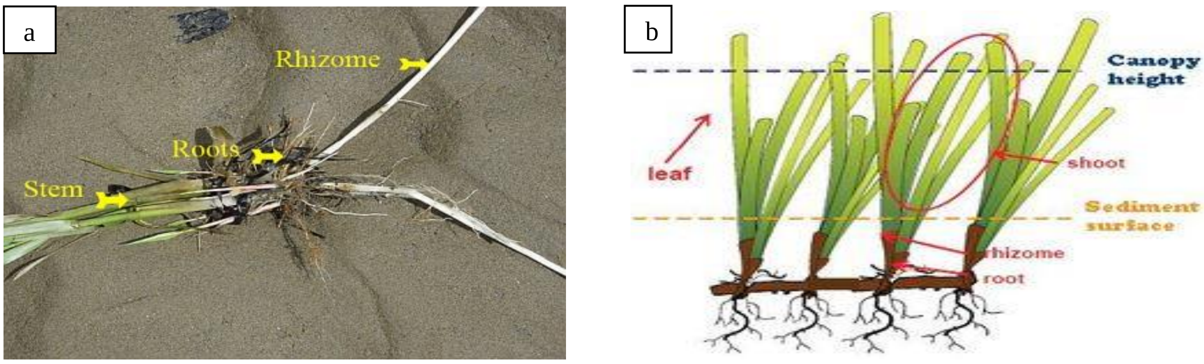

Figure 3: Salt marsh vegetation (a) showing stems, roots and rhizomes (Zottoli, 2011) (b) spreading of vegetation species by rhizomes system (Koch et al., 2006).

1.2 Salt marshes

Salt marshes generally dominate the tidal wetlands in temperate climatic zones and their existence is restricted to the upper intertidal zones of sheltered sedimentary coasts and estuaries. Salt marshes expand in those areas where there is net sediment accumulation due to the tides and they tend to spread out both vertically and horizontally (Redfield, 1972).

Geomorphology of salt marshes

Both the tidal range and the tidal regime (semidiurnal, mixed or diurnal) influence the flow over the marsh surfaces (Adam, 1990; French & Stoddart, 1992). On the basis of spring tidal range, salt marshes can be divided into micro-tidal (< 2 m), meso-tidal (2–4 m) and macro-tidal marshes (>4) (Davies, 1980). Again, macro-tidal salt marshes can be subdivided into low macro-tidal (4–6 m) and high macro-tidal (>6 m) (Robin et al., 2002).

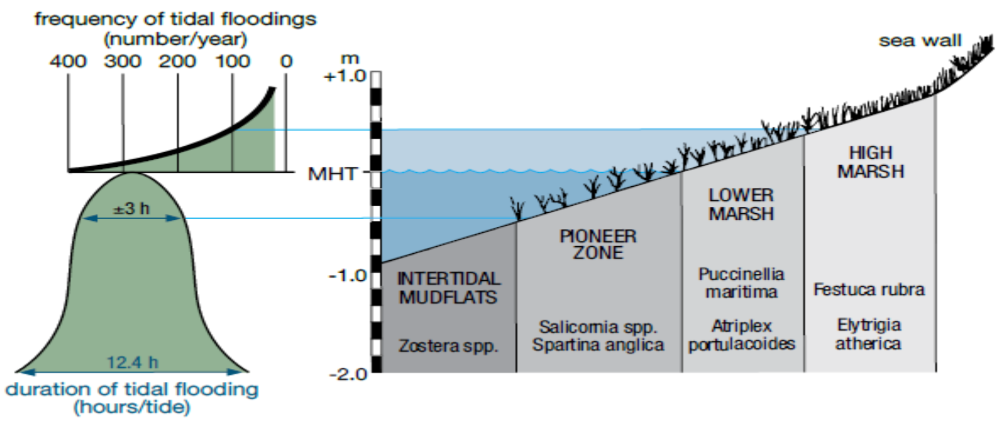

Figure 4: Schematic structure of a salt marsh on a Dutch Barrier Island with vegetation zones in relation to inundation duration and inundation frequency (Bakker, 2014).

Salt marsh vegetation

Salt marsh species vary with elevation (Adam, 1990; Dijkema, 1984; Vernberg, 1993). In salt marsh areas, four zones can be found depending on the elevation: the lower mudflat zone (no vegetation); the intermediate pioneer zone; the lower marsh area which is characterized by low species density; and the higher marsh area which is characterized by higher numbers of plant species (Niering & Warren, 1980) (Figure 4). The difference in inundation period and inundation gradient affect the availability, diversity and growth of the marsh vegetation. For example, a wide diversity of salt marsh species can be found in Europe due to the smaller inundation period and height (Beeftink & Rozema, 1988).

The mudflat and pioneer zones are the two most dynamic parts of the salt marshes subjected to inundation by every high tide with rapid sedimentation and erosion activities (Daloffire et al., 2006). On the other hand, the high marsh plants only submerge for brief periods during spring tides. Therefore, pioneer vegetation is the first to disappear when tidal flats are eroded due to waves (Balke, 2013).

Bio-geomorphic succession of salt marshes

The bio-geomorphic succession of a salt marshes (Figure 5) starts with the establishment of pioneer vegetation. When a critical biomass is reached, bio-geomorphic feedbacks generate bio-protection (sediment binding, energy attenuation) and bio-construction (sediment trapping, organic matter production) (Bouma et al., 2009). Without large disturbances, this bio-geomorphic succession may subsequently cause the salt marsh to develop towards a biological stable state, where the vegetation may disconnect from the physical processes and the biological interactions determine the future vegetation structure (Corenblit et al., 2007). However, scouring around the patches of vegetation may inhibit their lateral expansion (Bouma et al., 2009). High hydrodynamic energy, either from waves or tidal currents, will generally cause mudflat–salt marsh ecosystems to reduce in size due to erosion. Once the salt marshes are totally eroded and change to a bare mudflat, it takes a long time to re-establish the salt marsh environment again (Bouma et al., 2009).

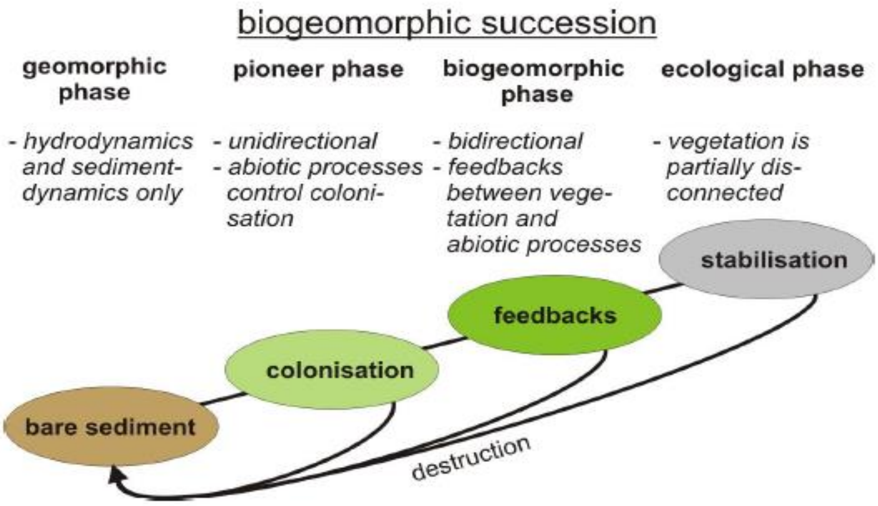

Figure 5: Bio-geomorphic succession of salt marshes adapted from (Corenblit et al., 2007). Plants colonise bare areas which are frequently disturbed (by both hydrodynamics and sediment dynamics) and can create bio-geomorphic feedbacks when they exceed a critical density threshold. Eventually, the vegetation is separated from the physical environment and hence develops into a biological stable state.

1.3 Hydrodynamics in salt marshes

Salt marsh vegetation induces several hydrodynamic processes, sometimes with large-scale consequences. The presence of salt marsh grasses can alter the environment by attenuating the hydrodynamic energy. Möller and Spencer (2002) measured wave heights and wave energy at two salt marsh–mudflat transition sites named Tillingham (UK) and Bridgewick (UK) and found considerable dissipation of wave energy and wave height over the inhomogeneous salt marshes compared to the mudflats. This apparent energy dissipation can be explained by the complex process in which vegetation roughness reduce the wave energy (Möller & Spencer, 2002). Wave attenuation by vegetation was also studied under controlled laboratory experiments with natural vegetation (Fonseca & Cahalan, 1992; Tschirky et al., 2000). Besides, several numerical studies are also available on the wave attenuation over the salt marsh vegetation surfaces (Dalrymple et al., 1984; Lima et al., 2006; Lowe et al., 2007; Méndez & Losada, 2004; Méndez & Losada, 1999). This wave attenuation gradually increases the accumulation of sediments and sediment elevation gradient in the salt marsh. Severe erosion of exposed sediments due to wave actions of storm event helps the formation of salt marsh cliff (Van de Koppel et al., 2005). In this study, the focus will be given to the salt marsh cliff soil erosion, hence further details of the hydrodynamics in salt marshes are omitted here.

Not lot of papers are available that focused on the formation of salt marsh cliff. The mechanism helps to the formation of salt marsh cliff was explained by Van de Koppel et al., (2005). Below a threshold bottom shear stress, vegetation can establish in the pioneer zone. After the initial establishment of the vegetation, the positive feedback between the plant growth and the sediment accumulation helps to the spatial development of the salt marshes. No vegetation development occurs at the mudflat side because the conditions are too adverse to the plant growth. Gradually, sediment elevation increases due to the accumulation of sediments trapped by the vegetation. As a result, salt marsh platform develops and strongly sloping sediment elevation occurs between the edge of the vegetated and un-vegetated part of the gradient (Figure 6). This edge is sensitive to the disturbance. Due to wave action, the vegetation in the exposed edge may collapse. Thus, the collapse of vegetation in turn leads to severe erosion of the exposed sediments and helps to the formation of the salt marsh cliff (Van de Koppel et al., 2005).

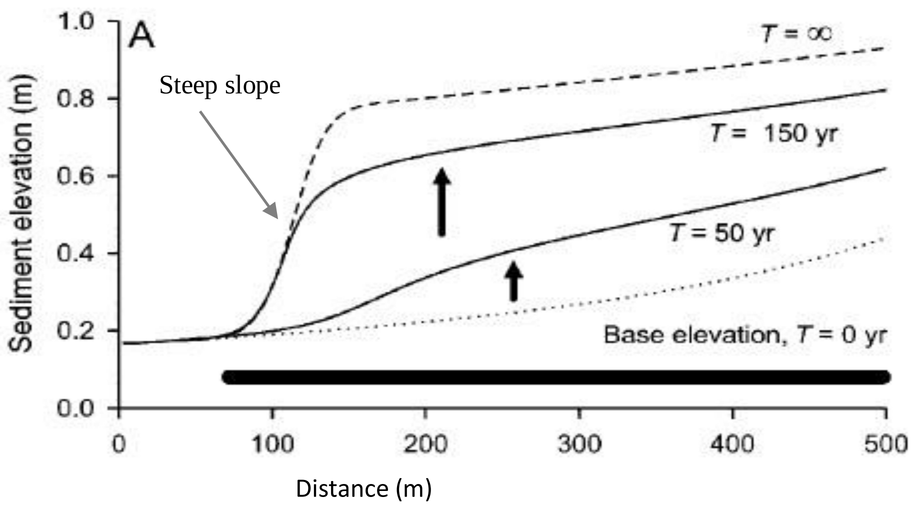

Figure 6: Development of the salt marshes from an un-vegetated tidal flat (steep slope exist between the vegetated and un-vegetated edge).

1.4 Sediment dynamics in salt marshes

Sediment dynamics, which includes both sediment deposition and erosion, are important to understand whether salt marshes will accrete/develop or erode/disappear. Salt marsh vegetation actively traps sediments by attenuating the local hydrodynamics and thereby contributes to its own lateral and vertical extension. However, due to the ongoing sediment deposition in the salt marshes, an elevation gradient may develop creating a cliff between the mudflat and the salt marsh. This cliff may erode due to wave action. Additionally, the topsoil of the salt marsh surface may erode under the continuous action of tides and waves. Therefore, there are two types of noticeable erosion processes in salt marshes: cliff soil erosion and topsoil erosion. The bed shear stress is an important factor that determines whether sediment deposition or topsoil erosion will occur on a sediment bed, which is explained in the next section.

1.4.1 Bed shear stresses

The bed shear stress is the key hydrodynamic parameter that controls the deposition and topsoil erosion of the sediment in salt marshes. The bed shear stress (τ_b) is the bed friction force per unit area due to exposure to waves and currents. When water flows over salt marsh beds, drag and turbulence is caused by the interaction with the bed and the vegetation. The presence of vegetation creates roughness and hence, affects the (orbital) flow velocity, which will further affect the shear velocity and bed shear stress. The present study will focus on cliff erosion rates, hence further details of this bed shear stress are omitted from this report. To know more about the calculation of the bed shear stress, readers are referred to the papers by Shi et al. (2012; 2014). For topsoil erosion to occur on the salt marsh surfaces, the bed shear stress needs to exceed a certain critical value: the 'critical bed shear stress'. Several studies (Christiansena et al., 2000; Shi et al., 2012; Shi et al., 2014; Tolhurst et al., 1999) are available on the calculation of critical bed shear stresses for topsoil erosion.

1.4.2 Sediment deposition mechanism

The formation of salt marshes is largely dependent on sediment deposition (Allen, 2000). Several field observations demonstrate that salt marsh vegetation increases sediment deposition and protects the bed against erosion due to reduced bed shear stresses in the vegetation (Brown et al., 1998). This sediment deposition phenomenon in salt marshes depends on the sediment properties, sediment concentration, flow turbulence and marsh topography. Earlier studies have addressed several aspects of sediment deposition on salt marsh surfaces. For example, accumulation of sediment occurs during times when the vegetated marsh surfaces are flooded and suspended sediment moves toward the marsh surfaces (Leonard & Luther, 1995; Wang et al., 1993).

1.4.3 Sediment erosion mechanism

The 'erodibility' of the sediment represents the sensitivity of the sediment to be eroded. It can be represented typically by the 'erosion threshold' and the 'erosion rate'. General aspects of the salt marsh erosion will be discussed with a focus on the cliff erosion from the salt marsh edges.

Topsoil erosion of salt marsh vegetation surfaces

The topsoil erosion is an important phenomenon in salt marsh environments. The presence of vegetation can significantly alter the erosion characteristics of salt marsh substrates (Paterson, 1989; Sutheland et al., 1998). Studies are available on the erodibility of the topsoil vegetated surfaces, which includes determination of both 'erosion thresholds' and 'erosion rates' (Houwing, 1999; Widdows et al., 2000). Sediment properties, such as grain size distributions and organic matter content, and vegetation parameters, such as vegetation density, affect the topsoil erosion. The study done by Grabowski et al. (2011) revealed, that the erodibilty of cohesive sediments is controlled by the physical sediment properties such as particle size distribution, bulk density, water content and organic matter, as well as biological properties such as the presence of roots and rhizomes.

Cliff soil erosion at the salt marsh edges

Cliff erosion is an inevitable and intrinsic consequence of the bio-morphological dynamics of salt marshes (Van de Koppel et al., 2005). High hydrodynamic energy such as a storm surge generally initialize this erosion process (Van Belzen et al., 2015). At exposed edge of salt marshes, sediment is vulnerable to wave and current action. The erodibility of the salt marsh edges (i.e. salt marsh cliff) can also be characterized by an 'erosion threshold' and an 'erosion rate'. The erosion threshold in case of cliff soil erosion is represented by the term 'critical salt marsh sediment elevation gradient', the maximum gradient that a salt marsh can withstand. The closer the marsh gets to this threshold, the more vulnerable it becomes to the disturbance (Van de Koppel et al., 2005) (Figure 7). Previous researches are available on the quantification of cliff soil erosion thresholds by measuring salt marsh elevation gradients (May, 1973; Scheffer et al., 2001; Van de Koppel et al., 2005). Further explanation of the salt marsh elevation gradient is beyond the scope of this study and hence is omitted here.

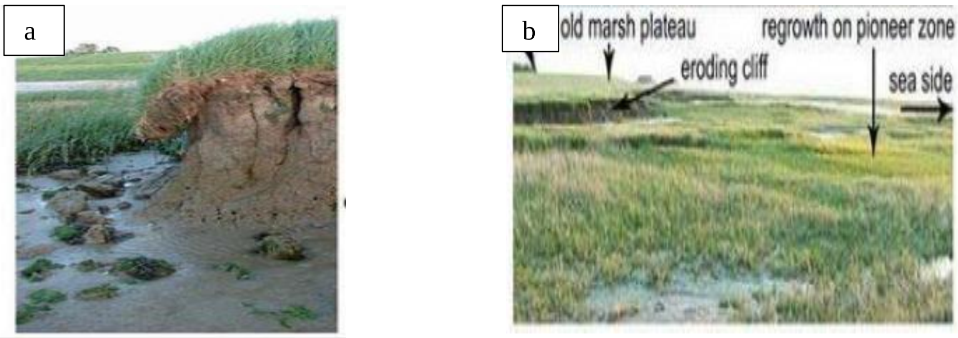

Figure 7: (a) Critical elevation gradient causes cliff erosion in the salt marsh edges (b) *Salt marshes showing eroding cliffs and regrowth of marshes on pioneer zone* (Van Belzen et al., 2015).

However, only few studies exist that looked into cliff erosion rates. Studies showed the severity of this cliff erosion: A study carried out during the period of 1993-1995 in the Lagoon of Venice, showed that strong wave action caused rapid erosion to most of the exposed salt marsh edges (Day et al., 1998). A comparison between the map of 1933 and 1970 done by Cavazzoni and Gottardo (1983) on the same place, found that marshes eroded at a rate of 0.8-2.7 m/yr.

While these are the outcomes of field studies on the erosion rates of salt marsh cliff edges, limited laboratory findings are available on this topic. A laboratory study done by Feagin et al., (2009) on the impact of the vegetation to wave erosion in the salt marsh edges found that the erosion rates do not significantly reduced by the presence of the salt marsh plants. However, Feagin et al., (2009) found that soil type is the primary variable that influences the cliff erosion rate in the wetland edges. Coops et al. (1996) carried out an experimental study at Delft Hydraulics (The Netherlands) on the interactions between waves, bank erosion and vegetation presence. Although this study was focused on the bank erosion, the vegetation and sediment parameters are expected to act in similar way as in case of cliff erosion due to wave action. Coops et al. (1996) found that the presence of belowground mass of the vegetation cover strongly reduces the erosion rate due to the soil reinforcement. Coops et al. (1996) also found that sediment composition is a major factor affecting the spatial distribution of erosion.

From the above literature study, it is noticeable that the cliff erosion rate depends on the sediment properties and the vegetation parameters. Therefore, the present study focusses on the cliff erosion rate and the effect of different vegetation characteristics and sediment properties on this cliff erosion rate.

1.5 Research problem

The findings by Feagin et al., (2009) challenges the common perception that salt marsh plants prevent lateral erosion along wetland edges by binding soil with live roots. No additional study is available that can support or reject the conclusion done by Feagin et al., (2009). The findings of Coops et al. (1996) generally support the common perception that the salt marshes help to reinforce the soil and hence reduce the erosion rate, but this experiment was carried out on the bank erodibility. Comparing the erosion rate between the two species *Phragmites autralis* and *Scirpus lacustris*, Coops et al. (1996) found the net erosion in *Phragmites australis* was significantly lower than the *Scirpus lacustris*. The findings of two studies hardly support each other. Additional, although some field studies are available on the cliff erosion rates in salt marshes, controlled experimental studies of cliff erosion rates are still very limited. No extensive study is available on the correlation between cliff erosion rates and different salt marsh vegetation and sediment properties. All these research gaps described above lead to the following research problem.

> *It is not well known yet how and to what extent the vegetation characteristics and the sediment properties affect the cliff erosion rates in salt marshes.*

Different vegetation species with varying vegetation density and amount of biomass are expected to show different cliff erosion rates. Investigating cliff erosion rates for different vegetation parameters and species requires an extensive laboratory study. The laboratory experiment provides us the insights to identify the important parameters that contribute to the cliff erosion rates in a controlled environment. Different sites have different soil properties and variable hydrodynamic exposures. To compare cliff erosion rates among different sites, it is required to use the same type of disturbance effect. Additionally, from field studies, it is hard to obtain data on the cliff erosion rate of the densely vegetated or higher elevated salt marsh areas, as erosion in these areas is an individual and slow process. Therefore, in order to study cliff erosion for different vegetation species and densities within a small time frame, laboratory studies are required.

1.6 Research objective

The objective of this study is:

To quantify salt marsh cliff erosion rates through controlled laboratory wave tank experiments and to quantify the effects of the sediment properties (median sediment grain size and organic carbon content) and the vegetation characteristics (vegetation species, vegetation density, amount of aboveground and belowground biomass) on the salt marsh cliff erosion rates.

1.7 Research questions

The following research questions have been formulated for this study:

1. How do vegetation characteristics and sediment properties generally vary in salt marsh areas?
2. How to assess the cliff erosion of salt marsh substrates in a controlled experimental set-up?
3. What are the typical cliff erosion of salt marshes collected across a range of field conditions?
4. What is the impact of vegetation characteristics and sediment properties on the cliff erosion of the salt marsh?

1.8 Approach and report outline

The research approach and outline of the report is based on the formulated research questions stated in section 1.7. To answer the research questions, experiments were carried out in a controlled laboratory setting at the faculties of NIOZ in Yerseke. Sediment samples and sediment cores were collected from the field. Detailed information of the sampling locations will be provided in section 2.1. The vegetation characteristics and sediment properties of the collected samples will be analysed and the procedure will be described in section 2.2. The collected sediment cores will be used in the wave tank experiment to determine the cliff erosion of the salt marshes. The detailed processes of measuring the cliff erosion rates will be described in section 2.3, followed by a description of data analysis technique in section 2.4.

The results of all measurements and tests will be presented in chapter 3. Section 3.1 and 3.2 will present the results of sediment properties and vegetation characteristics, respectively. Section 3.3 will present the quantification of sediment volume loss from the sediment cores of wave tank experiments. Section 3.4 will present the suitable trend lines fitted to the obtained eroded sediment volume graphs. The correlation of the observed cliff erosion rates to the sediment properties and vegetation characteristics will be analysed in section 3.5. Discussion of this study will be given in chapter 4, followed by conclusions and recommendation in chapter 5.

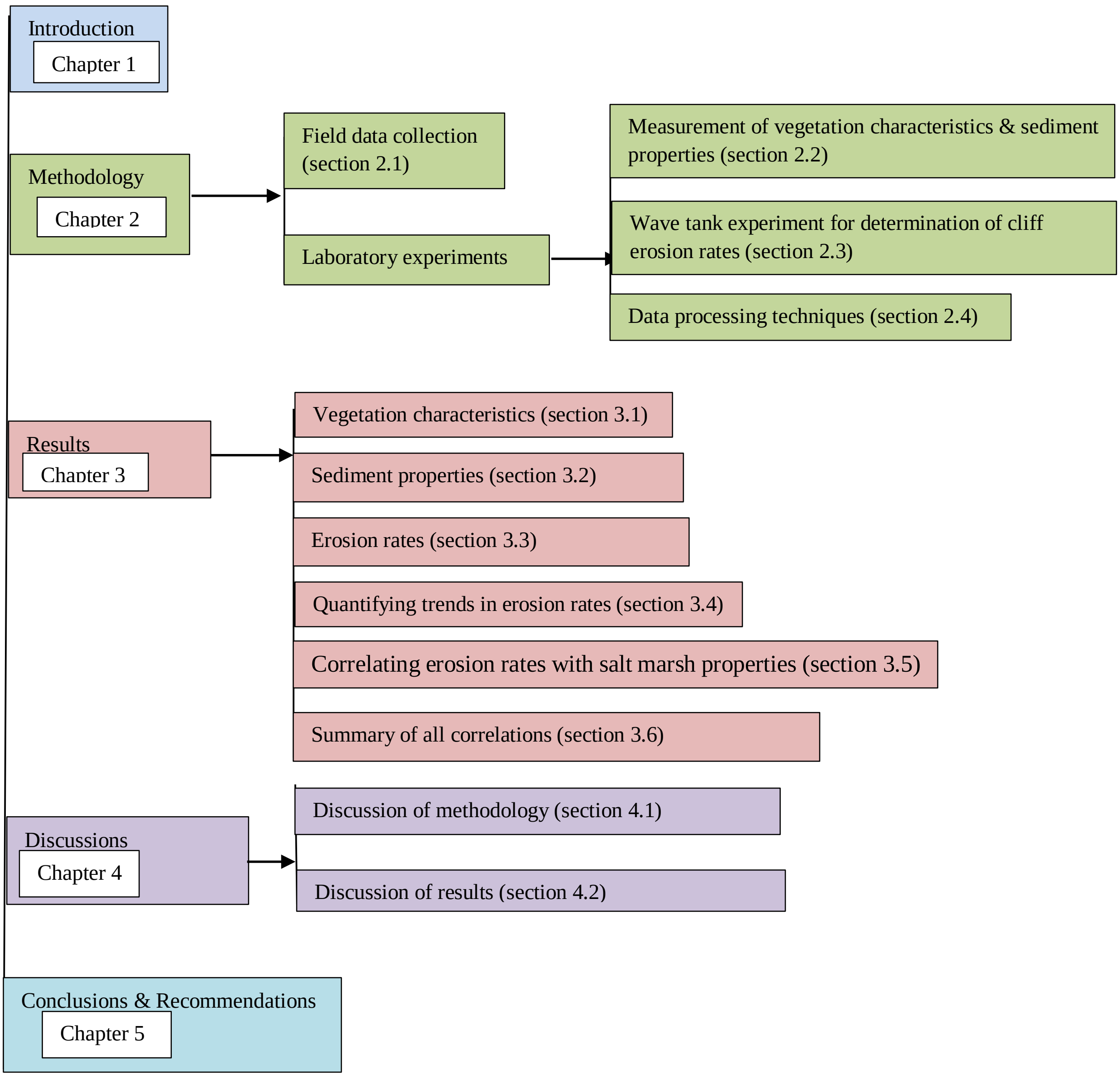

Figure 8: Schematised outline of the thesis

Chapter 2

2. Methodology

This chapter describes the research methods deployed in this study. At first, introduction and description of the field sites that have been selected for this study are given. The sampling locations and sample collection techniques are provided here. After that, laboratory experiment procedure for the quantification of the physical properties of the collected sediment samples are described, which includes determination of sediment properties and vegetation characteristics. Next, the experimental set-up of wave tanks is explained followed by the image collection techniques. 3D image analysis method of determining the eroded sediment volume is described. Finally, the validation of the 3D image analysis method is described. The schematised diagram showing the procedures involved in the methodology chapter is given below in Figure 9.

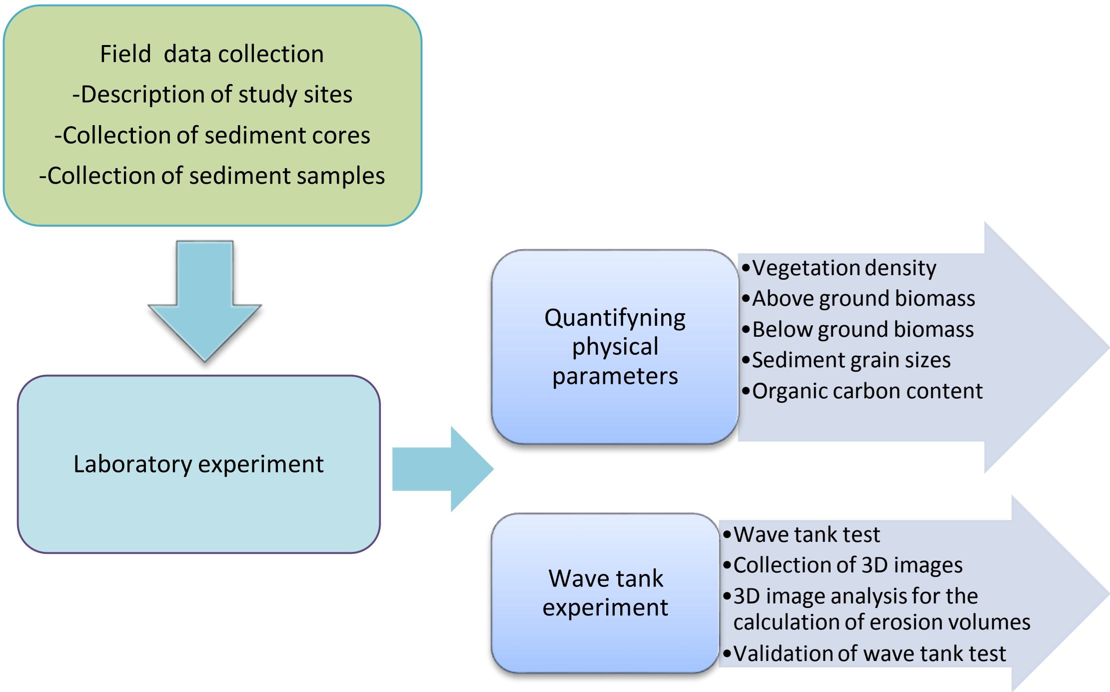

Figure 9: Schematised diagram of the experimental methods.

2.1 Field data collection

To carry out the experiments, sediment cores for the wave tank experiments and sediment samples for analysing sediment properties were collected from five different study sites covering a range of vegetation and sediment properties. In this section, the study sites are introduced, along with the underlying reasons for selecting the five study sites. Next, the sediment coring and sediment sampling techniques are presented.

2.1.1 Study Sites

The study sites were selected along the Western Scheldt estuary and the Nieuwe Maas because vegetation characteristics vary for tidal influenced and river influenced areas. Sediment properties vary across tidal and riverine environments as well. Therefore, the selected study sites can be classified based on the salinity of the water. Further, the specific vegetation characteristics and sediment properties of every field site will affect the cliff erodibilty of the salt marsh substrates. Therefore, the study sites have been selected to cover a wide range of vegetation characteristics and sediment properties.

Four of the study sites are located at the Dutch Coast along the Western Scheldt estuary, and one study site named De Zaag, is located along the Nieuwe Maas (Figure 10). The name of the study sites, latitude, longitude, vegetation species and salinity are given in the table 1.

Table 1: The study sites where sediment and vegetation samples were collected: locations (Latitude & Longitude), salinity condition of water and vegetation species.

Site name	Latitude	Longitude	Species	Salinity of water	water body
Zuidgors	51°23'13.0"N	3°49'20.2"E	*Spartina anglica*	Salt water	Western Scheldt
Hellegatpolder	51°21'58.74"N	3°57'06.12"E	*Spartina anglica*	Salt; freshwater inlet	Western Scheldt
Bath	51°24'12.1"N	4°11'01.4"E	*Spartina anglica, Scirpus maritimus, Phragmites australis*	Very brackish water (more salt water, less fresh water)	Western Scheldt
Groot Buitenschoor	51°21'57.8"N	4°14'45.6"E	*Scirpus maritimus*	Brackish water(more fresh water, less salt water)	Western Scheldt
De Zaag	51°53.610'N	4°36.233'E	*Phragmites australis*	Fresh water	Nieuwe Maas

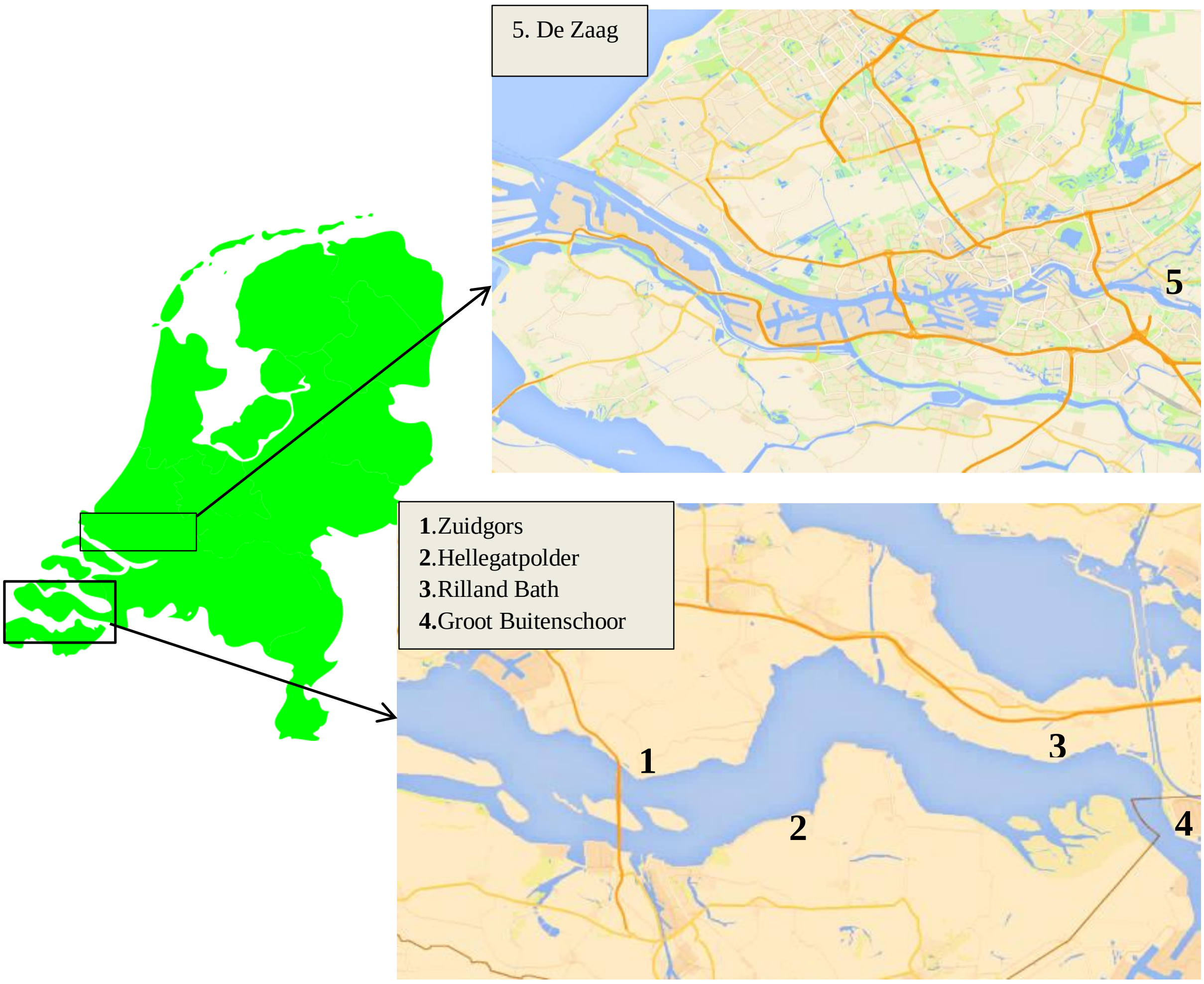

Figure 10: Location of study sites.

<u>Description of the study sites</u>

The focus of this study was to observe the effect of vegetation characteristics (species, density, amount of biomass) and sediment properties (grain sizes and organic carbon) on cliff erosion rates. The selected field sites cover various degrees of salinity, from salt water via brackish to freshwater. The salinity determines the type of species but is not a determinant in the erosion process. For the experiments it is important to account for the natural salinity to avoid dispersion or flocculation of the sediments. The description of the five study sites is given below:

1. **Zuidgors** is a tidal dominated, hence salt water influenced area located along the Western Scheldt estuary (Figure 10). *Spartina anglica* is the common vegetation type for this site and this marsh has only two characteristic zones: the non-vegetated mudflat and a densely vegetated upper marsh zone. The sediment type in this area is sandy.

2. **Hellegatpolder** is a salt water dominated area also located along the Western Scheldt (Figure 10), but it has a fresh water inlet. The vegetation type in this site is *Spartina anglica*. In the salt water influenced area, three characteristic zones can be found: the higher marsh with densely vegetated *Spartina anglica*, the sparsely vegetated pioneer zone and the un-vegetated mudflat zone. The sediment type is very sandy for this area. The areas closer to the fresh water inlet can be taken as the very brackish water

influenced area. In this area, two zones can be found: un-vegetated mudflat zone and vegetated higher marsh zone with *Spartina anglica*. The sediment type is clayey.

3. The study site **Rilland Bath** (Figure 10) has both salt and fresh water influence, hence the water is very brackish. In this area, three types of salt marsh species can be found, *Spartina anglica*, *Scirpus maritimus* and *Phragmites australis*. *Scirpus maritimus* is the dominated species in this area with three distinctive zones: mudflat, sparsely vegetated and densely vegetated zone. The *Spartina anglica* has only two characteristic zones: mudflat and vegetated zone. For *Phragmites australis*, only vegetated zone exist. The sediment type is clayey.

4. The study site **Groot Buitenschoor** (Figure 10) is brackish water influenced area. The common vegetation type in this zone is *Scirpus maritimus* with three distinctive zone: mudflat, sparsely vegetated and densely vegetated areas. The sediment type is very clayey.

5. The study site **De Zaag** is a fresh water influenced area as it is located along the river Nieuwe Maas (Figure 10). The vegetation species is *Phragmites australis*. The sediment type is clayey.

2.1.2 Collection of sediment cores and samples

Sediment cores for the salt marsh cliff erosion experiments in the wave tanks and sediment samples for the analysis of grain sizes and organic carbon were collected from all field sites. In total, 51 sediment cores and 50 sediment samples were collected (Figure 11). Among the 51 cores, 33 cores were taken from areas of existing salt marshes, whereas 18 sediment cores were collected from mudflats. At each location, 3 replicates were collected to make up for local variations in vegetation and sediment properties. The characteristics of the samples collected at each field site are as follows (summarized in Figure 11):

1. Zuidgors: From this site, 6 sediment cores and 6 sediment samples were collected; 3 sediment cores and 3 sediment samples from the mudflat zone and 3 sediment cores and 3 sediment samples from the vegetated zone with dense *Spartina anglica* species.
2. Hellegatpolder: At this site, overall 15 sediment cores and 14 sediment samples were collected; 9 sediment cores and 9 sediment samples from a salt water influenced area consisting of mudflat, sparsely vegetated and densely vegetated area. 6 sediment cores and 5 sediment samples were collected from a fresh water influenced area: 3 sediment cores from the mudflat and 3 sediment cores from vegetated area. Among the 5 sediment samples: 2 from mudflat and 3 from vegetated zone were collected.
3. Rilland Bath: From this site, overall, 18 sediment cores and 18 samples were collected: 9 sediment cores and 9 sediment samples were collected from the area dominated by *Scirpus maritimus*: mudflat zone, sparsely vegetated and densely vegetation zones (3 sediment cores and 3 sediment samples from each of the zone). In the zone of *Spartina anglica*, 6 sediment cores and 6 sediment samples were collected; 3 cores and 3 sediment samples from the mudflat zone and 3 cores and 3 sediment samples from the vegetated zone. The remaining 3 sediment cores and 3 sediment samples were collected in a zone with *Phragmites australis* species.
4. Groot Buitenschoor: 9 sediment cores and 9 sediment samples were collected from this *Scirpus maritimus* dominated site including 3 sediment cores and 3 sediment samples from each of the location: the mudflat, the sparsely vegetated and the densely vegetated areas.
5. De Zaag: From this site, only 3 sediment cores and 3 sediment samples were collected from the *Phragmites australis* vegetated zone.

Figure 11 gives an overview of sediment cores and sediment samples collected from the five different field sites.

Figure 11: Flow chart showing the natural water conditions, locations, salt marsh species types and total numbers of sediment cores and sediment samples collected from five different field sites. Green colour represents the collected sediment cores and sediment samples places; intensity of colour changes with the increasing of vegetation density, SC=Sediment cores, SS=Sediment samples. Numbers of sediment cores and sediment samples are same with one sediment sample less in case of very brackish water-Hellegatpolder-unvegetated zone.

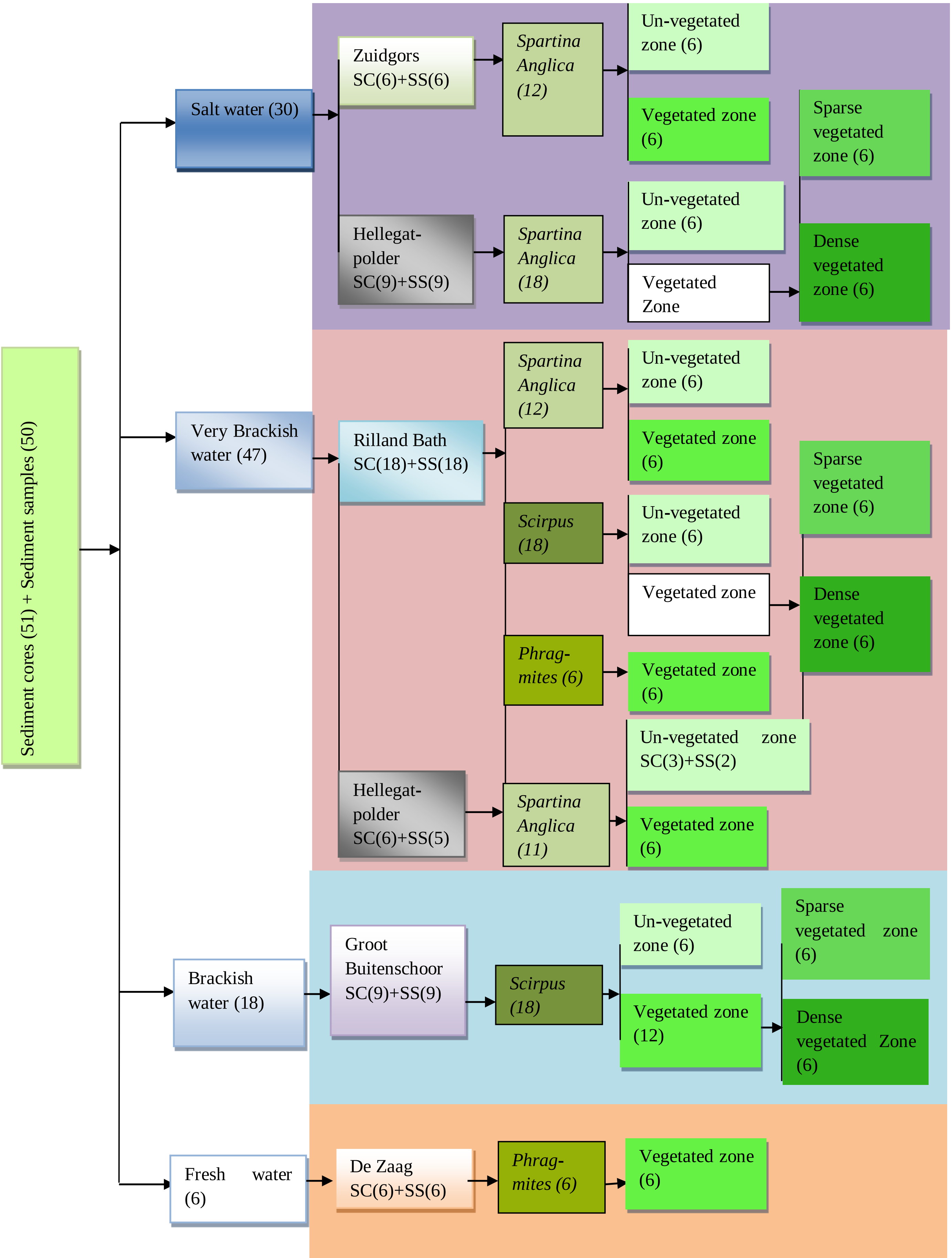

The sediment cores were collected two hours before the incoming high tides as to make sure that enough time was available to collect the sediment cores. The sediment cores at all the sites were collected in the same way. The hollow plastic sediment core tubes are 30 cm high and 15 cm in diameter, with a blue cap to close the bottom (Figure 12a). The empty tubes were placed in the selected zones (mudflat, sparse vegetated or dense vegetated zone) of each site and hammered into the ground until around 25 cm of the tube penetrated into the ground as shown in Figure 12c. After that, the soil around the tube was removed with the help of a spade so that the tube filled with sediment, the sediment core, could be taken out smoothly without disturbing the core bottom (Figure 12e). After taking out the sediment cores from the ground, the blue cap was attached at the bottom so that the sediments would not fall out when transporting to the laboratory. The collected sediment cores were either placed in the wave tank directly or stored in a tank for some days in the same type of water as in the field, until the wave tank was ready for the run. The storing period was always less than one week to avoid compaction and drying of the sediments.

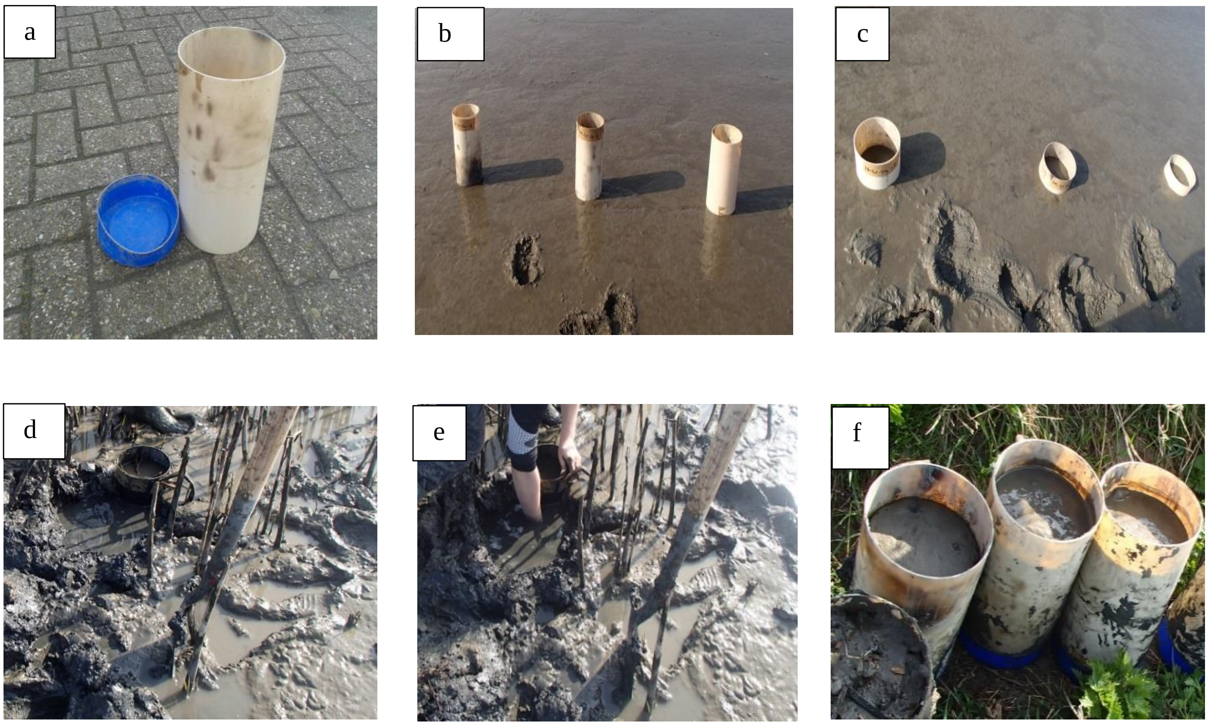

Figure 12: a) Empty sediment core, b) Placing of sediment cores in mudflat zone, c) Hammered sediment cores into the ground, d) Spading to remove the soil around the core, e) Taking out of sediment core from ground, f) Collected sediment cores.

To collect the sediment samples, 30 cm PVC tubes with a diameter of 4.3 cm were used, with a red cap to close the bottom. Sediment samples were collected similar to the collection of the sediment cores. The tubes for the sediment samples were placed in each zone and hammered into the ground until around 20 cm (Figure 13a). With the help of a spade, the samples were taken out carefully and the caps were put on the bottom of the tubes.

Figure 13: a) Placing and hammering of sediment samples to the ground, b) Collected sediment samples and sediment cores.

2.2 Quantifying vegetation and sediment properties

2.2.1. Measuring vegetation density

The vegetation density is expressed as the number of individual plants per square meter area. From the five study sites, 11 vegetated zones were sampled and for each of these zone the vegetation density was measured. The square area measuring ruler was placed in the vegetated area and the number of plants within that square was counted. However, this procedure of counting vegetation density does not refer to the vegetation density on each of the collected sediment cores. For this reason, the vegetation density on each of the collected sediment cores was measured. As this was not planned beforehand, the number of plants on the sediment cores was not counted before doing wave tank experiments. Therefore, the numbers of plants were counted in the images of the sediment cores taken during the wave tank experiments.

2.2.2. Measuring aboveground biomass

The aboveground biomass consists of the stems and leaves of the salt marsh plants above the sediment. The aboveground plant material on top of the sediment cores was cut at the time of collecting the sediment cores. Some of the upper biomass that was not collected during that period, was collected after finishing the wave tank experiment and before cleaning of the cores. The fresh weight of aboveground biomass was measured. After that, it was dried in an oven at 60°C for a 5 day period and weighted again to get the dry aboveground biomass.

2.2.3. Measuring belowground biomass

The belowground biomass consists of roots and rhizomes of the salt marsh plants in the soil. The eroded sediment cores after finishing the wave tank experiments were collected. The roots in the remaining sediment volume were cleaned to measure fresh and dry biomass of the roots. The roots were washed by spraying water over the sediments using a 1 mm sieve so that no biomass was lost during washing. No brush was used to avoid the possibility of damaging the roots. The stones, worms, crabs and shells were removed by hand. After cleaning, all the roots were stored in a refrigerator at a temperature of 4°C. After that, the fresh root biomass was measured. The fresh roots were dried in the oven at a temperature of 60°C for around 5 days. After 5 days, when the root biomass became very brittle, the samples were taken out from the oven and the mass was measured, which indicates dry biomass. Pictures of the dry biomass during the measurements are shown in Figure 14a and 14b.

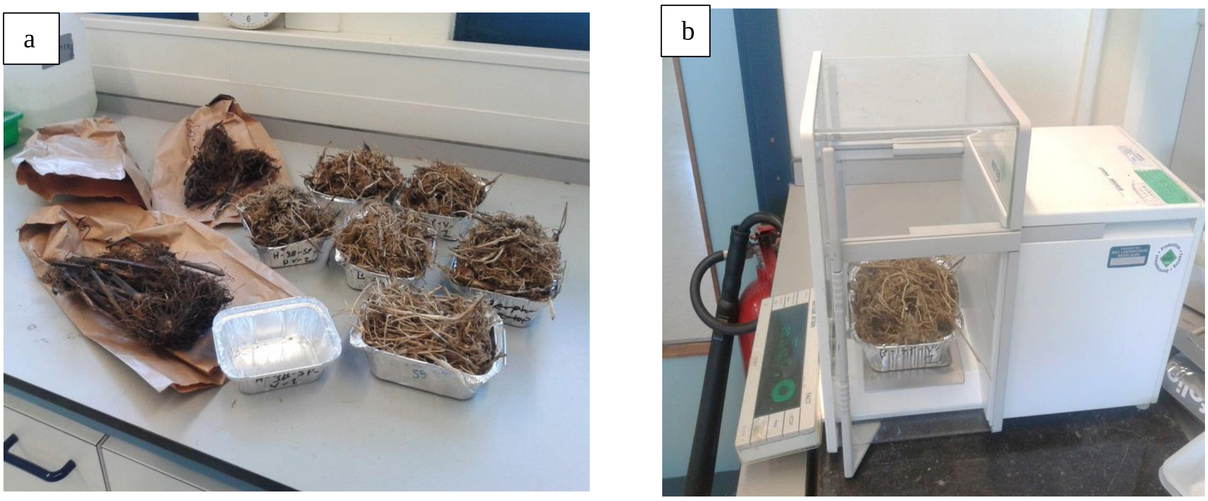

Figure 14: a) Oven dry root biomass, b) weighing of the root biomass using a digital balance.

2.2.4. Measuring sediment grain sizes

Preparation of the sediment samples

After the collection of the sediment samples from the field, the samples were further prepared for grain size analysis and organic carbon measurement.

- By using a stand, the collected sediment samples (each about 20 cm long) were divided in two layers with height of 10 cm each and weighted in the laboratory.
- These samples were put in plastic bags and labelled,
- The plastic bags with sediment samples were kept in a box and the box was stored in a freezer at a temperature of -20°C.

The reason for dividing the samples in two parts was to make them fit in the freeze dryer, which was further needed to prepare the sediment samples for the grain sizes and organic carbon measurements. Therefore, from the collected 50 sediment samples, 100 samples of 10 cm height were obtained.

The stored sediment samples were taken out of the freezer and put into the freeze dryer at -60°C. This freeze drying needed to be repeated several times depending upon the numbers and the available space in the freeze dryer (placing of sediment samples in three layers of freeze dryer) (Figure 15a and 15b). After distributing the sediment samples in the layers of freeze dryer, the mouths of the plastic bags were opened as to make it possible for the water to escape. In this case, the freeze dryer preferred instead of using oven because the freeze drying removes the moisture without greatly altering the physical structure of the sediment.

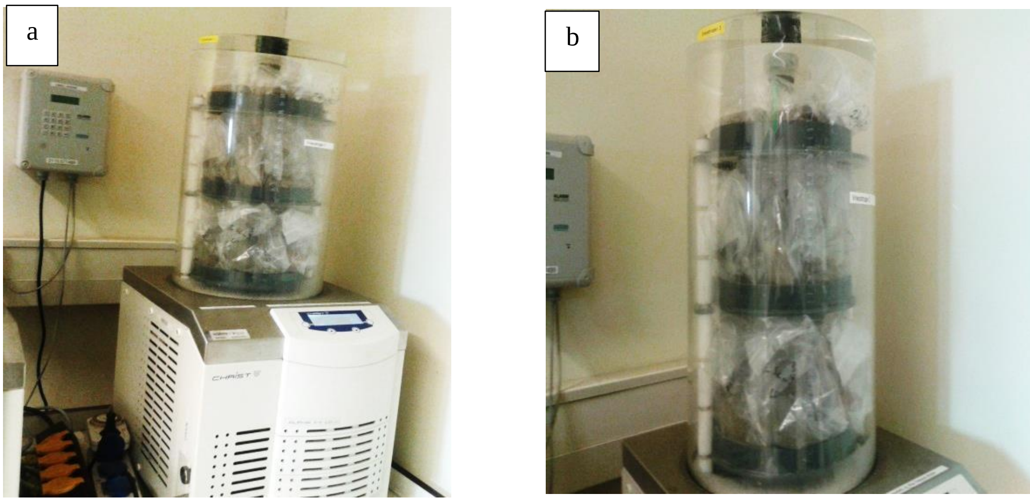

Figure 15: a) Freeze dryer with vacuum chamber in top, b) Sediment samples placed in three layers of the freeze dryer.

The freeze drying was done for around 5 days as to make sure the samples were perfectly dried. After that, the mass of each sample was measured. The freeze dried samples were smashed thoroughly (not giving full strength to avoid the possibility of breaking the larger grains) for the further test. From each of the smashed samples, some portions were sieved using a 1 mm sieve and the sieved samples were divided in two parts, keeping each of them in separate red cap containers with specific labels (Figure 16a and 16b). The content of one of the red cap containers was used to measure the grain size distributions and the rest were used for organic carbon analysis.

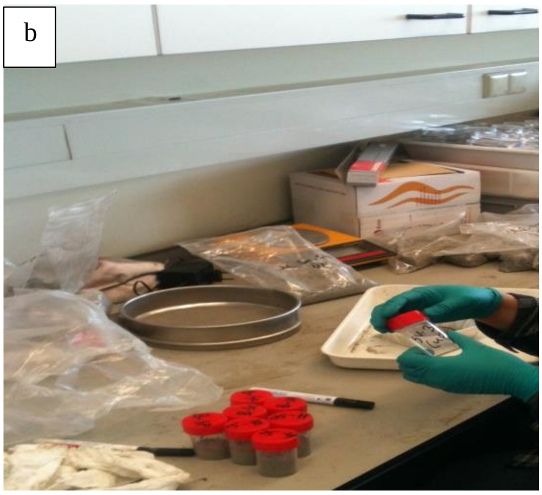

Figure 16: a) & b) Sediment samples preparation for the grain size and organic carbon test.

Grain Size Distribution

This test was performed to determine the percentage of different grain sizes within the sediments. In the laboratory, a Coulter Counter was used to determine the grain size distributions of the sediment samples. Grain size analysis provided the grain size distribution of the sediments that was used to classify the soil.

2.2.5. Measuring organic carbon content

The organic carbon content determines the percentage of organic compound existed in the sediment. Due to the available time limit, this test was not carried out directly. This measurement was done in the laboratory of NIOZ- Yerseke.

2.3. Cliff erosion experiments

2.3.1 Wave tank test

In order to measure the cliff erosion rates from the collected sediment cores, wave tank experiments were performed at NIOZ (Yerseke) in April 2015. There were four wave tanks available at the laboratory, each with three slots. Therefore, 12 sediment cores could be put into the four wave tanks at a time. In this case, the 51 sediment cores were collected in field sites with four different characteristic salinities: salt water, very brackish water, brackish water and fresh water. To avoid differences in flocculation or dispersion of the sediment, the salinity of the water used in the tank was made as close as possible to the natural conditions.

Wave tank set-up

A schematized diagram of wave tank is shown in Figure 17. Each wave tank was 3.5 m long, 0.89 m wide and 0.79 m deep. Inside the tank, the following items can be found:

- Wave paddle: A wave paddle is placed in the tank that can generate waves by moving back and forth over a distance of 32 cm (Figure 17). In this case, the applied pressure to the wave paddle is 8 bars (Figure 18b). The produced waves are one big waves with various smaller irregular waves as to create more natural conditions. When big waves attack the exposed front of the sediment cores, the wave height is around 38 cm from the bottom of the wave tank and about 20 cm from the bottom of the sediment cores (Figure 17). 5 big waves can be produced per minute by the forward and backward movement of the wave paddle. The time difference between the start of the movement of wave paddle is 10 s.
- Tank slots: In each tank, three parallel slots for placing the cylindrical metal sediment cores are provided at a distance of 2.76 m from the wave paddle (Figure 18d).
- Sloping bottom: The slots are located on an elevated horizontal bottom of 50 cm. The height of the horizontal bottom is 18 cm above the bottom of the tank. In front of the elevated bottom, the height is covered by a sloping bottom with a horizontal length of 22 cm (Figure 17).

The tank was filled with water up to a height of 19 cm from the bottom of the tank, which is 1 cm from the bottom of the sediment cores.

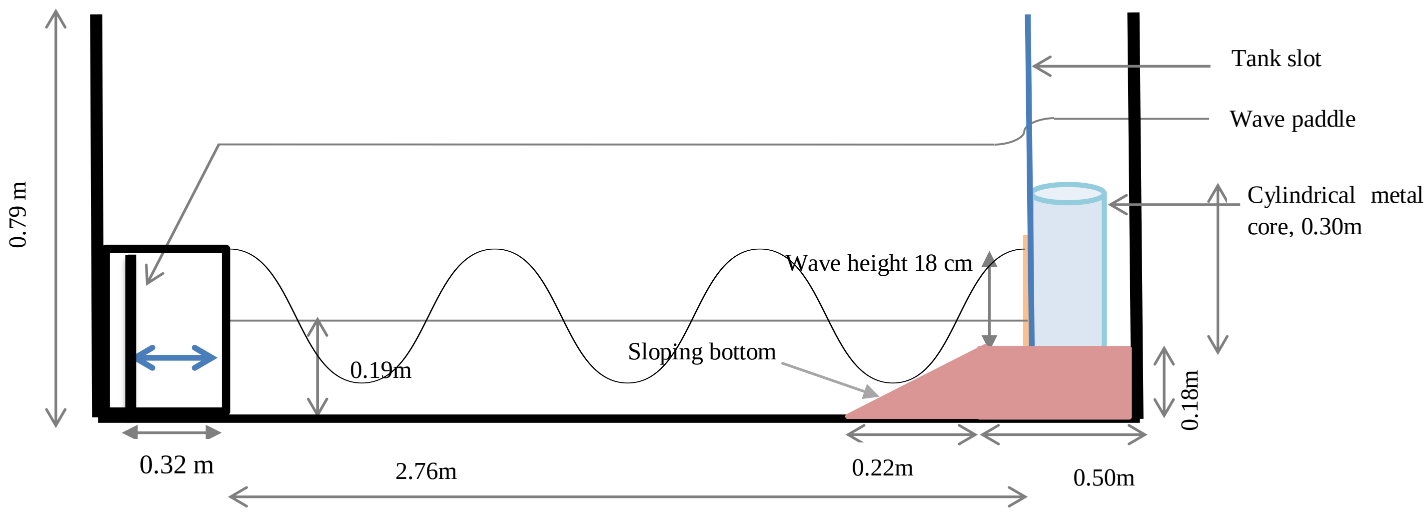

Figure 17: A Schematized side view of the wave tank to measure cliff erosion rates in the laboratory.

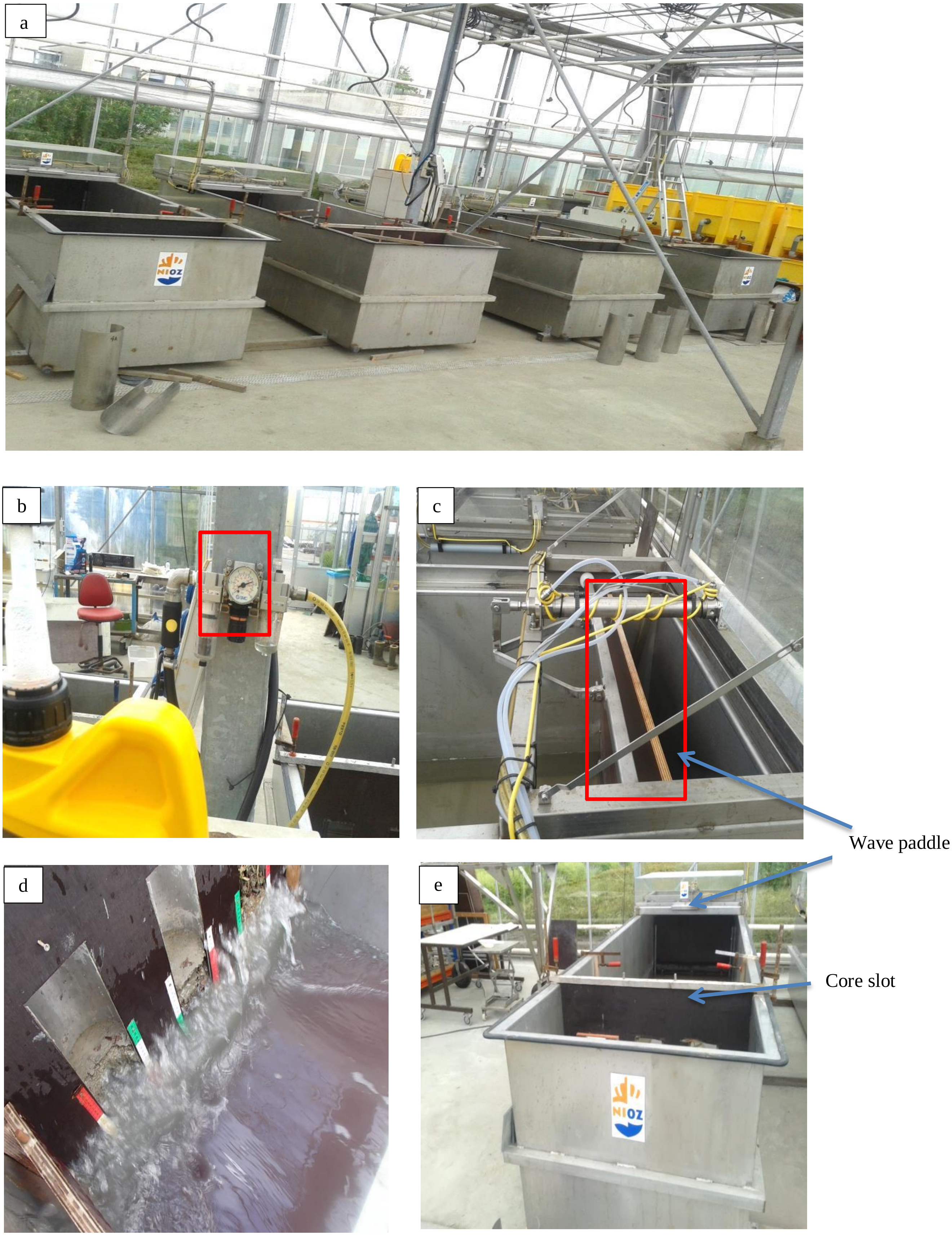

Figure 18: a) Four wave tanks in the laboratory, b) Pressure gauge, c) Wave paddle, d) Wave tank slots with sediment cores during wave attack, e) Entire wave tank showing wave paddle and core slot.

Table 2: Specification of the wave experiment.

Site name	Locations	Species	Number of sediment cores	water condition	water height (cm)	water condition at tank	Salinity of water (ppt)	Total (cores)
Zuidgors	Mudflat; Marsh zone	*Spartina anglica*	mudflat (3); marsh zone (3)	Salt water	19	salt water	30	6
Hellegatpolder	Mudflat; Pioneer zone, Marsh zone	*Spartina anglica*	mudflat (3); pioneer zone (3); marsh zone (3)	Salt water	19	salt water	30	9
Rilland Bath; Hellegatpolder	Mudflat, Marsh zone	*Spartina anglica*	Spartina (Bath) (6); Spartina (Hellegatpolder)(6)	Very Brackish water	19	14 cm salt water and 5 cm fresh water	22	12
Rilland Bath	Mudflat, Pioneer zone, Marsh zone	*Scirpus maritimus; Phragmites australis*	Scirpus (9); Phragmites (3)	Very Brackish water	19	14 cm salt water and 5 cm fresh water	22	12
Groot Buitenschoor	Mudflat; Pioneer zone, Marsh zone	*Scirpus maritimus*	mudflat (3); pioneer zone (3); marsh zone (3)	Brackish water	19	5 cm salt water and 14 cm fresh water	8	9
De Zaag	Marsh zone	*Phragmites australis*	marsh zone (3)	Fresh water	19	fresh water	0	3

The salinity of the water in every experiment is adapted to the natural condition for the cores and can be found in table 2. In the wave tanks, the provided water was the water available in the estuary near the Yerseke-NIOZ laboratory. The salinity of this water is 30 ppt, which was taken as salt water. The fresh water was taken as salinity of 0 ppt. The salinity was taken as 22 ppt for the sediment cores collected from the very brackish water of Bath and Hellegatpolder with a fresh water inlet area and this was done by providing 14 cm of salt water and 5 cm of fresh water in the wave tanks. The salinity condition of very brackish water for the sediment cores collected from the Groot Buitenschoor was taken as 8 ppt, which was the combination of 5 cm salt water and 14 cm fresh water.

Before placing the sediment cores in the wave tanks, they needed to be prepared. After preparing and placing the sediment cores in the slots, the paddle movement was started and run for 48 hours. During this 48 hours period, the wave paddle was stopped several times to take camera shots of the sediment cores. The procedure of colleting the images is described in section 2.3.2.

After finishing the running of the wave tank experiment, the eroded sediment cores were put in plastic bags and labelled. Water was drained out of the tank and sediments were removed, and prepared for the next run.

<u>Preparation of sediment cores</u>

Before placing the sediment cores in the wave tank slots, the sediment cores needed to be prepared.

- The sediment cores were taken out from the storage tank and the bottom caps were removed.
- A partial cylindrical metal core with one side opening of width 12 cm was hammered into the sediment core such that the sediment would reach up to 20 cm height (Figure 19b & 19c).
- With the help of a stand, the plastic sediment tube was removed keeping the sediments in the cylindrical metal core (Figure 19d).
- The metal core with the sediments in it was taken to the ground (Figure 19e). With the help of a knife, the sediment was levelled off with the edge of the metal core (Figure 19f). The exposed area of the

front plane of the sediment core is 240 cm^2 (Figure 19g). For all sediment cores, exactly the same procedure was carried out.

- These prepared metal sediment cores were placed into the slots in the wave tanks.

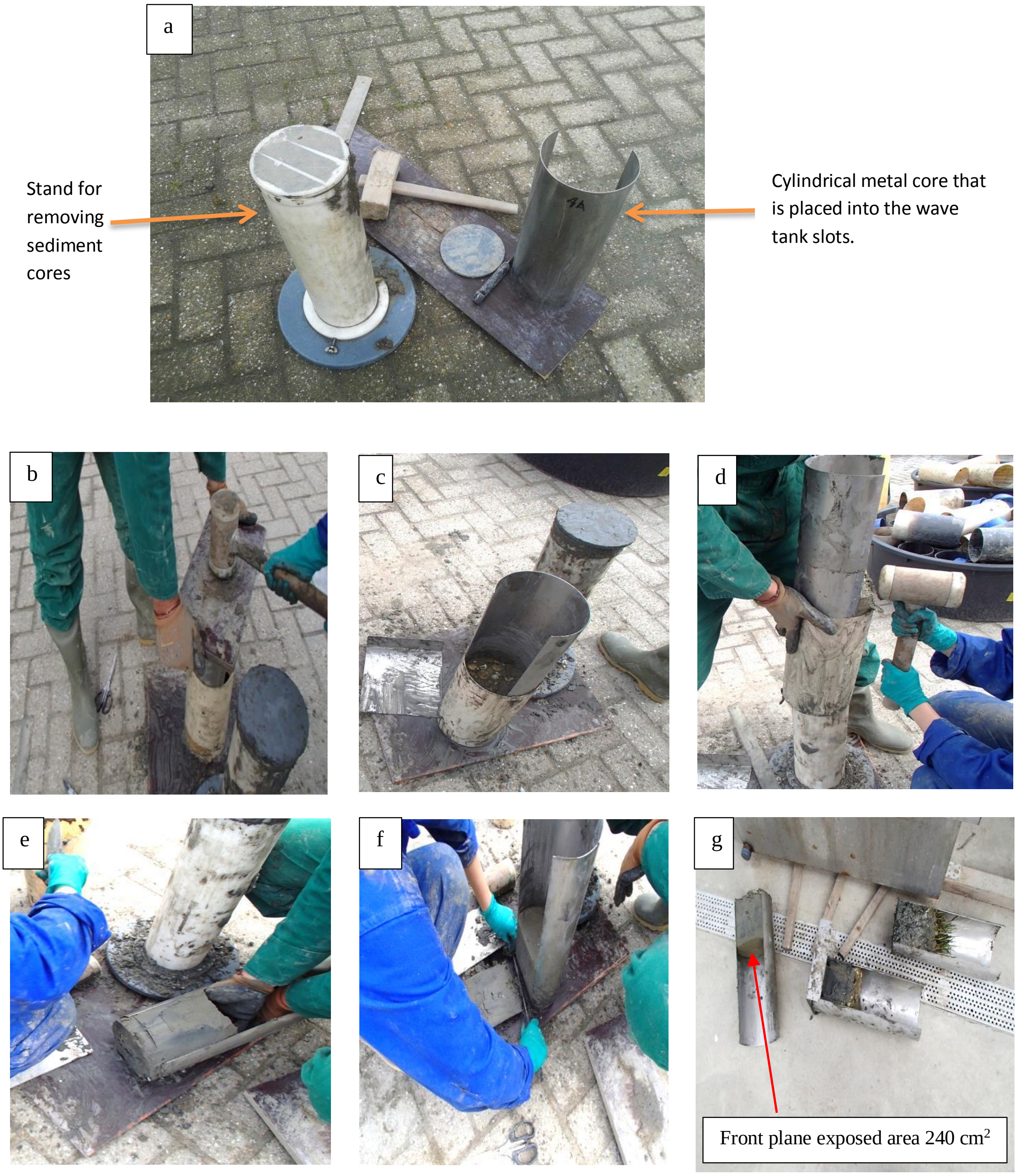

Figure 19: a) Instruments used for the preparation of sediment cores, b), c) and d) Hammering of cylindrical metal core into the sediment core, e) Cylindrical metal sediment core placed in the ground, f) Levelling of the sediments to fit in the metal core edge, g) Prepared sediment cores placed in front of wave tank.

2.3.2. 3D images

To measure the eroded volume of the sediment cores during the wave tank experiments, a 3D imaging technique was applied. A water proof camera was used to collect images, which was operated manually. After placing the cylindrical metal cores in the tank slots, more than 40 pictures were taken for every sediment cores from more than 40 different angles. The wave paddle started to run for a total of 48 h, with stopping the paddle after 1 h, 2 h, 4 h, 8 h, 16 h, 24 h, 32 h, 40 h and 48 h. Images were taken at each of these time steps. The camera setting was 'automatically adjusted'. The 'flash' option of the camera was used for the pictures taken at night. The procedure of analysing the images is described in the section 2.4.1.

2.4 Data processing techniques

2.4.1 3D image analysis for the calculation of erosion volumes

To analyse the digital images of the erosion experiments, three programs were used: Visual SFM, Meshlab and Matlab. Visual SFM is an image processing software, used for 3D reconstruction of images. This software constructs 3D pictures from the input of the 2D images taken from 40 different angles. After the 3D reconstruction, three reference points were added to the 3D images manually to form a triangular mesh. The triangular mesh was further analysed using Meshlab. Meshlab is an open source program for processing and editing this unstructured 3D triangular mesh. The resultant mesh files obtained from the Meshlab can be imported in Matlab, which then calculates the sediment volume loss. The detailed procedure of the 3D image reconstruction (by VisualSFM), mesh formation in 3D images (by Meshlab) and Volume loss calculation (by Matlab) is given in Appendix A. The Matlab scripts used to calculate erosion volume was developed by J. van Belzen, a scientist in the NIOZ-Yerseke. The stepwise procedure of image analysis is summarized in Figure 20.

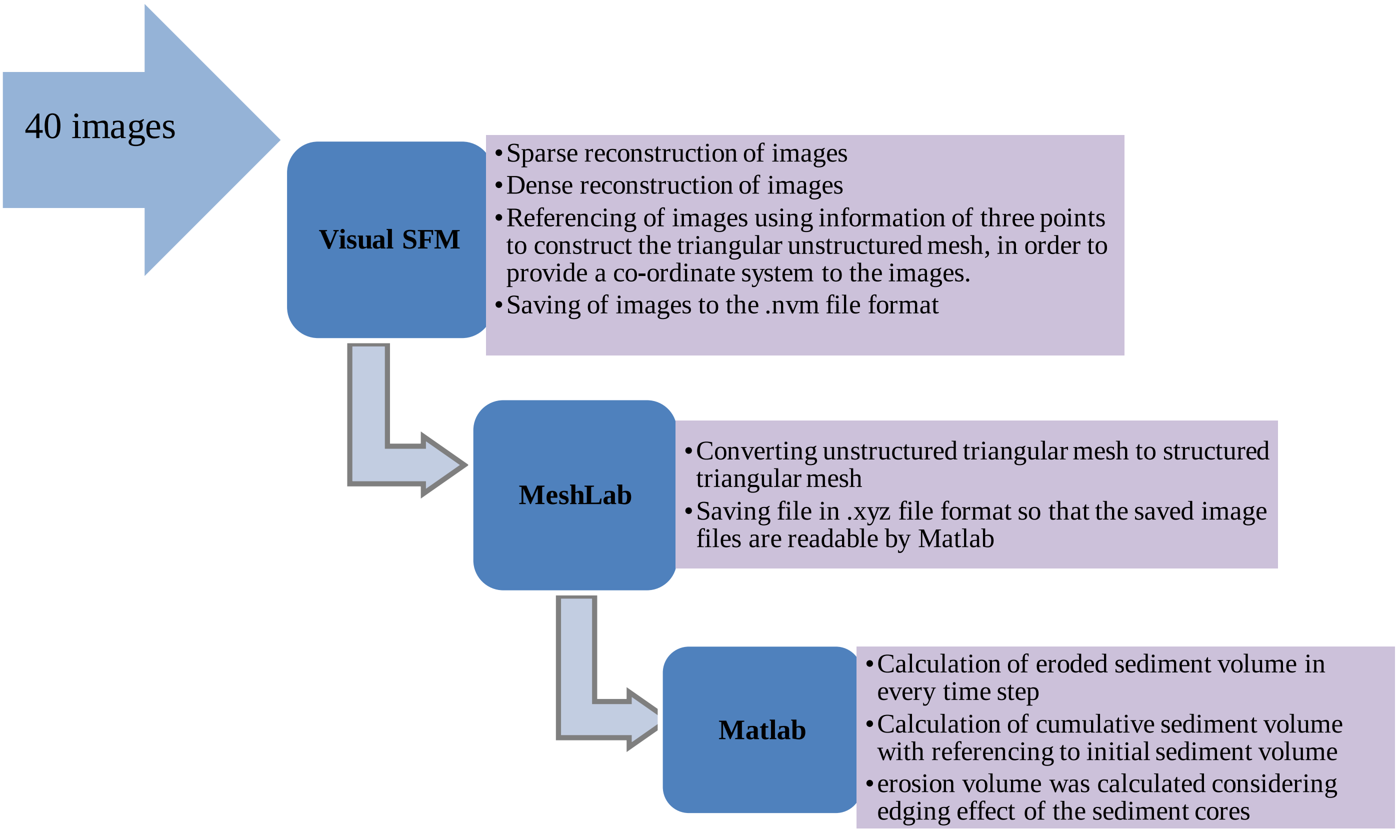

Figure 20: Stepwise procedure of 3D image analysis technique.

Compensating for edge effects

The height of the sediments in all the metal cores was 20 cm. However, sometimes the top of the sediments had an uneven surface, which causes a variation in the height (not exactly 20 cm). This gives rise to variations in the calculation of the exposed plane area and consequently in the initial volume of the sediments in the metal cores. The edge of the sediments in the metal cores was levelled to make the exposed plane as even as possible. However, due to the presence of roots, this action could not be done perfectly and as a result, for some of the sediment cores, especially for the vegetated cores, the exposed surface of the sediments could not be fully levelled off with the edge of the metal cores. This incidentally caused additional errors in the calculation of the initial total sediment volume in the metal cores.

To avoid these errors in the calculation of the eroded sediment volume, these edge effects were considered in the 3D image analysis procedure. In this case, the total dimension of the sediment cores was not considered but instead just part of it was taken. This approach was applied for all the sediment cores. The actual height of the sediment core was 20 cm and the actual width was 12 cm. Therefore, the total sediment volume was 2880 cm^3. However, the total sediment volume in the Matlab program was calculated differently. The rectangle plane taken during the image analysis considering edging effect was 16 cm X10 cm (Figure 21a). The dimension along the Z-axis was 12 cm (Figure 21b). Therefore, total sediment volume of the metal sediment core analysed during the image analysis is 1920 cm^3. Top surface area of the metal sediment core was 159.51 cm^2.

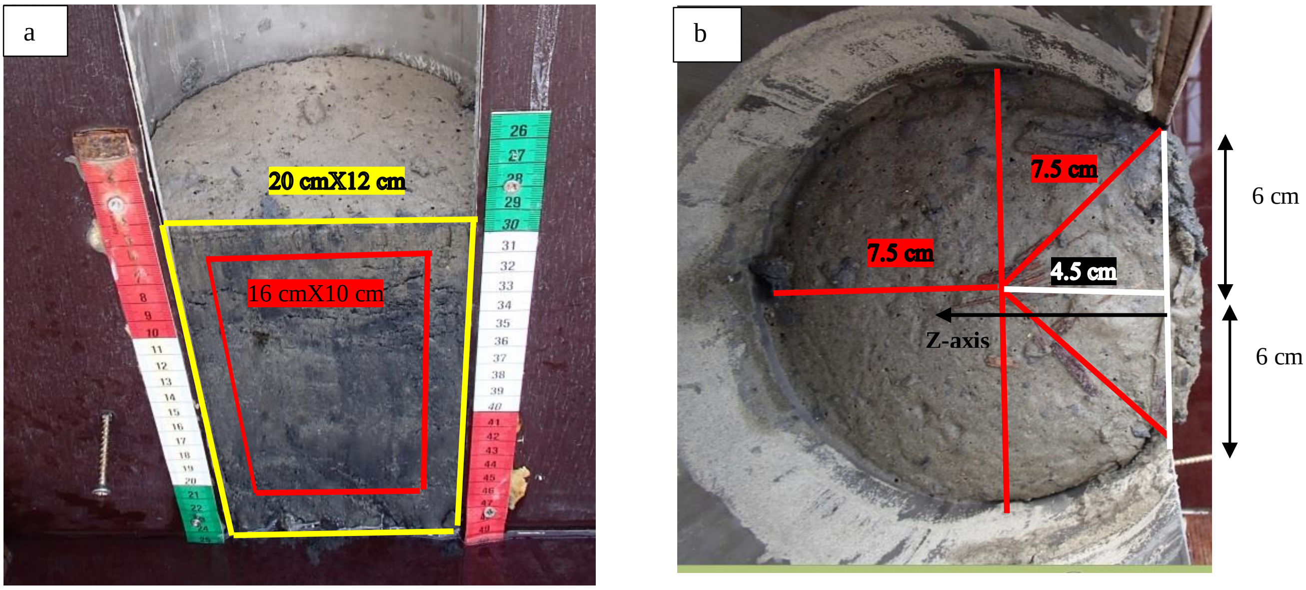

Figure 21: Calculation of the initial sediment volume in the cylindrical metal sediment cores in case of 3D image analysis procedure (a) showing considered exposed area, (b) showing the dimension along the Z-axis (top surface area).

2.4.2. Validation of the sediment erosion volume measurement

To know whether the method of calculating the eroded sediment volumes is a good representation of the actual eroded volume from the sediment cores under wave actions, this method has been validated by comparing the results obtained using this method with manually calculated erosion volumes. Due to the time limit, the validation was not carried out directly instead using the same calibration during the development of this method.

The used sediment core for this case is 20 cm high, which was prepared as explained in section 2.3.1. This core was placed in the 1st wave tank slot in its cylindrical metal core. The pictures of the placed sediment core are shown in Figure 22.

Subsequently, an approximately square shaped sediment amount was cut from the front plane of the sediment core as shown in Figure 22a. This sediment amount was weighted in the laboratory. Dividing this weight with the specific density of the sediments, the volume of the artificially eroded soil was obtained.

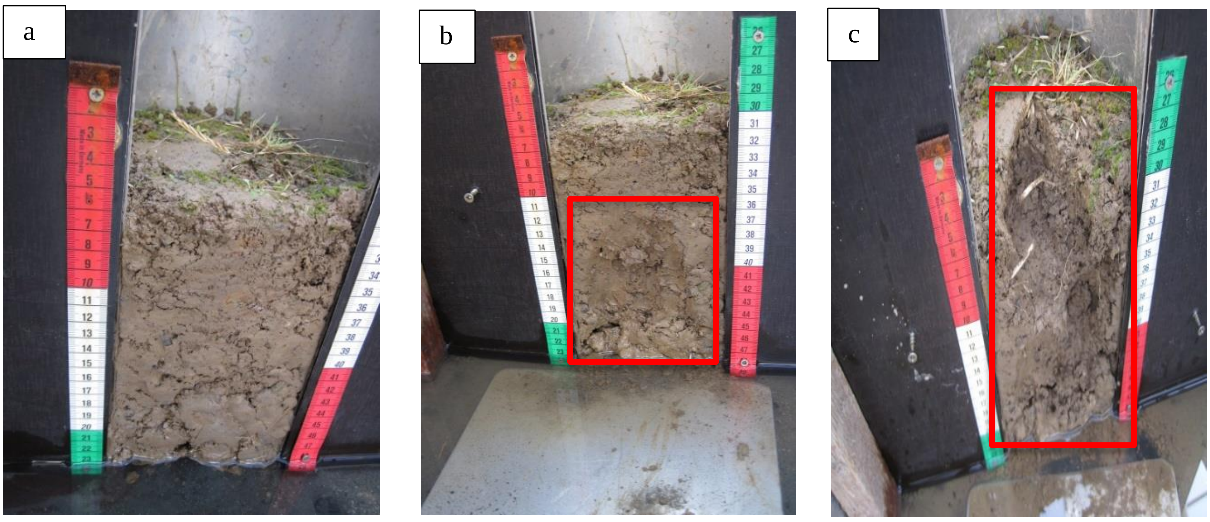

Figure 22: Sediment core used for the calibration operation, a) at the time step T0, b) at time step T3 with manually removed sediments from front plane, c) at time step T5 (with manually removed sediments).

After that, 40 images were taken from different angles of the same sediment core. These images were analysed through 3D image analysis method in section 2.4.1. This eroded volume represents the volume loss in the time step one (T1). For each case, the digital imaging technique was repeated two times for the same time step. Both these procedures (manual procedure and using 3D image analysis method) were carried out for six time steps. For every time step, sediments were removed manually and the 'erosion' was measured by weighing the eroded sediments as well as by the method of 3D image analysis to obtain the volume loss.

The obtained values of the eroded sediment volumes by both methods are given in table 3.

Table 3: Eroded sediment volume calculated by the 3D image analysis technique and manually measurement

Time step	**Number of steps**	**Calculated I**	**Calculated II**	**Measured**	
		V (cm³)	**V (cm³)**	**Weight (g)**	**V (cm³)**
T0	0	0	0	0	0
T1	1	73	60	48	29
T2	2	99	81	81	82
T3	3	157	137	107	147
T4	4	250	229	177	251
T5	5	305	289	94	303
T6	6	351	332	115	369

The measured eroded volume in the laboratory and the calculated eroded volume using 3D image analysis method are plotted in Figure 23(A). In the graph, Calculated I represents the eroded volume of sediments calculated using the 3D image analysis method. Calculated II represents the eroded volume of sediments calculated using the same method for repeated measurement. 'Measured' represents the manually calculated eroded volume.

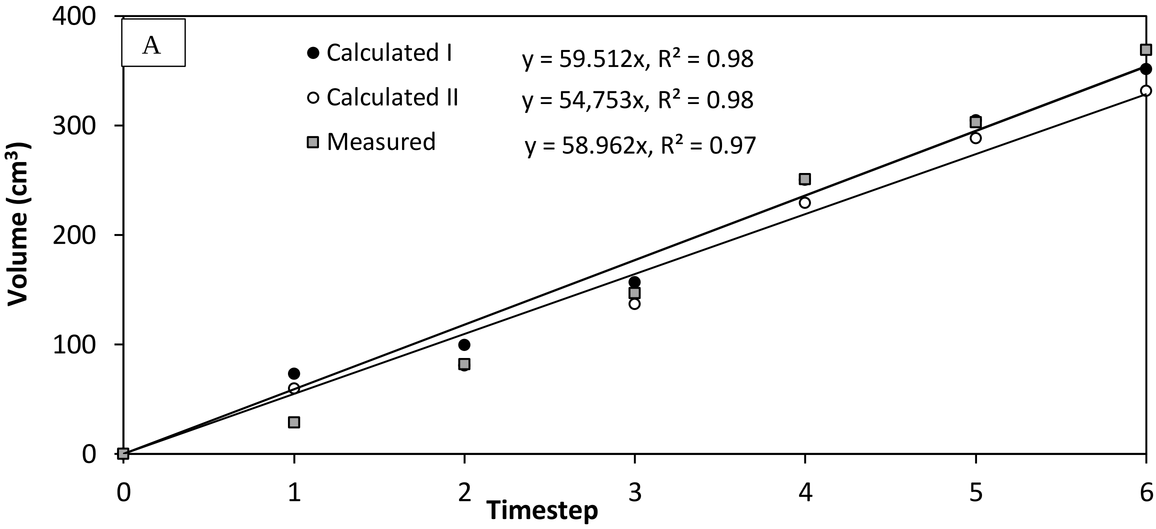

Figure 23: (A) Graph of eroded volume calculation using the 3D image analysis technique and manually measurement.

Both Calculated I (R^2=0.97) and Calculated II (R^2=0.98) give very high values of R^2, when the data is drawn against the manually measured sediment volume (Figure 23(B) & 23(C). The high values of R^2 mean that eroded volume calculated by using the image analysis method compares well to the measured volume of eroded sediments.

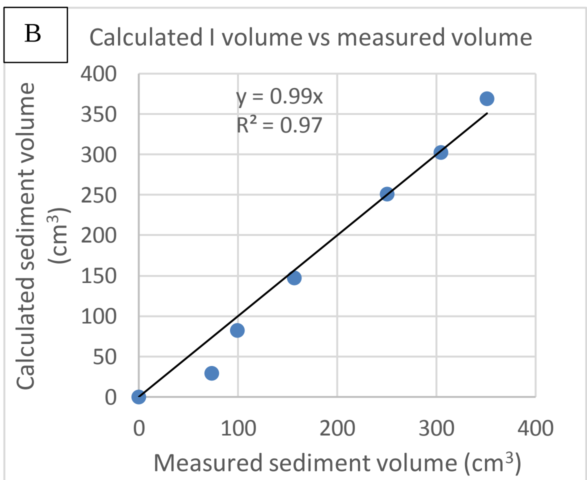

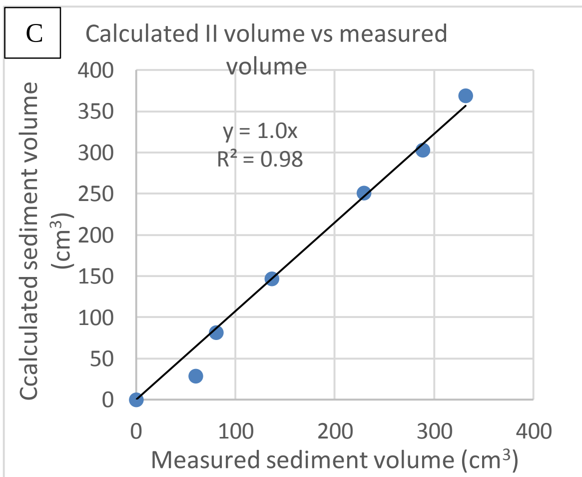

Figure 23: (B) Plot of measured eroded sediment volume and calculated I eroded sediment volume with linear regression fit and R^2 value. (C) Plot of measured eroded sediment volume and calculated II eroded volume with linear regression fit and R^2 value.

Chapter 3

3. Results

In this chapter, the results of this study will be presented. The chapter starts with the results of the sediment properties and vegetation characteristics, followed by the results of the observed erosion rates from the sediment cores in the wave tank experiments. Next, the observed erosion rates will be interpreted and converted into two coefficients characterizing the erosion properties of the sediment cores: the erosion rate and the erosion maximum. The vegetation and sediment characteristics will be correlated with these two coefficients to find out the parameters influencing the erosion of the sediment cores in the wave tank experiments.

3.1 Vegetation characteristics

3.1.1 Vegetation density

The number of stems counted on the cylindrical area of each sediment core (159.51 cm^2) is expressed as number of stems per square meter. The results of the stem density (stems/m^2) can be found in table 4. (Original data and Intermediate results can be found in table 2 of Appendix B). Stem density is higher for the sediment cores with *Spartina anglica* species with a range around 1003-3260 stems/m^2. The stem density of *Phragmites australis* sediment cores is around 439-1254 stems/m^2. The stem density of *Scirpus maritimus* species is around 63-1066 stems/m^2. These ranges were taken as considering sparsely vegetated and densely vegetated cases. Obviously, the stem density in the densely vegetated sediment cores is higher than the stem density for the sparsely vegetated cores for every species.

3.1.2 Aboveground biomass

Aboveground biomasses were calculated as the amount of dry biomass per m^2 surface area. These data were obtained from the vegetation that was present on each of the cores that were taken from the field.

The amount of aboveground biomass varied depending upon the study sites and species. Higher amounts of aboveground biomass were found for the sediment cores collected from the *Phragmites australis* dominated study sites with a range of around 1596-3794 g/m^2, whereas smaller amounts of aboveground biomass were obtained for the sediment cores collected from *Scirpus maritimus* species dominated study sites with a range of around 114-962 g/m^2. The aboveground biomass found for the *Spartina anglica* was in a range of 162-977 g/m^2. Within the same study area, the aboveground biomass was higher for the sediment cores collected from densely vegetated locations than for the sediment cores of sparsely vegetated location. The amount of aboveground biomass of *Spartina anglica* species differed among study sites: higher amounts were found for the sediment cores collected from Zuidgors and Hellegatpolder, whereas smaller amounts were found for the sediment cores collected from Rilland Bath. The results of the aboveground biomass analyses can be found in table 4. (Original data and Intermediate results can be found in table 3 of Appendix B).

3.1.3 Belowground biomass

The belowground biomass was calculated as the amount of dry roots and rhizomes biomass per square meter of surface area. Dry belowground biomass also varied with study sites and species. For *Spartina anglica species,* higher amounts of belowground biomass were found for the sediment cores collected from Rilland Bath (13156-18859 g/m^2), whereas smaller amounts of belowground biomass were found for the sediment cores collected from Hellegatpolder with fresh water areas (1381-4741 g/m^2) and salt water areas (2621-6835 g/m^2). The belowground biomass of *Phragmites australis* varied around 4500-5125 g/m^2 for Rilland Bath, whereas it was around 6000-14000 g/m^2 for De Zaag. Among the three species, the smallest amount of belowground biomass was obtained for the *Scirpus maritimus*. Within each of the study sites, the amount of belowground biomass in the sediment cores was different for different locations. The amount of belowground biomass increased for the sediment cores collected from the densely vegetated locations compared to the sediment cores collected from the sparsely vegetated zones. The results of the belowground biomass can be found in table 4. (Original data and Intermediate results can be found in table 4 of Appendix B).

Table 4: Results of stem density, aboveground and belowground biomass of 33 vegetated sediment cores (Name of the sediment cores was chosen as location (2=vegetated, 3=sparse vegetated, 4=dense vegetated)-Study sites (B=Bath, H=Hellegatpolder, Z=Zuidgors, G=Groot Buitenschoor, D=De Zaag)-Vegetation species (Sc=Scirpus maritimus, Sp=Spartina anglica, Ph=Phragmites australis)-Characteristics vegetation (SV=Sparse vegetated, DV=Dense vegetated, V=Vegetated)-number of replicate (1, 2, 3)).

Name of the sediment cores	Stem density (stems/m²)	Dry aboveground biomass (g/m²)	Dry belowground biomass (g/m²)	Name of the sediment cores	Stem density (stems/m²)	Dry aboveground biomass (g/m²)	Dry belowground biomass (g/m²)
3B_Sc_SV_1	313	114.73	4627.80	**4H_Sp_DV_1**	2382	944.14	5009.72
3B_Sc_SV_2	188	117.23	2730.99	**4H_Sp_DV_2**	1881	707.79	6835.46
3B_Sc_SV_3	63		1653.94	**4H_Sp_DV_3**	2132	654.50	6429.47
4B_Sc_DV_1	1442	320.36	9969.88	**2Z_Sp_V_1**	2006	977.37	11629.57
4B_Sc_DV_2	1755	431.32	6338.23	**2Z_Sp_V_2**	2696	880.82	8173.56
4B_Sc_DV_3	1066	376.78	8033.33	**2Z_Sp_V_3**	2633	677.70	5722.20
2B_Ph_V_1	878	3794.75	4789.18	**3G_Sc_SV_1**	251	516.58	1408.06
2B_Ph_V_2	1254	2782.27	5633.87	**3G_Sc_SV_2**	125	505.92	2085.14
2B_Ph_V_3	752	2530.25	5125.25	**3G_Sc_SV_3**	313	779.89	2950.91
2B_Sp_V_1	2758		18859.01	**4G_Sc_DV_1**	752	687.10	7939.16
2B_Sp_V_2	3260	162.37	10597.77	**4G_Sc_DV_2**	376	541.66	6525.40
2B_Sp_V_3	2570		13156.34	**4G_Sc_DV_3**	564	962.95	5785.99
2H_Sp_V_1	2382	808.10	2399.96	**2D_Ph_V_1**	752	3054.98	13965.35
2H_Sp_V_2	2194	672.69	1381.37	**2D_Ph_V_2**	878	3121.43	10042.46
2H_Sp_V_3	2006	628.80	4741.76	**2D_Ph_V_3**	439	1596.77	6098.39
3H_Sp_SV_1	1881	488.37	3340.77				
3H_Sp_SV_2	1066		2622.02				
3H_Sp_SV_3	1003		2621.50				

3.2 Sediment properties

3.2.1 Sediment grain sizes

Sediment grain sizes (including D_{50}) were analysed for all the vegetated and un-vegetated sediment samples considering two layers: the top 0-10 cm (top layer) and the lower 10-20 cm (bottom layer). Besides, the averaged D_{50} was calculated for the two layers. The grain size distributions of the sediments varied depending upon the study sites. The results of the sediment grain sizes can be found in the table 5. (Original results can be found in table 5 of Appendix B)

3.2.2 Organic carbon content

The organic carbon content of all the sediment samples were obtained for the same two layers as the grain sizes. Besides, average organic carbon content of the two layers were calculated as well. The results of organic carbon content can be found in the table 5 (Original results can be found in table 6 of Appendix B).

Table 5: Sediment sizes (D_{50}) and organic carbon content averaged of the two layers (Name of the sediment samples was chosen as location (1=mudflat/unvegetated, 2=vegetated, 3=sparse vegetated, 4=dense vegetated)-Study sites (B=Bath, H=Hellegatpolder, Z=Zuidgors, G=Groot Buitenschoor, D=De Zaag)-Vegetation species (Sc=Scirpus maritimus, Sp=Spartina anglica, Ph=Phragmites australis)-Characteristics vegetation (Un=unvegetated, SV=Sparse vegetated, DV=Dense vegetated, V=Vegetated)-number of replicates (1, 2, 3)).

Name of the sediment samples	Average sediment sizes of two layers (SD_{50}) (µm)	% org C. Average of two layers	Name of the sediment samples	Average sediment sizes of two layers (SD_{50}) (µm)	% org C. Average of two layers
1B_Sc_Un_1	57.30	1.47	**3H_Sp_SV_1**	127.23	0.35
1B_Sc_Un_2	56.48	1.72	**3H_Sp_SV_2**	113.47	0.31
1B_Sc_Un_3	54.46	1.78	**3H_Sp_SV_3**	105.08	0.48
3B_Sc_SV_1	58.50	1.10	**4H_Sp_DV_1**	111.24	0.32
3B_Sc_SV_2	105.47	0.25	**4H_Sp_DV_2**	114.13	0.28
3B_Sc_SV_3	96.45	0.28	**4H_Sp_DV_3**	109.03	0.33
4B_Sc_DV_1	77.60	0.45	**1Z_Sp_Un_1**	57.94	0.69
4B_Sc_DV_2	77.97	0.32	**1Z_Sp_Un_2**	58.89	0.86
4B_Sc_DV_3	77.30	0.56	**1Z_Sp_Un_3**	46.34	0.73
2B_Ph_V_1	88.74	0.24	**2Z_Sp_V_1**	64.06	0.72
2B_Ph_V_2	83.68	0.27	**2Z_Sp_V_2**	46.91	0.98
2B_Ph_V_3	85.26	0.38	**2Z_Sp_V_3**	45.20	0.89
1B_Sp_Un_1	84.65	0.38	**1G_Sc_Un_1**	68.40	0.98
1B_Sp_Un_2	87.40	0.39	**1G_Sc_Un_2**	59.25	1.02
1B_Sp_Un_3	83.74	0.30	**1G_Sc_Un_3**	64.55	1.07
2B_Sp_V_1	88.83	0.27	**3G_Sc_SV_1**	100.65	0.82
2B_Sp_V_2	86.98	0.25	**3G_Sc_SV_2**	62.78	1.14
2B_Sp_V_3	86.50	0.34	**3G_Sc_SV_3**	80.90	0.92
1H_Sp_Un_1	23.78	1.22	**4G_Sc_DV_1**	24.80	1.89
1H_Sp_Un_2	56.18	1.03	**4G_Sc_DV_2**	25.64	1.76
1H_Sp_Un_3			**4G_Sc_DV_3**	66.40	1.44
2H_Sp_V_1	105.22	1.17	**2D_Ph_V_1**	113.07	1.10
2H_Sp_V_2	63.27	1.51	**2D_Ph_V_2**	107.07	1.12
2H_Sp_V_3	94.59	1.55	**2D_Ph_V_3**	105.27	2.03
1H_Sp_Un_1	129.76	0.19			
1H_Sp_Un_2	129.06	0.17			
1H_Sp_Un_3	134.23	0.27			

3.3 Erosion rates of sediment cores

3.3.1 Collected erosion data

The relative sediment volume due to erosion was calculated by dividing the cumulative erosion volume calculated in each time step by the total sediment volume (1920 cm^3) considered during the image analysis technique. The relative sediment volume was calculated for each of the 51 sediment cores. Example graphs of the relative sediment volume eroded of sediment cores collected from Rilland Bath are given in Figure 24.

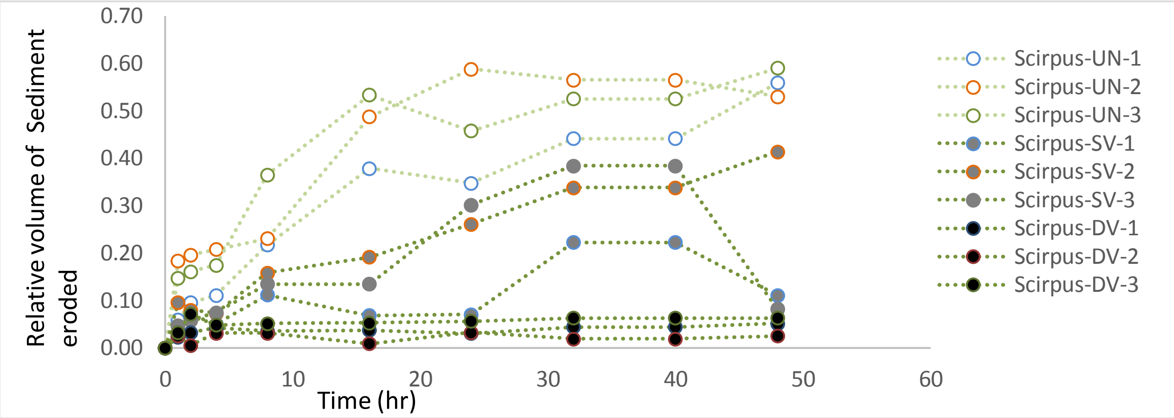

Figure 24: Relative sediment volume eroded for 9 sediment cores from the study site at Rilland Bath, which is very brackish water dominated area (DV=densely vegetated zone; SV= sparsely vegetated zone; UN=mudflat zone). Three replicates were taken at each site (numbered 1, 2, 3).

The amount of the relative eroded sediment volume of the sediment cores taken from the mudflat, sparsely vegetated and densely vegetated zones varies significantly. The higher volume loss was obtained for the 3 replicates collected from the mudflat zone, whereas the lower erosion volumes were found for the 3 replicates taken from the densely vegetated zone (Figure 24).

Erosion rate (cm^3/s) for all the time steps was obtained for the cumulative sediment volume in every time step divided by the time step to get an idea about the actual rate of erosion from the sediment cores. The calculated erosion rates for the 9 sediment cores of *Scirpus maritimus* species collected from Rilland Bath are given in Figure 25.

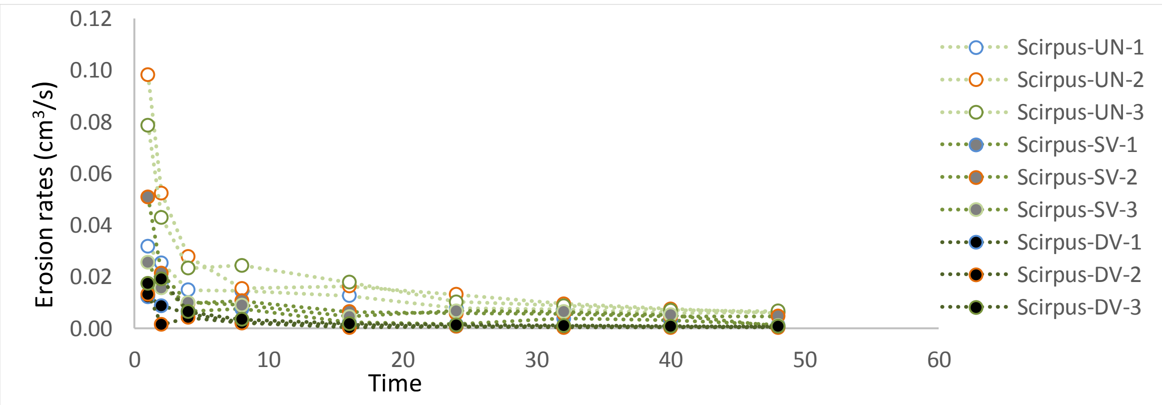

Figure 25: Erosion rates of 9 sediment cores collected from Rilland Bath (black marker=sediment cores collected from densely vegetated zone, grey marker=sediment cores collected from sparsely vegetated zone, white marker=sediment cores collected from the mudflat zone. In legend, name was selected as vegetation species (Scirpus)-location of sediment cores taken (UN=mudflat, SV=sparse vegetated, DV=Dense vegetated)-replicates number (1, 2, 3)).

Within the same study site, clear differences are noticeable in the erosion rates of the sediment cores collected from three different zones (i.e. mudflat zone, sparsely vegetated zone and densely vegetated zone). All the sediment cores showed highest erosion rates during the first time step (T1=1hr) and gradually decreased towards zero. The erosion rates of the mudflat sediment cores were around 0.08-0.10 cm^3/s after 1 hour of wave action. In this period, the erosion rates of the sediment cores collected from sparsely vegetated zone were around 0.02-0.05 cm^3/s, whereas erosion rates of the sediment cores collected from densely vegetated zone were around 0.01-0.02 cm^3/s.

3.3.2 Comparison of relative sediment volume eroded among study sites

The sediment cores were collected from five field sites covering three salt marsh species with their three different zones (i.e. mudflat zone, sparsely vegetated zone and densely vegetated zone). Same salt marsh species was found in two study sites or more than two sites. For example, *Scirpus maritimus* was found in Rilland Bath and Groot Buitenschoor. *Phragmites australis* was found in Rilland Bath and De Zaag. *Spartina anglica* was found in Rilland Bath, Hellegatpolder and Zuidgors. All these five study sites are different in their influenced water salinity conditions and soil properties. Therefore, it is interesting to know whether the erosion of the sediment cores collected from five study sites are different or not. For this reason, comparisons were drawn for the same vegetation species found in two different sites. The two Figures (Figure 26 and 27) present the relative sediment volume eroded for the sediment cores collected from Rilland Bath and Groot Buitenschoor for the same species '*Scirpus maritimus*'.

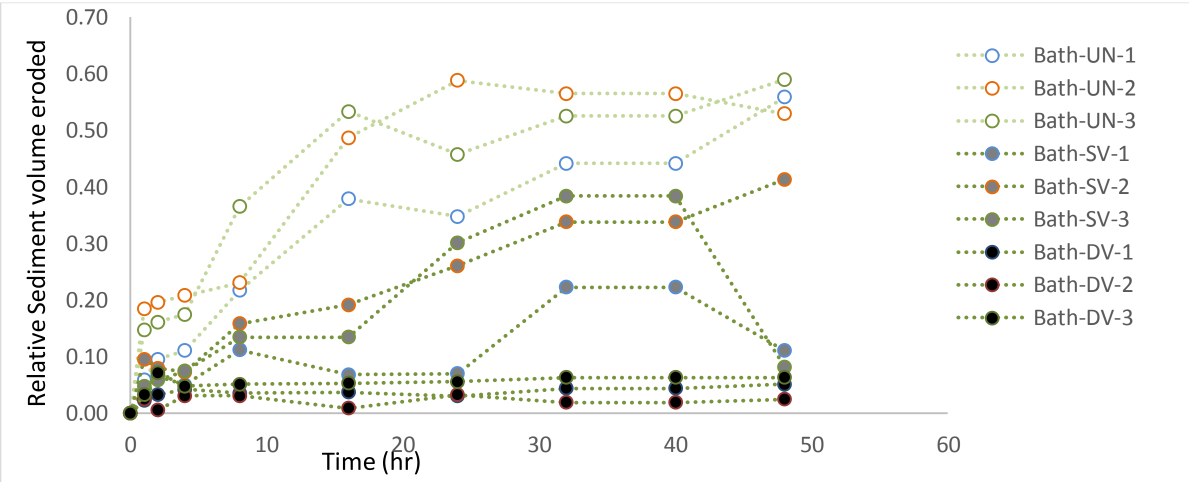

Figure 26: Relative sediment volume eroded for 9 sediment cores of Scirpus maritimus collected from study site Rilland Bath (black marker=sediment cores from densely vegetated zone, grey marker=sediment cores from sparsely vegetated zone, white marker=sediment cores from the mudflat zone; this Figure is same as Figure 24 but shown again for easy comparison with Figure 27).

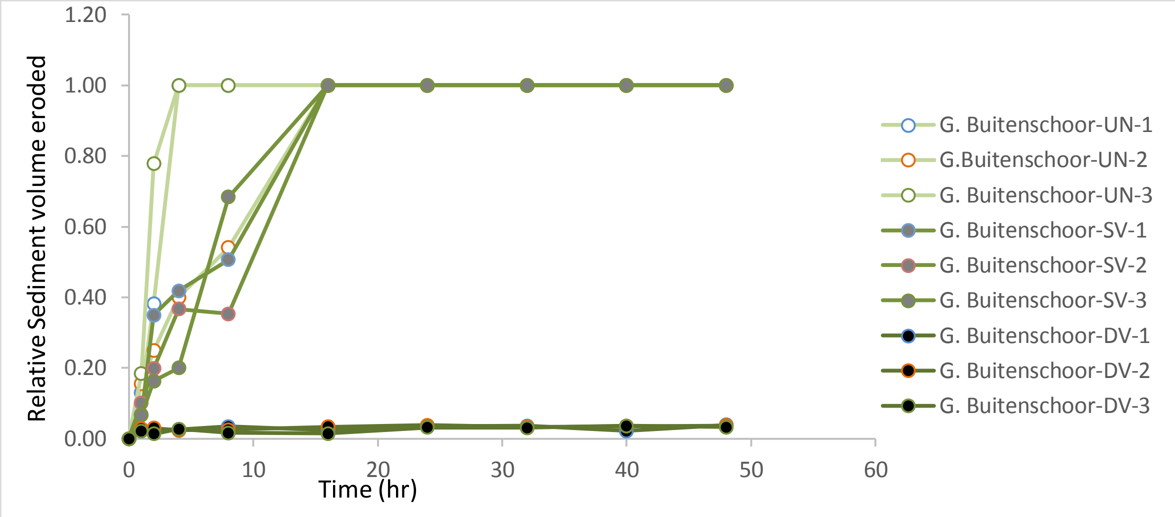

Figure 27: Relative sediment volume eroded for 9 sediment cores of Scirpus maritimus collected from Groot Buitenschoor (black marker=sediment cores collected from densely vegetated zone, grey marker=sediment cores collected from sparsely vegetated zone, white marker=sediment cores collected from the mudflat zone).

Figure 26 and Figure 27 show the difference in relative erosion of the sediment cores collected for the same species, *Scirpus maritimus* from two different study sites, Rilland Bath and Groot Buitenschoor. The relative eroded volumes of the sediment cores collected from the densely vegetated areas for the two study sites was in the same order of magnitude (Figure 26 and 27). Higher relative sediment volume eroded was found for the Groot Buitenschoor mudflat sediment cores than that of Rilland Bath. Therefore, the erodibility of the sediment cores collected from the Groot Buitenschoor was more than the sediment cores collected from the Rilland Bath.

Spartina anglica was found in Hellegatpolder and Rilland Bath. Both Rilland Bath and Hellegatpolder is very brackish water dominated areas. To compare the difference in erodibility between these two study sites for the *Spartina anglica*, Figure 28 and 29 are presented.

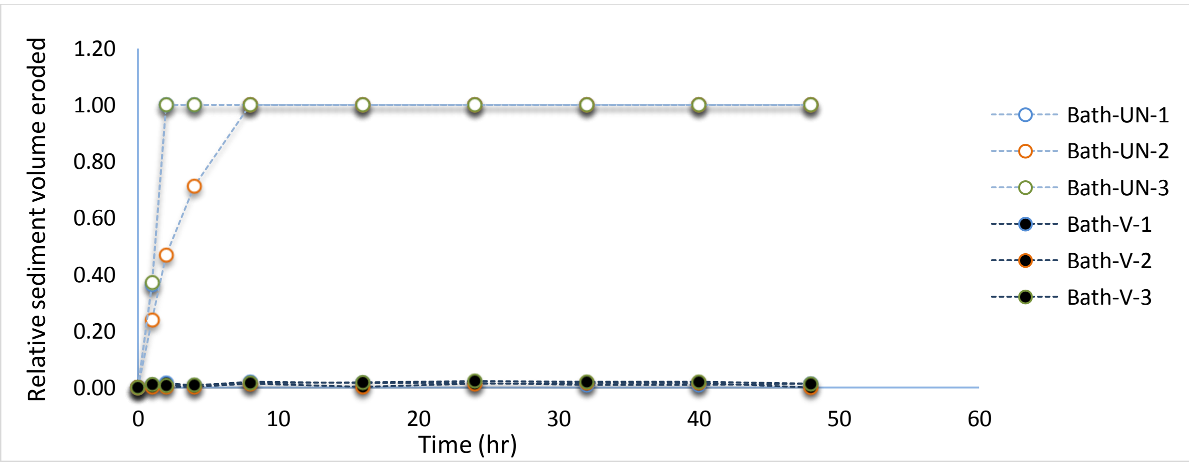

Figure 28 Relative sediment volume eroded of 6 sediment cores of Spartina anglica collected from study site Rilland Bath (black marker=sediment cores from densely vegetated zone, white marker=sediment cores from the mudflat zone. In legend, name was selected as study site (Bath)-location of sediment cores taken (UN=mudflat, V= vegetated)-replicates number (1, 2, 3)).

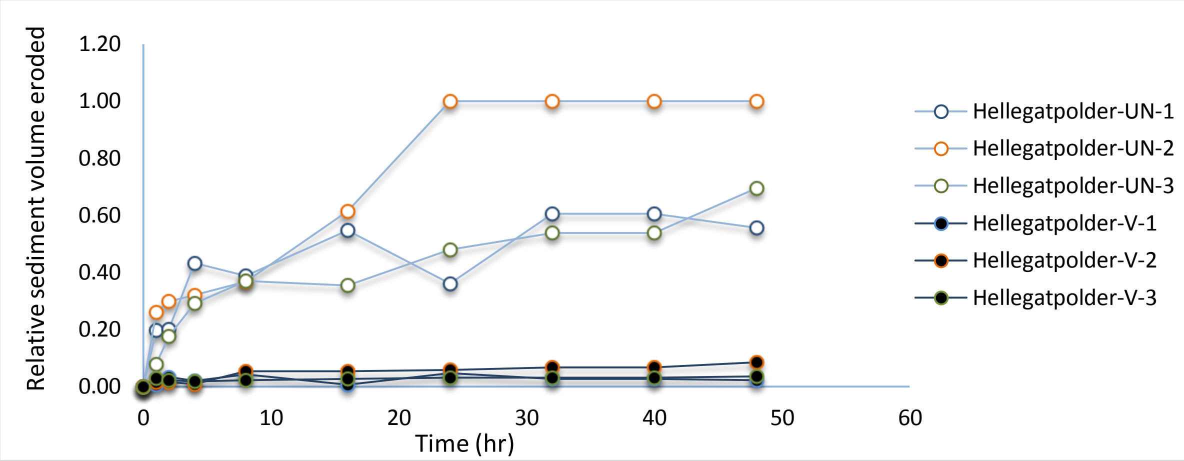

Figure 29: Relative sediment volume eroded of 6 sediment cores of Spartina anglica collected from study site Hellegatpolder with very brackish water dominated area (black marker=sediment cores from densely vegetated zone, white marker=sediment cores from the mudflat zone. In legend, name was selected as study site (Hellegatpolder)-location of sediment cores taken (UN=mudflat zone, V=vegetated zone)-replicates number (1, 2, 3)).

From Figure 28 and 29, it is clear that the relative erosion of the mudflat sediment cores of Rilland Bath was higher than those of Hellegatpolder. The relative erosion of the densely vegetated sediment cores for these two study sites was in the same order of magnitude. The erodibilty of the sediment cores collected from the Rilland Bath was more than those of the Hellegatpolder.

3.3.3 Comparison of relative sediment volume eroded among different species

Comparisons were also made to see whether the relative sediment erosion for the three species are different. The relative erosion of the sediment cores of *Spartina anglica, Scirpus maritimus and Phragmites australis* collected from the Rilland Bath is given in Figure 30.

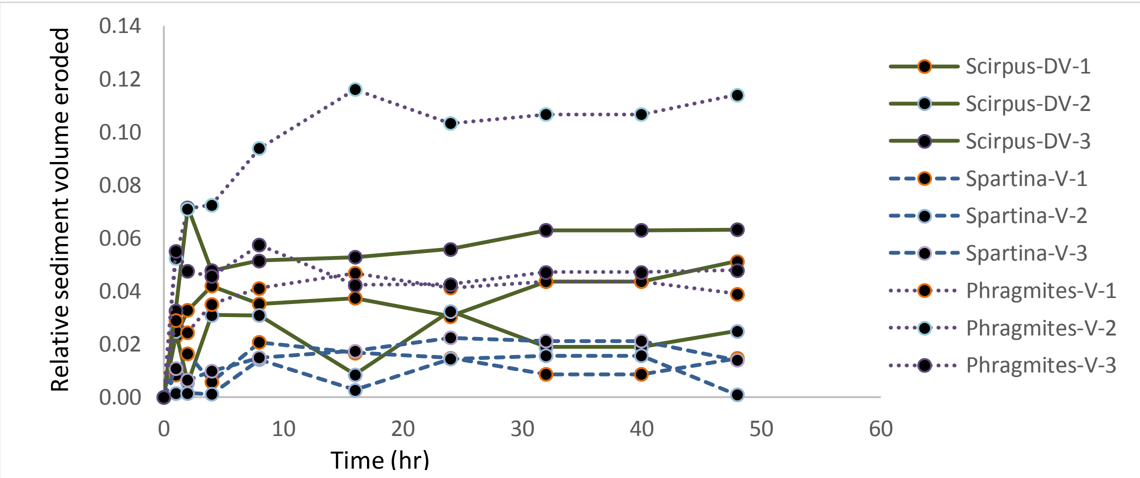

Figure 30: Relative sediment volume eroded of sediment cores for three species collected from Rilland Bath. In legend, name was selected as species names (Spartina/Scirpus/Phragmites)-location of sediment cores taken (V=Marsh zone, DV=densely vegetated)-replicates numbers (1, 2, 3)).

From Figure 30, among the three species, *Spartina anglica* showed less relative sediment erosion than the other two species, whereas this erosion was similar for *Scirpus maritimus* and *Phragmites australis*.

3.3.4 Comparison of relative sediment volume eroded among the mudflat sediment cores collected from different study sites

The estimation of sediment erosion from only the mudflat sediment cores is a good way to understand how the erodibility differs among the study sites with different sediment properties. Because, in this case, no vegetation characteristics are involved. The relative erosion of the mudflat sediment cores collected from four study sites is given in Figure 31.

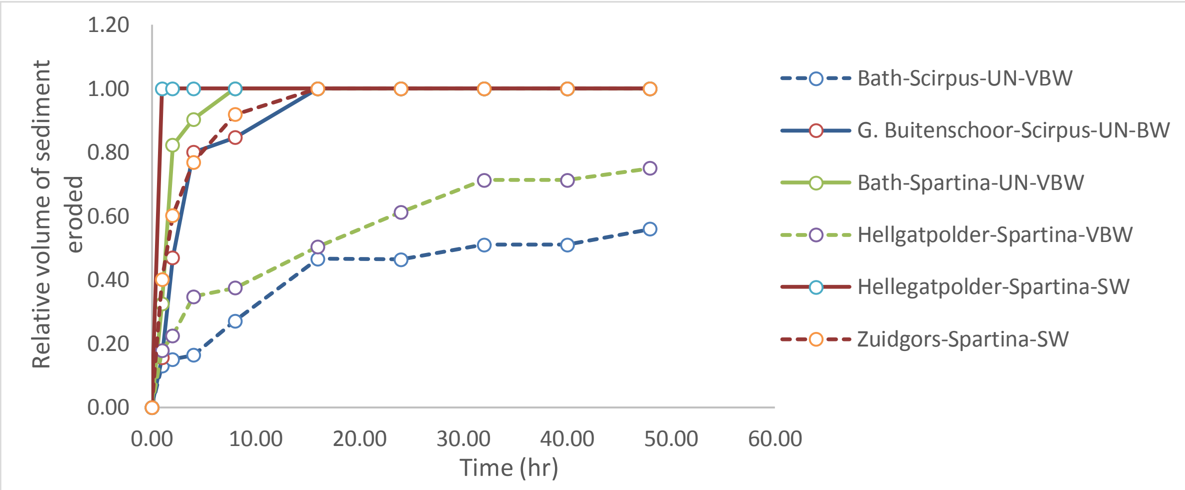

Figure 31: Relative volume of sediment eroded for only the mudflat sediment cores collected from Rilland Bath, Groot Buitenschoor, Hellegatpolder and Zuidgors (in the legend, the name was chosen as sites name (Bath/G. Buitenschoor/Hellegatpolder/Zuidgors)-species name-salinity of water (BW=Brackish water, VBW=Very brackish water, SW=Salt water)).

From Figure 31, higher amount of the relative sediment erosion was found for the mudflat cores collected from Hellegatpolder with salt water dominated area, whereas smaller erosion was found for the mudflat sediment cores of Rilland Bath with very brackish water influenced area. Interestingly, the relative erosion of the mudflat sediment cores collected from Zuidgors and Groot Buitenschoor was in the same order of magnitude.

3.4 Quantifying trends in erosion rates

The erosion process in the wave tank experiments show exponential growth behaviour. At first, the erosion from the sediment cores was large due to the availability of relatively loose sediments. With the passing of time and progressing erosion, the remaining sediments were strongly bonded by adhesive forces between soil particles and root biomass in the sediment cores. Therefore, the same wave energy cannot erode the remaining sediments easily. More wave energy is needed to erode the remaining sediments but in this case, the wave energy is not changing. For this reason, with increasing time, the sediment erosion reduced and this process can be expressed by the exponential function (1) given below:

$$E=M(1-e^{-\varepsilon t}), \qquad (1)$$

Where,
E= relative erosion of sediments from the sediment cores (dimensionless)
ε= erosion rate coefficient (hr^{-1}) further referred to as 'erosion rate'
M=relative maximum amount of sediments that can be eroded if time (t) goes to infinity further referred to as 'erosion maxima' with a maximum value of 1 (all sediments in the cores is eroded).

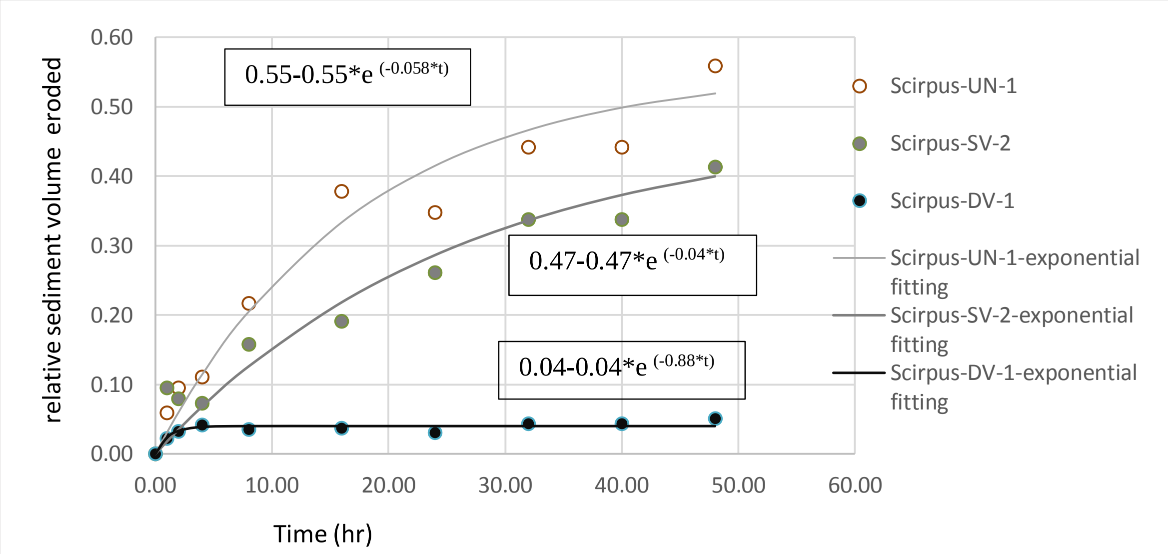

Figure 32: Exponential trend lines fitted to the graphs of relative sediment volume eroded for three sediment cores of Rilland Bath. 'Erosion rates (ε)' and 'erosion maxima' can be found for the fitted trend lines.

The trend line fitting for the erosion of three sediment cores from Rilland Bath is shown in Figure 32. For all 51 sediment cores, exponential trend lines were fitted and the two coefficients were extracted. In this case, erosion maximum and erosion rate are taken as the characteristic coefficients for the exponentially growth behaviour of sediment volumes from all the sediment cores due to wave action. R^2 values are calculated for all the sediment cores with fitted curve. R^2 values obtained for the mudflat sediment cores are very high and remain in range of 0.84-1.0. The sparsely vegetated sediment cores showed R^2 values of range 0.51-0.97, the densely vegetated sediment cores showed R^2 values with range of 0.35-0.93. Therefore, the exponential growth function used in this case gives a very good representative of the observed sediment erosion from the mudflat sediment cores. This exponential fitting is also representative of the observation erosion in case of densely vegetated sediment cores with some small values of R^2. Overall, this exponential function represents the observed erosion behaviour.

The procedure of curve fitting was carried out in excel using an add-in named 'Solver'. First, the value of erosion maximum (M) was assumed by observing the graph. The value of erosion rate (ε) was obtained by fitting simple exponential function in the existing graph. Using these two values in the equation (1), relative sediment eroded values were calculated for every time step. After that, root mean square error was calculated using the original relative sediment eroded values and the new sediment eroded values obtained using equation (1). In the 'Solver' program, this root mean square error was set to minimise by optimizing erosion maximum (M) and erosion rate (ε). When the program was run, erosion maximum (M) and erosion rate (ε) were optimized and subsequently the relative sediment eroded values were calculated by optimized values of erosion maximum and erosion rate. Finally, R^2 value was calculated using the original relative sediment eroded values and newly obtained relative sediment eroded values. This procedure was carried out for all the sediment cores.

3.5 Correlating erosion rates with salt marsh properties

All resulting erosion rates, erosion maxima and vegetation and sediment characteristics are summarized in Table 6.

Table 6: Result matrix including erosion rates (ε) and erosion maxima, all the vegetation characteristics (i.e. dry aboveground biomass, dry belowground biomass, stem density) and sediment characteristics (i.e. D_{50} and organic carbon averaged over two layers (Name of the sediment samples was chosen as location (1=mudflat/unvegetated, 2=vegetated, 3=sparse vegetated, 4=dense vegetated)-Study sites (B=Bath, H=Hellegatpolder, Z=Zuidgors, G=Groot Buitenschoor, D=De Zaag)-Vegetation species (Sc=Scirpus maritimus, Sp=Spartina anglica, Ph=Phragmites australis)-Characteristics vegetation (Un=unvegetated, SV=Sparse vegetated, DV=Dense vegetated, V=Vegetated)-number of replicates (1, 2, 3)).

Name of the sediment cores	Erosion rates (hr^{-1})	Erosion maxima (b) (-)	Dry belowground biomass (g/m^2)	Dry aboveground biomass (g/m^2)	Stem density ($stem/m^2$)	Average sediment sizes of two layers (D_{50}) (µm)	Org C. Average of two layers (%)
1B_Sc_Un_1	0.05	0.55				57.30	1.47
1B_Sc_Un_2	0.11	0.57				56.48	1.72
1B_Sc_Un_3	0.14	0.55				54.46	1.78
3B_Sc_SV_1	0.16	0.13	4627.80	114.73	313	58.50	1.10
3B_Sc_SV_2	0.04	0.47	2730.99	117.23	188	105.47	0.25
3B_Sc_SV_3	0.12	0.24	1653.94		63	96.45	0.28
4B_Sc_DV_1	0.88	0.04	9969.88	320.36	1442	77.60	0.45
4B_Sc_DV_2	11.63	0.02	6338.23	431.32	1755	77.97	0.32
4B_Sc_DV_3	1.30	0.06	8033.33	376.78	1066	77.30	0.56
2B_Ph_V_1	0.68	0.04	4789.18	3794.75	878	88.74	0.24
2B_Ph_V_2	0.48	0.11	5633.87	2782.27	1254	83.68	0.27
2B_Ph_V_3	11.32	0.05	5125.25	2530.25	752	85.26	0.38
1B_Sp_Un_1	0.78	1.02				84.65	0.38
1B_Sp_Un_2	0.31	1.01				87.40	0.39
1B_Sp_Un_3	0.79	1.02				83.74	0.30
2B_Sp_V_1	1.22	0.01	18859.01		2758	88.83	0.27
2B_Sp_V_2	0.19	0.01	10597.77	162.37	3260	86.98	0.25
2B_Sp_V_3	0.25	0.02	13156.34		2570	86.50	0.34
1H_Sp_Un_1	0.34	0.50				23.78	1.22
1H_Sp_Un_2	0.07	1.07				56.18	1.03
1H_Sp_Un_3	0.11	0.58					
2H_Sp_V_1	0.73	0.03	2399.96	808.10	2382	105.22	1.17
2H_Sp_V_2	0.08	0.08	1381.37	672.69	2194	63.27	1.51
2H_Sp_V_3	14.97	0.03	4741.76	628.80	2006	94.59	1.55
1H_Sp_Un_1	6.40	1.00				129.76	0.19
1H_Sp_Un_2	6.40	1.00				129.06	0.17
1H_Sp_Un_3	6.40	1.00				134.23	0.27

Rest of table 6:

Name of the sediment cores	Erosion rates (ε) (hr^{-1})	Erosion maxima (b) (-)	Dry belowground biomass (g/m^2)	Dry aboveground biomass (g/m^2)	Stem density ($stem/m^2$)	Average sediment sizes of two layers (D_{50}) (µm)	Org C. Average of two layers (%)
3H_Sp_SV_1	1.02	0.17	3340.77	488.37	1881	127.23	0.35
3H_Sp_SV_2	0.51	0.17	2622.02		1066	113.47	0.31
3H_Sp_SV_3	1.73	0.13	2621.50		1003	105.08	0.48
4H_Sp_DV_1	0.22	0.03	5009.72	944.14	2382	111.24	0.32
4H_Sp_DV_2	0.27	0.02	6835.46	707.79	1881	114.13	0.28
4H_Sp_DV_3	7.30	0.02	6429.47	654.50	2132	109.03	0.33
1Z_Sp_Un_1	0.92	1.01				57.94	0.69
1Z_Sp_Un_2	0.35	0.98				58.89	0.86
1Z_Sp_Un_3	0.25	1.01				46.34	0.73
2Z_Sp_V_1	1.39	0.01	11629.57	977.37	2006	64.06	0.72
2Z_Sp_V_2	0.40	0.02	8173.56	880.82	2696	46.91	0.98
2Z_Sp_V_3	2.33	0.01	5722.20	677.70	2633	45.20	0.89
1G_Sc_Un_1	0.35	1.02				68.40	0.98
1G_Sc_Un_2	0.12	1.03				59.25	1.02
1G_Sc_Un_3	0.52	1.02				64.55	1.07
3G_Sc_SV_1	0.13	1.03	1408.06	516.58	251	100.65	0.82
3G_Sc_SV_2	0.10	1.06	2085.14	505.92	125	62.78	1.14
3G_Sc_SV_3	0.11	1.05	2950.91	779.89	313	80.90	0.92
4G_Sc_DV_1	1.05	0.03	7939.16	687.10	752	24.80	1.89
4G_Sc_DV_2	1.88	0.03	6525.40	541.66	376	25.64	1.76
4G_Sc_DV_3	0.72	0.03	5785.99	962.95	564	66.40	1.44
2D_Ph_V_1	17.59	0.02	13965.35	3054.98	752	113.07	1.10
2D_Ph_V_2	3.38	0.02	10042.46	3121.43	878	107.07	1.12
2D_Ph_V_3	0.41	0.06	6098.39	1596.77	439	105.27	2.03

Erosion maximum and erosion rate showed different values for the sediment cores collected from five field sites, three vegetation species and zones (i.e. mudflat zone, sparsely vegetated zone and densely vegetated zone) from the same study site. Five field sites are different in their vegetation characteristics and sediment properties from each other. Therefore, to find the relation between the erodibility of the sediment cores and the vegetation characteristics or sediment properties, erodibility coefficients are plotted against these vegetation characteristics and sediment properties separately. The vegetation characteristics were stem density, dry aboveground biomass and dry belowground biomass. The sediment properties were median grain sizes and organic carbon content. In the following section, the dependency of the erosion maxima and erosion rates with all the vegetation characteristics and sediment parameters are presented.

3.5.1 Correlating erosion properties to the belowground biomass

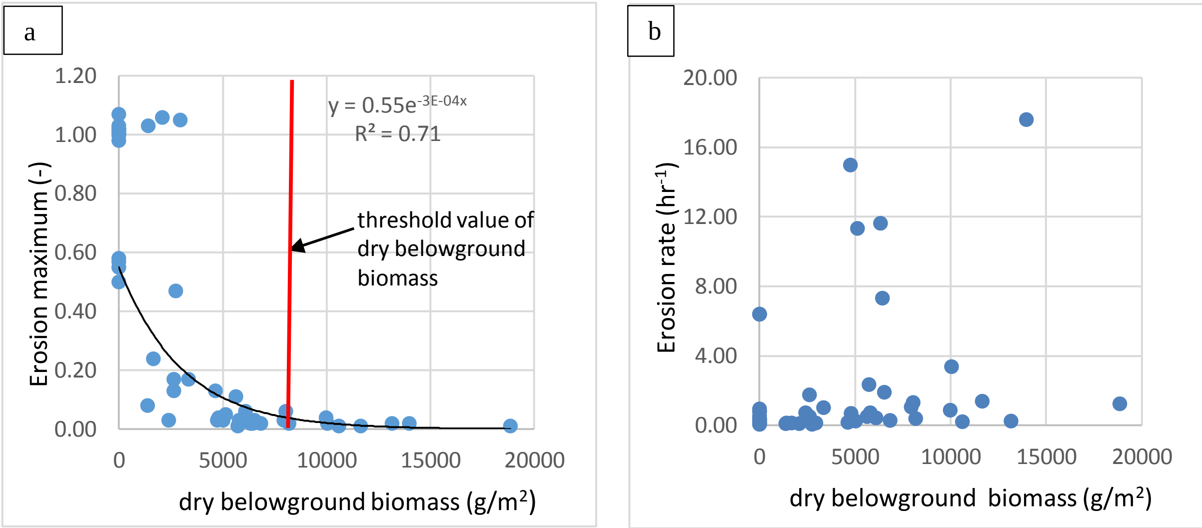

Figure 33: Relation of dry belowground biomass (g/m²) with (a) erosion maximum, in the Figure the red line represents the threshold values of dry belowground biomass (b) erosion rate.

Figure 33 shows the relation of erosion maxima (Figure 33a) and erosion rates (Figure 33b) with the dry belowground biomass for all the collected sediment cores. Once exceeding a certain value of the dry belowground biomass (around 8000 g/m^2), the erosion of the sediments was not so negligible and below this amount the erosion rapidly increased. This value was taken as the threshold amount of dry belowground biomass that prevents the soil from erosion (Figure 33a). An exponential relation was found between the dry belowground biomass and the erosion maxima with an R^2-value of 0.71. According to this relation, if the amount of dry belowground biomass increases, the maximum amount of sediments that can be eroded will decrease. No clear pattern was visible between the erosion rates (*ε)* and dry belowground biomass (Figure 33b).

3.5.2 Correlating erosion properties with aboveground biomass

To find out the relation between the erosion maxima or erosion rates with dry aboveground biomass, Figure 34a and 34b can be obtained.

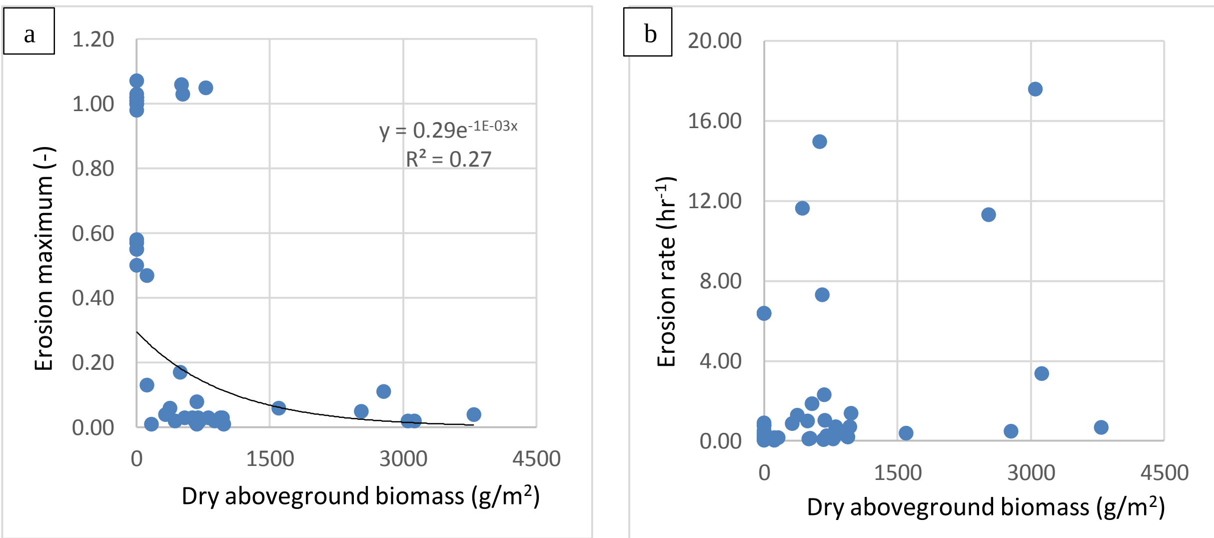

Figure 34: Relation of dry above ground biomass (g/m²) with (a) Erosion maximum, (b) erosion rate.

From Figure 34a, an exponential relation was found between the erosion maxima and dry aboveground biomass such that the erosion maxima reduces exponentially due to increase of the aboveground biomass. The R^2 value is 0.27, which means obtained relation between them was not so strong. Again, the erosion rates did not show any clear relation with dry aboveground biomass (Figure 34 b).

3.5.3 Correlating erosion properties with stem density

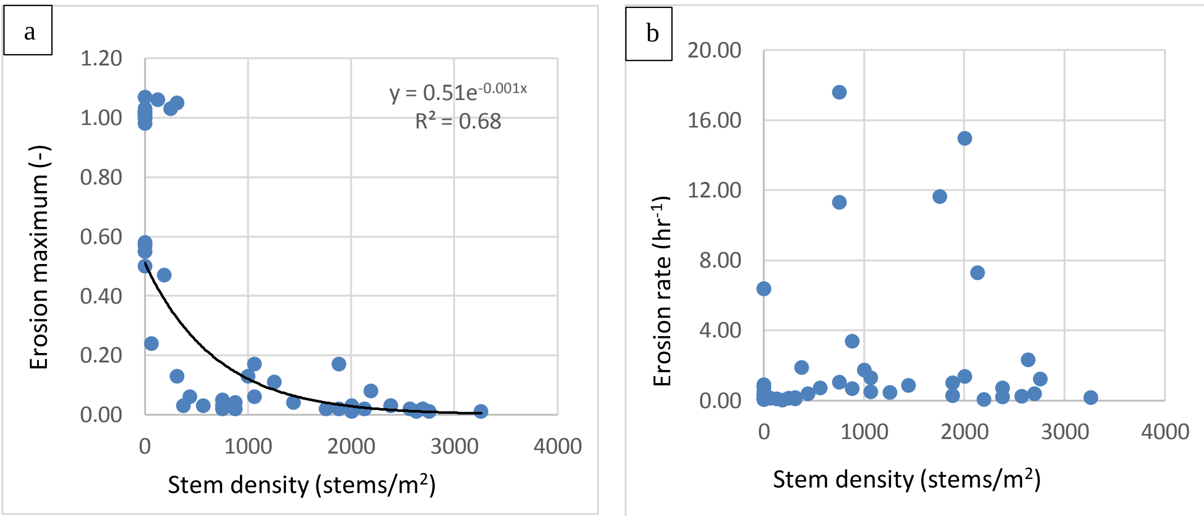

Figure 35: Relation of the stem density with (a) erosion maximum (b) erosion rates.

Figure 35a and 35b present the relation between the erosion maxima and erosion rates with stem density. Similar type of exponential relation existed between the stem density (stems/m^2) and erosion maxima as found in previous two cases. The value of R^2 is 0.68, indicates this exponential relation is a good representative of the underlying relation between the erosion maxima and stem density. No clear pattern was obvious between erosion rates and the stem density (Figure 35b).

3.5.4 Correlating erosion properties with median grain sizes

To determine whether the sediment gain sizes influence the erosion of the sediment cores from five field sites, erosion maxima and erosion rates are presented against the sediment grain sizes. The obtained graphs are shown in Figure 36.

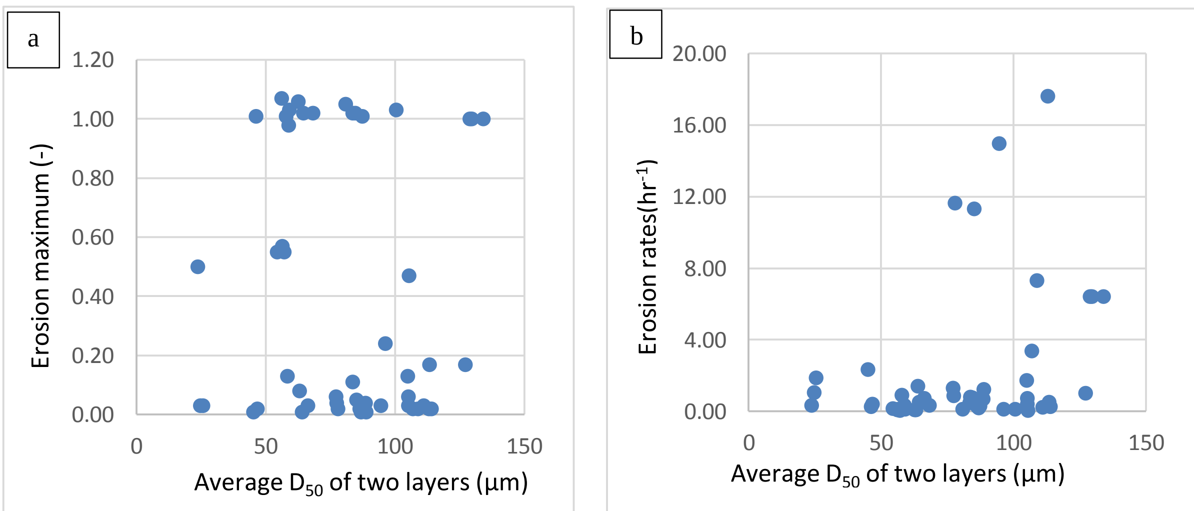

Figure 36: Relation of average D_{50} of the sediments with (a) Erosion maximum (b) erosion rate.

From Figure 36a, no clear relation was obtained between erosion maxima and erosion rates and median grain size averaged over two layers.

3.5.5 Correlating erosion properties with organic carbon content

Another sediment properties, organic carbon content was also correlated with the erodibility quantifying coefficients, erosion maxima and erosion rates. The obtained graphs are shown in Figure 37a and 37b.

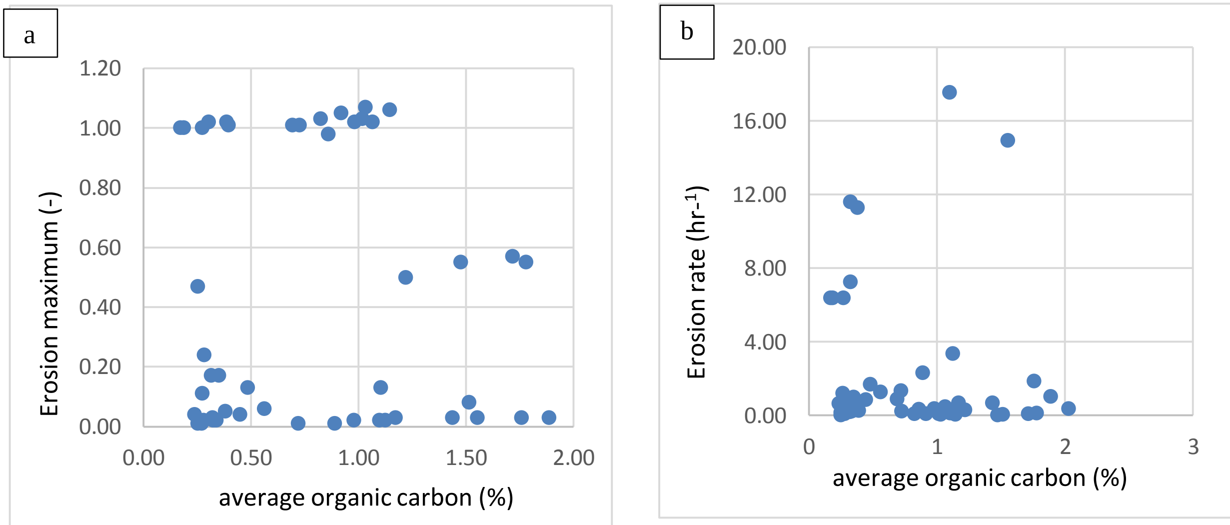

Figure 37: Relation of average organic carbon content with (a) Erosion maximum (b) erosion rate.

From Figure 37a, and 37b, no clear pattern was obtained between the erosion maxima or erosion rates with organic carbon content averaged over two layers.

3.5.6 Correlating erosion properties of mudflat sediment cores with median grain sizes

Sediment gain sizes and organic carbon content are different for the five study sites. To see the difference in erodibilty of the five study sites for differing the sediment properties, only mudflat sediment cores were considered. In Figure 38, erosion rates are presented against the average sediment sizes (D_{50}) for only the mudflat sediment cores.

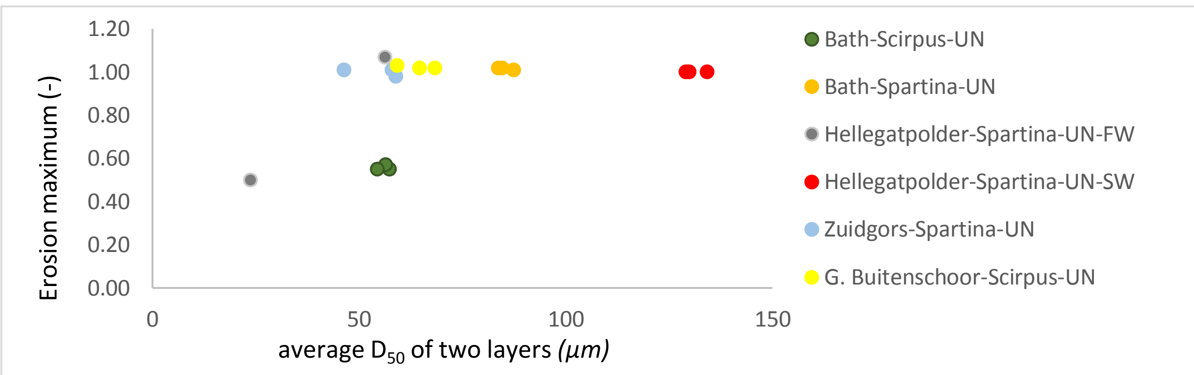

Figure 38: Relation between average D_{50} (µm) of mudflat sediment cores and erosion maximum. (Legend was taken as study sites-species-UN (mudflat). For Hellegatpolder, two types of water condition exist, FW= fresh water influenced area, SW=Salt water influenced area).

From Figure 38, threshold value was found for D_{50}, means if the median grain sizes exceeds 50 µm, then the mudflat sediment cores eroded completely except for the study site Rilland Bath with *Scirpus maritimus* dominated area.

To see how the erosion rate behaves with average median grain sizes over two layers, erosion rate is presented against the average D_{50} (Figure 39) collected for only mudflat sediment cores.

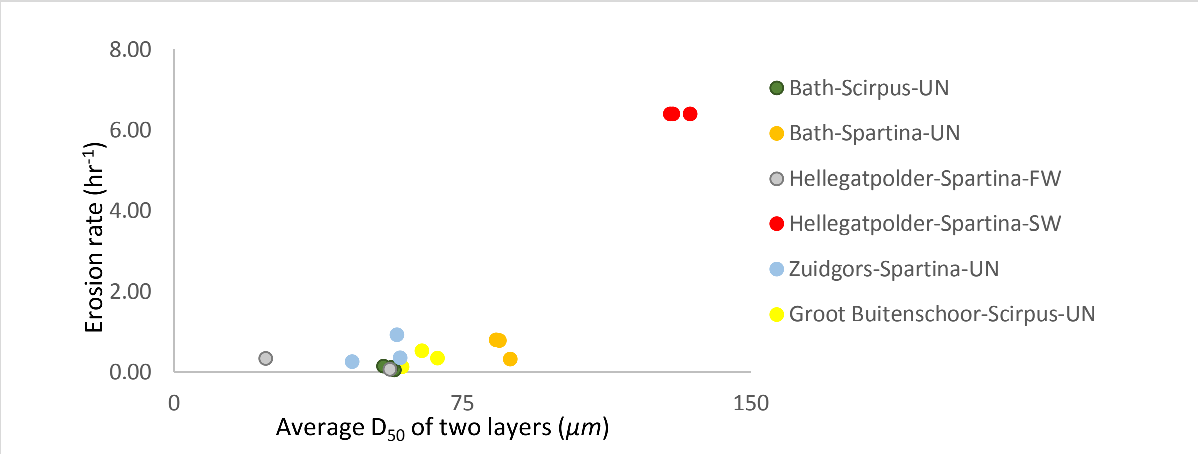

Figure 39: Relation between average D_{50} (µm) of mudflat sediment cores and erosion rate (hr^{-1}) (Legend was taken as study sites-species-UN (mudflat). For Hellegatpolder, two types of water condition exist, FW= fresh water influenced area, SW=Salt water influenced area.

A clear pattern is visible from the graph of erosion rates and median grain sizes. The larger the grain sizes, the higher the erosion rates observed in case of mudflat replicates. Linear trend line was fitted in the graph of figure 43a. Maximum erosion rates were found for the sediment cores taken from the salt water dominated area of Hellegatpolder, whereas minimum erosion rates occurred for the mudflat sediment cores taken from study site Rilland Bath.

3.5.7 Correlating of erosion properties of mudflat sediment cores with organic carbon content

The correlation between the erosion maxima and organic carbon content is shown in Figure 40.

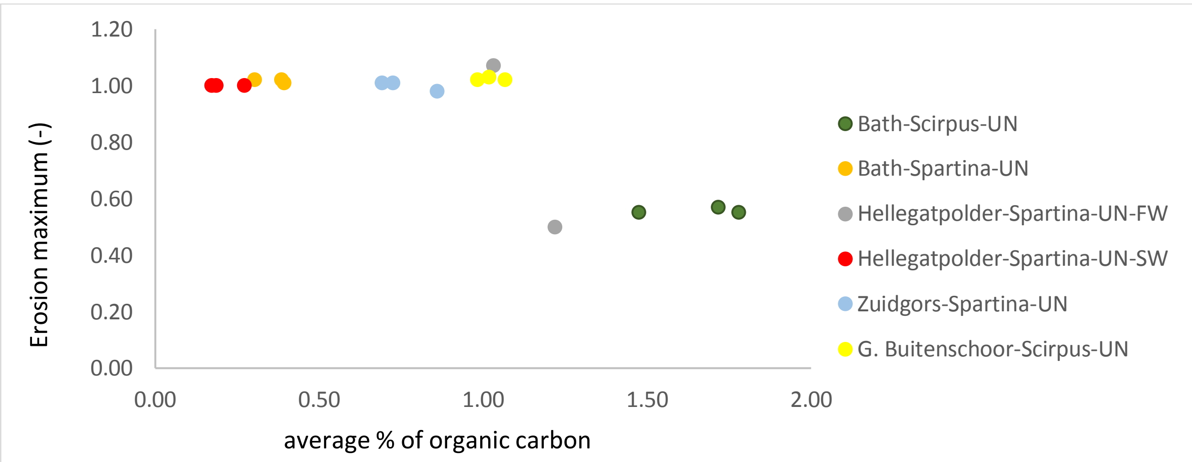

Figure 40: Relation between average organic carbon content (%) of mudflat sediment cores and erosion maximum. (Legend was taken as study sites-species-UN (mudflat). For Hellegatpolder, two types of water condition exist, FW= fresh water influenced area, SW=Salt water influenced area).

From Figure 40, a threshold value was found for organic carbon content. Below and around the value of 1.00 of the organic carbon content (%), the erosion maximum was highest.

Organic carbon content are presented against the erosion rate to see how the organic carbon content correlated with erosion rates (Figure 41)

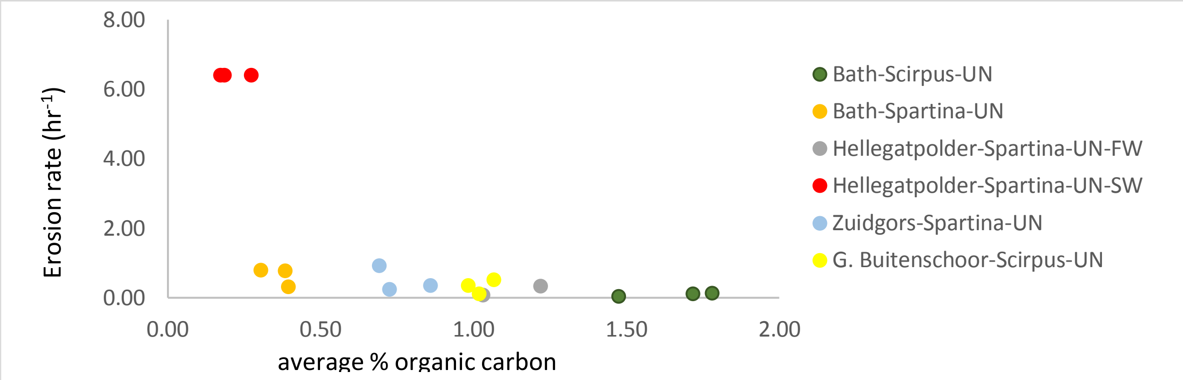

Figure 41: Relation between average organic carbon (%) of mudflat sediment cores and erosion rate (hr^{-1}). (Legend was taken as study site name-species (Scirpus/Spartina)-UN (mudflat). For Hellegatpolder, FW=cores taken from fresh water dominated area, SW= cores taken from salt water dominated area.

From Figure 41, erosion rates decrease with the increase of organic carbon content. Smaller amounts of organic carbon were related with higher erosion rates in case of sediment samples collected from Hellegatpolder with salt water dominated area (Figure 41). Larger amount of organic carbon content was related to smaller erosion rates of mudflat sediment samples taken from Rilland Bath in front of *Scirpus maritimus* dominated area. Linear trend line fitting of this graph was shown in Figure 43b.

3.6 Summary of all correlations

To summarize, the relations between erosion maxima and all the vegetation characteristics (i.e. dry aboveground biomass, dry belowground biomass, and stem density) and sediment properties (i.e. D_{50} and organic carbon content) for all sediment cores, only vegetated sediment cores and only mudflat sediment cores are given in Figure 42.

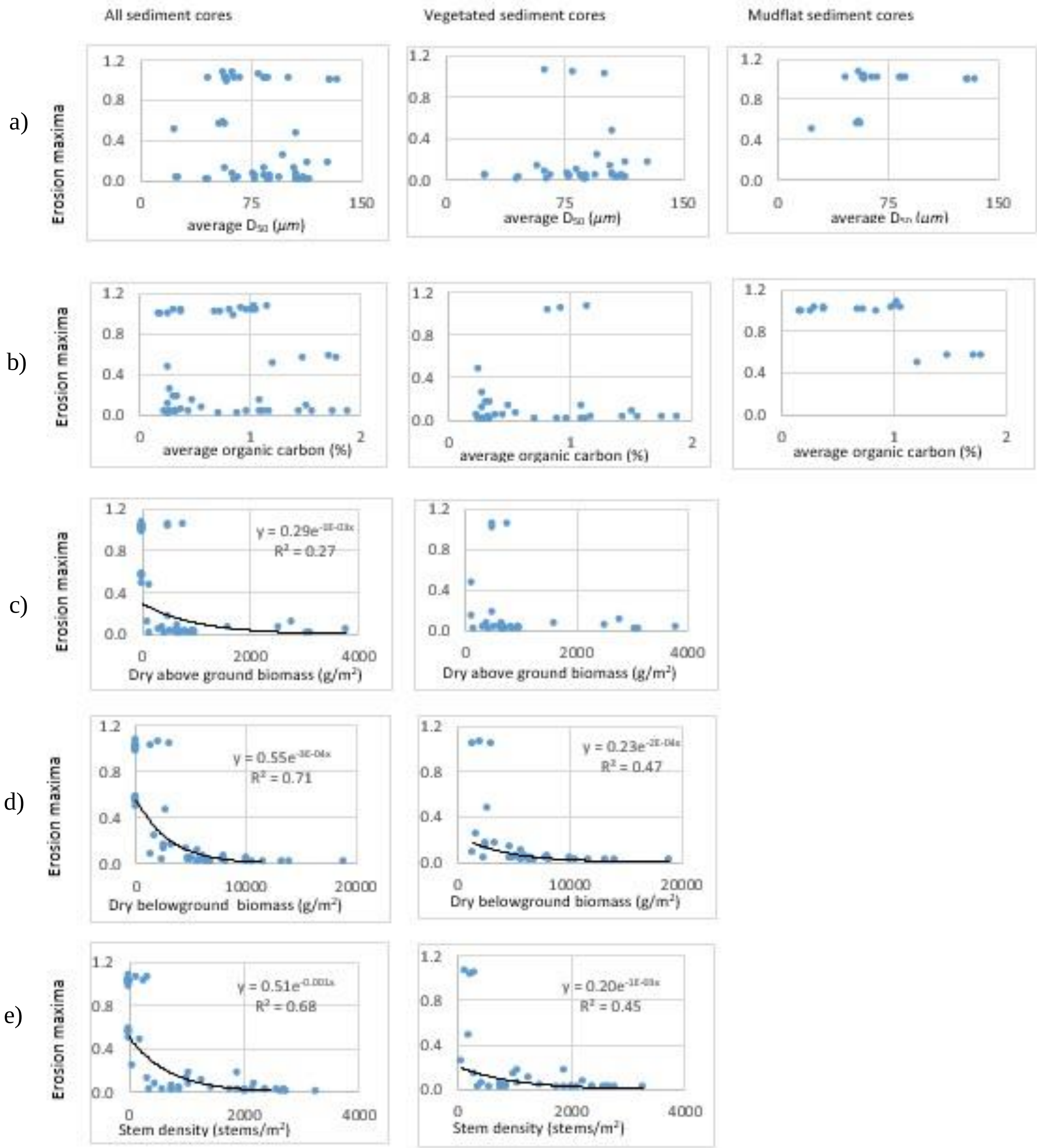

Figure 42: (a) Relation between average D_{50} and erosion maxima for all sediment cores, only vegetated sediment cores, only mudflat sediment cores, (b) Relation between erosion maxima and organic carbon content for all sediment cores, only vegetated sediment cores, only mudflat sediment cores, (c) Relation of above ground biomass with erosion maxima for all sediment cores, only vegetated sediment cores and only mudflat sediment cores, (d) Relation between amount of belowground biomass and erosion maxima of all sediment cores, only vegetated sediment cores and mudflat sediment cores, (e) Relation between erosion maxima and stem density for all sediment cores, only vegetated sediment cores and only mudflat sediment cores.

For all the sediment cores, dry belowground biomass (R^2=0.71, $P<0.05$) and stem density (R^2=0.68, $P<0.05$) showed the best relation with erosion maxima. No significant relation could be found between the erosion maxima with D_{50} or organic carbon content considering sediment cores all together. In case of only vegetated cores, both dry belowground biomass and stem density showed exponential relation with erosion maxima with R^2 value 0.47 ($P<0.05$) and 0.45 ($P<0.05$) respectively. For mudflat sediment cores, the organic carbon content and D_{50} values showed threshold values, with 50 µm for the D_{50} and 1% for the organic carbon content.

Correlation coefficients and P values were calculated between the erosion maxima and all the vegetation characteristics and sediment properties for three cases separately (i.e. all sediment cores, only vegetated sediment cores, only mudflat sediment cores). The calculated correlation coefficients and P values are summarized in table 7. Stem density and dry belowground biomass showed higher negative correlation values with 0.73 and 0.72 respectively in case of taking all the sediment cores. For the mudflat sediment cores, the correlation coefficients of organic carbon content was higher with a value of 0.72. D_{50} gave a positive correlation coefficient of 0.46.

Table 7: Correlation coefficients and P values calculated between the erosion maxima and dry aboveground biomass, dry belowground biomass, stem density, D_{50} and organic carbon content for all the sediment cores together, only vegetated sediment cores and only mudflat sediment cores.

	Correlation coefficient			**P value**		
Correlation analysis with erosion maxima and vegetation characteristics and sediment properties given below	All sediment cores	Only vegetated sediment cores	Only mudflat sediment cores	All sediment cores	Only vegetated sediment cores	Only mudflat sediment cores
Dry aboveground biomass (g/m²)	-0.48	-0.2		0.000315	0.24	
Dry belowground biomass (g/m²)	-0.72	-0.45		0	0.007	
Stem density (g/m²)	-0.73	-0.5		0	0.002	
D_{50} (µm)	-0.066	0.03	0.46	0.64	0.82	0.05
Organic carbon content (%)	-0.054	0.02	-0.72	0.7	0.89	0.0066

To know the relation between erosion rates and all the vegetation characteristics and sediment properties, erosion rates with vegetation characteristics and sediment properties for all the sediment cores together, only vegetated sediment cores and only mudflat sediment cores are presented in Figure 43.

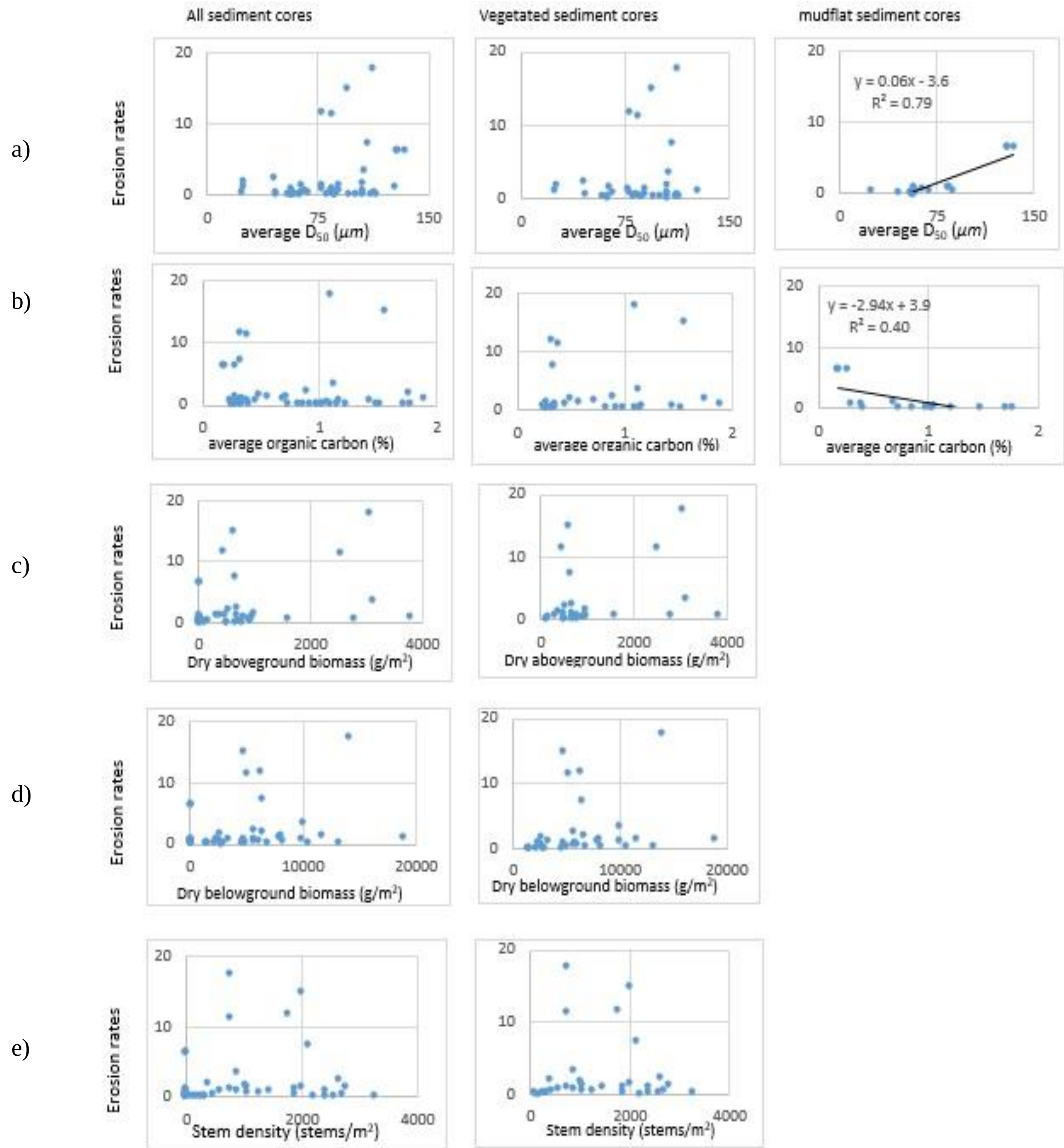

Figure 43: (a) Relation between average D_{50} and erosion rates for all sediment cores, only vegetated sediment cores, only mudflat sediment cores, (b) Relation between erosion rates and organic carbon content for all sediment cores, only vegetated sediment cores, only mudflat sediment cores, (c) Relation of above ground biomass with erosion rates for all sediment cores, only vegetated sediment cores and only mudflat sediment cores, (d) Relation between amount of belowground biomass and erosion rates of all sediment cores, only vegetated sediment cores and mudflat sediment cores, (e) Relation between erosion rates and stem density for all sediment cores, only vegetated sediment cores and only mudflat sediment cores.

From Figure 43, considering all sediment cores together, the erosion rates did not show any relation with any of the vegetation characteristics (i.e. dry aboveground biomass, dry belowground biomass and stem density) or sediment properties (i.e. D_{50} and organic carbon content). For only vegetated sediment cores, no relation was found for any of the sediment or vegetation characteristics. While considering only mudflat sediment cores, the

D_{50} showed the best predictor of the linearly varying erosion rates with R^2 value 0.79 ($P<0.05$). In this case, organic carbon content also showed linear decreasing relation with erosion rates ($R^2=0.40$, $P<0.05$).

Correlation coefficients and P values were calculated between the erosion rates and all the vegetation characteristics and sediment properties for three cases separately (i.e. all sediment cores, only vegetated sediment cores, only mudflat sediment cores). The calculated correlation coefficients and P values are given in table 8. Taking all the sediment cores and the vegetation sediment cores, none of the vegetated and sediment properties gave higher correlation values. However, D_{50} gave higher correlation coefficient in case of the mudflat sediment cores. The correlation coefficient calculated for the organic carbon content was 0.64.

Table 8: Correlation coefficients and P values calculated between the erosion rates and dry aboveground biomass, dry belowground biomass, stem density, D_{50} and organic carbon content for all the sediment cores together, only vegetated sediment cores and only mudflat sediment cores.

	Correlation coefficient			**P value**		
Correlation analysis with erosion rates and vegetation characteristics and sediment properties given below	All sediment cores	Only vegetated sediment cores	Only mudflat sediment cores	All sediment cores	Only vegetated sediment cores	Only mudflat sediment cores
Dry aboveground biomass (g/m²)	0.33	0.29		0.01	0.09	
Dry belowground biomass (g/m²)	0.24	0.2		0.08	0.24	
Stem density (stem/m²)	0.11	0.02		0.42	0.89	
D_{50} (µm)	0.34	0.16	0.89	0.01	0.36	0
Organic carbon content (%)	-0.07	0.07	-0.64	0.6	0.67	0.004

Chapter 4

4. Discussion

In this study, laboratory experiments were performed to quantify the eroded sediment volume from sediment cores, mimicking wave attacks on salt marsh cliffs, considering the vegetation characteristics and sediment properties. In this chapter, the validity of the used method and some propositions about this method will be discussed. Furthermore, the results of this study will be compared to the available results of previous studies.

4.1 Discussion of the methodology

Wave tank experiment

- Hydrodynamic conditions in the wave tank: It is already stated that the hydrodynamic conditions such as wave height, wave frequency and wave energy in the wave tank are important factors to consider during the calculation of the sediment erosion as erosion maximum and rate will change with these parameters. Although rough estimates of these hydrodynamic parameters were carried out, it is necessary to estimate the hydrodynamic conditions correctly. Due to the limited time available of this thesis, the measurement of hydrodynamic conditions was not carried out.
- Wave set-up in the wave tanks: Although the set-up of all the four wave tanks was expected to be similar, there may be some wave set-up effect (different wave conditions from one tank to another), which is not clear at this moment. This wave tank set-up effect will influence the comparative results of eroded sediment volumes found for different sediment cores. This effect was minimised by distributing the three replicates in three different wave tanks.
- Placement of sediment cores in the tank slots: The placed sediment cores started to disperse in the stagnant water before starting the wave action, during the collection of pictures for the initial time step (Figure 44, yellow marked). This erosion of the sediments before starting the wave action may affect the calculation of the sediment erosion volume. However, the rectangular portion counted during the image analysis procedure resolves this problem. The still water depth at the bottom of the wave tank slot was 1 cm. The sediments from the first 1 cm above the bottom will be affected by this dispersion, whereas the rectangular frame of image analysis was taken 2 cm above the bottom of the sediment cores. Therefore, it can be stated that this process has negligible impact on the image analysis and the calculation of the eroded sediments volume.
- Image quality: The use of image analysis techniques for the calculation of the eroded sediment volume required good quality images that are suitable for the 3D image reconstruction. To get the 3D image reconstruction properly, the images should be taken from 40 different angles. In this experiment, there was no fixed predefined design for taking these images. Therefore, it may happen that the taken images in some cases were not from 40 different angles, which may have affected the quality of the reconstructed images and the calculation of the eroded volume for some sediment cores. Fixed predefined design for taking images is required.

Figure 44: Dispersion of sediments in the bottom of the sediment cores in stagnant water before starting of wave actions.

Validation of the data analysis procedure

- The calibration operation was carried out without taking the wave effects into account. Therefore, the sediment volume loss was not due to wave action, instead the sediment was removed manually in different time steps. To know whether this image analysis technique is good enough to represent the eroded sediment amount, it is better to carry out the measurement taking the wave effect. For example, weighing the sediment cores before the wave action and subsequently measuring the weight after some time steps of wave actions. The difference in the weights of the sediment cores at different time steps will represent the sediment weight loss for different sediment cores.
- The presence of roots in the eroded sediment cores may have effect on the calculation of eroded sediment volume. An assumption in this case is, without roots, the calculated eroded volume using this method will give more accurate results than that one with roots. The reason for this, the hanging roots may cause 'shadow effect' in the images and subsequently to the method of the 3D image analysis and underestimate to the eroded sediment volume results.

4.2 Discussion of results

Effect of the presence of plant roots on sediment erosion

The eroded sediment volumes measured in the case of mudflat sediment cores range around 1000-1920 cm^3, which is higher than the range 20-200 cm^3 of the measured eroded sediment volume for the densely vegetated sediment cores. The sediment cores collected from the sparsely vegetated areas show sediment erosion volumes in the range of 300-700 cm^3, except in Groot Buitenschoor (1920 cm^3). The results of the eroded sediment volume is given in table 9-table 14 of appendix B. The main reason for the decrease in the amount of the eroded sediment volume is the presence of the plant roots in the vegetated sediment cores. Correlating results of the belowground biomass and the amount of eroded sediment show that the belowground biomass is negatively correlated with the amount of sediment erosion measured in the experiments.

This finding was compared to the results found in the paper of Feagin et al. (2009). In this paper, the erosion of sediment was quantified as a wet weight loss (g). When exposed to waves in a similar experimental set-up as deployed in this study, no significant difference in the amount of sediment erosion was found between sediment cores with and without plant roots. Feagin et al. (2009) stated that the presence of plants and their roots made no statistically significant difference to the amount of sediment erosion from the sediment cores in the wave flume. Instead, Feagin et al., (2009) concluded that vegetation contributes to soil stability due to its long-term effect on soil properties.

The study carried out by Coops et al. (1996) on the effect of the presence of vegetation in bank erosion due to wave action supports our findings that the presence of vegetation reduces the sediment erosion due to the soil reinforcement.

To compare the order of magnitude of the eroded sediment volumes obtained in the present study and the results found in the paper of Feagin et al. (2009), the cumulative erosion volume (cm^3) was converted to the weight loss (g) by multiplying the erosion volume with the bulk density of the sediments. The bulk density of the sediment samples was calculated during the stage of sample preparation for grain sizes and organic carbon test. The value of the bulk density for the sediment cores is given in table 15 of appendix B. After 48 hours of wave action, the cumulative weight loss of sediments was found to be roughly in a range of 1800-3300 g for the mudflat sediment cores, whereas this range varies between roughly 21-300 g for the sediment cores collected from densely vegetated areas. For the 18 hours period of their flume runs, Feagin et al. (2009) found that sediment losses from both cores with and without plants ranged between 15-20 g. The combined effects of the hydrodynamic conditions, the exposure area of the sediment cores and the duration of wave exposure influence the large difference between these experimental results. The sediment losses in our study after the first 18 hours of wave action were roughly in a range of 1000-1600 g for the mudflat sediment cores (except some mudflat cores that fully eroded within 8 hours of wave action) and roughly in a range of 20-250 g in case of the densely vegetated sediment cores. The hydrodynamic conditions are different in our case with wave heights of 20 cm in front of the sediment cores and a frequency of 5 waves per minute. In between these largest waves, smaller irregular waves were generated due to reflections in the wave tanks. These smaller waves also contributed to the erosion of the sediment cores as well. In the study by Feagin et al. (2009) the significant wave heights was 7.38 cm only upon their impact on the marsh edge. According to the supplementary material found with the Feagin et al. (2009) paper, the frequency is slightly less than 2 Hz. Therefore, the hydrodynamic conditions are important factors for the large numerical difference in results of this experiment from the results of literature of Feagin et al. (2009). Therefore, the results obtained in this experiment could not be compared with the results of Feagin et al. (2009).

It was already stated that the paper of Coops et al. (1996) focused on the effect of the vegetation and sediment properties on the bank erosion. Additional, the hydrodynamic condition used in the study of Coops et al. (1996) was different than ours. Therefore, it was not possible to compare the order of magnitude of the eroded sediments.

Effect of vegetation species on the sediment erosion

Sediment cores were collected from three areas with different dominant vegetation species: *Spartina anglica, Scirpus maritimus* and *Phragmites australis.* The results of the eroded sediment volumes show differences across the various vegetation types. In this case, only the densely vegetated sediment cores for every species was considered. The eroded sediment volume after 48 hours was around 30-40 cm^3 for the *Spatina anglica,* around 60-130 cm^3 for *Scirpus maritimus* and around 60-250 cm^3 for the *Phragmites australis.* Therefore, the vegetation species has significant impact on the reduction of the sediment erosion.

Feagin et al. (2009) compared sediment erosion from two types of vegetation species: *Spartina alterniflora* with extensive roots and *Batis maritima* with weak and brittle root structure and found that the type of vegetation does not significantly reduce the lateral erosion. A possible reason behind the difference in finding with the present study is the difference in wave heights. Wave height in this experiment was 20 cm when impacting to the marsh edge, whereas the wave height found in Feagin et al. (2009) was 7.38 cm impacting the marsh edge.

Therefore, different wave height conditions might have impact on the sediment erosion from the vegetation differently.

The study of Coops et al. (1996) considered the sediment erosion for two types of salt marsh species named '*Scirpus lacustris'* and '*Phragmites australis'* and found that the sediment erosion in case of the presence of *Scirpus lacustris* is more than that of *Phragmites australis*. The possible reason stated in the paper of Coops et al. (1996) was the distribution of roots (i.e. *Phragmites australis* were more finely distributed in the soil than the *Scirpus lacustris*).

Effect of sediment properties on sediment erosion

The available literature, Feagin et al. (2009) showed a correlation between organic matter content and erosion rates (R^2=0.390). In our study, we calculated organic carbon content. Therefore it is not possible to compare our results to the findings of Feagin et al. (2009). Additional, Feagin et al. (2009) found that the bulk density provided the best linear predictor (R^2=0.721) for the observed sediment erosion, whereas in our study, no apparent relationship was found between any of the erosion coefficients and the bulk density (R^2=0.043 for erosion rates and R^2=0.095 for erosion maxima) of all the sediment cores together. Only noticeable relationships among the bulk density and the characterized erosion coefficients were found in case of mudflat sediment cores (R^2=0.386 for erosion rates and R^2=0.414 for erosion maxima). This finding also supports our previous finding that the grain size is an important parameter for the erosion maxima and erosion rates in case of mudflat sediment cores.

Validation of correlation analysis

For this study, the results of the sediment erosion experiments were characterised by using two coefficients: the erosion maximum, which is the maximum amount of sediments that was eroded from the sediment cores if the wave exposure in the wave tank would last infinitely long; and the erosion rate, measures the speed by which the sediment erosion approaches to maximum value (with this rate being the power of an exponential function). These two erosion coefficients were related to the vegetation characteristics and sediment properties in three ways: for all sediment cores together, for the vegetated sediment cores only and for the mudflat sediment cores only. For all the cases, the correlation analysis was done between each of the erosion coefficients and each of all the vegetation and sediment properties separately to show comprehensively the dependency of these erosion coefficients on the vegetation and sediment characteristics.

The function used to fit all the correlating graphs of erosion properties and vegetation characteristics or sediment properties was focused to give higher value of R^2. Taking all the sediment cores together and only vegetated sediment cores, the fitted curve was exponential function for the erosion maximum and vegetation characteristics. In this case, although the fitted function gave higher R^2 but it may possible that the trend line show other maximum values of erosion maximum when the vegetation characteristics values decrease. For the erosion rate graphs of mudflat sediment cores, the linear trend line fitted curve gives good R^2 values without any discussion.

Unfortunately, results on the vegetation cover or the amount of roots were not found for Feagin et al. (2009). The paper was focused more on the soil parameters. Therefore, it may be that the study gave a conclusion without carefully looking or taking the vegetation characteristics (presence of root biomass or number of stems). To draw a conclusion on the effect of both sediment properties and vegetation characteristics, it required to emphasize on both these parameters equally.

Chapter 5

5. Conclusions and recommendations

In this study, the erodibility of salt marsh cliffs has been investigated. The main aim was to quantify the effect of vegetation characteristics and sediment properties on salt marsh cliff erosion. In this chapter, the formulated research questions will be answered briefly. After that, some recommendations on future research will be given.

5.1 Conclusions

1. How do vegetation characteristics and sediment properties vary in salt marsh areas?

Vegetation characteristics such as vegetation species, vegetation density and the amount of aboveground and belowground biomass vary greatly with the salinity of the water at the study sites. For example, *Spartina anglica* species was found in the study sites Hellegatpolder and Zuidgors, both these places are salt water influenced areas. This species can also be found in Rilland Bath, which is very brackish water influenced study site. *Phragmites australis* dominates the study site De Zaag, which is fresh water influenced site (table 9). *Scirpus maritimus* is the common type of species found in the Rilland Bath. Relatively large vegetation densities were found for *Spartina anglica* with a range of 16-52 stems per sediment core. The amount of aboveground biomass was larger of *Phragmites australis* with a range of 25 g-60 g, which has higher stems and longer leaves. Smallest amount of dry aboveground biomass was found for *Scirpus maritimus* (between 1g-15 g), which is a sparsely distributed species. The amount of dry belowground biomass was largest for *Spartina anglica* with a range of 22 g-300 g. Stem density, amount of aboveground and belowground biomass vary largely from the sparsely vegetated areas to densely vegetated areas for the same species.

Table 9: Summary of vegetation characteristics of different study sites (only the densely vegetated cases). For aboveground biomass, Low was taken as 1 g-9 g, medium was 10 g-15 g and high was 16 g-60 g. For stem density, Low was taken as 1-15 stems per sediment core, medium was 16-38 stems per sediment core and high was 39-52 stems per sediment core. For belowground biomass, low was taken as 1 g-60 g, medium was 61-150 g, high was 151-300 g.

Study sites	**Salt water (Zuidgors & Hellegatpolder)**	**Very brackish water (Rilland Bath & Hellegatpolder)**	**Brackish water (Groot Buitenschoor)**	**Fresh water (De Zaag)**
Species	*Spartina anglica*	*Spartina anglica; Scirpus maritimus; Phragmites australis*	*Scirpus maritimus*	*Phragmites australis*
Aboveground biomass	Medium	*Spartina anglica* (low at Rilland Bath; medium at Hellegatpolder); *Scirpus maritimus* (low); *Phragmites australis* (high)	Medium	High
Stem density	High	*Spartina anglica* (medium); *Scirpus maritimus* (medium); *Phragmites australis* (low)	Low	Low
Belowground biomass	High- Zuidgors; Medium- Hellegatpolder	*Spartina anglica* (high-Rilland Bath; Low-Hellegatpolder); *Scirpus maritimus* (medium); *Phragmites australis* (medium)	Medium	High

No clear pattern in median grain sizes (D_{50}) or the organic carbon content can be found for areas where salt marshes are present with differing salinity conditions. However, an interesting relation pattern can be found for both D_{50} and the organic carbon content of mudflat areas influenced by different water salinities. D_{50} values are larger for the sediments of salt water influenced sites except Zuidgors, and they tend to be smaller for the sediments of brackish water influenced areas. The behaviour of the organic carbon content is reversed: a smaller organic carbon content can be found for the sediments of salt water dominated areas except Zuidgors and a larger organic carbon content can be found for the brackish water influenced areas.

Table 10: Sediment properties of salt marshes (only mudflat zones)

Study sites	**Salt water**	**Brackish & very brackish water**
D_{50}	Large	Small
Organic carbon content	Low	High

2. How to assess the cliff erosion of salt marsh substrates in a controlled experimental set-up?

Laboratory experiments are suitable approaches to assess the cliff erosion of salt marshes in a short period of time and under controlled conditions. At first, sediment cores from salt marshes had to be collected from field sites covering a wide range of field conditions. In the laboratory, a wave tank was used in which a cliff-like marsh edge was mimicked. Sediment cores were placed in the openings in the back-wall at the end of the sloping bottom of the tank. Irregular waves were then generated continuously, with significant wave heights of 20 cm and 30 s period impacting on the sediment cores' edges. Hence, erosion occurred at the opening side of the sediment cores. Images were collected at different time steps to quantify the erosion of the sediment cores after 1hrs, 2hrs, 4hrs, 8hrs, 16hrs, 24hrs, 32hrs, 40hrs, and 48 hrs. Forty images were taken of each sediment core at every time step. These images were post-processed by using image processing programs Visual SFM and MeshLab. After that, Matlab scripts were used to calculate the cumulative sediment loss from the processed images. The sediment losses over time were plotted for each core and suitable curves were fitted. Exponential fits (equation 1 in section 3.4) represented the dimensionless erosion data best, resulting in two characteristic cliff erosion coefficients: the 'erosion maximum' and the 'erosion rate'.

3. What are the typical cliff erosion parameters of salt marshes collected across a range of field conditions?

The cliff erosion of sediment cores collected across a range of salt marsh conditions varies depending upon their locations (e.g. mudflat, sparsely vegetated marsh zone or densely vegetated marsh zone) and species. The cliff erosion in our study was quantified by the 'erosion maximum' and 'erosion rate'. The erosion maximum is the relative maximum amount of sediments that was expected to erode from the samples during the infinite period of wave actions. Erosion rate is a rate coefficient and measures the speed by which sediment erosion approaches to erosion maximum. The cliff erosion maxima obtained for all the densely vegetated salt marshes were 0.02-0.11. The higher range of cliff erosion maxima was found for the cores retrieved from the mudflats with a range of 0.55-1.0. Therefore, the presence of vegetation in the salt marsh substrates is effectively reducing the maximum amount of sediment erosion. The typical cliff erosion maxima obtained for *Spartian anglica* were 0.01-0.02. The erosion maxima were higher for the *Phragmites australis* species with a range of 0.02-0.11. The range of erosion maxima for S*cirpus maritimus* was 0.02-0.06. Therefore, *Spartina anglica* is better in reducing the maximum amount of sediments eroded from the salt marsh substrates. The second erosion parameter, the 'erosion rate' also varies with the study sites, species and locations. However, it is not possible to give any typical range. Because the value of the cliff erosion rates for the species and locations fluctuated in a wide range and no clear relation could be found for the erosion rates with different species and locations.

4. What is the impact of vegetation characteristics and sediment properties on the cliff erosion of the salt marsh substrates?

The cliff erosion of salt marshes is influenced by vegetation characteristics and sediment properties. In this study, the vegetation characteristics were vegetation density, amount of dry aboveground and dry belowground biomass. The sediment properties were D_{50} and organic carbon content. The results reveal that the dry root biomass (R^2=0.71) and the stem density (R^2=0.68) provide the best predictor of the erosion maxima. Both these parameters showed negative correlation coefficients with erosion maxima in case of the vegetated salt marsh substrates. The organic carbon (R^2=0.55) and the D_{50} (R^2=0.20) are important predictors for the erosion maxima observed for the sediment cores retrieved from mudflat locations.

No significant relation was found between the erosion rates and D_{50} or the organic carbon content for the salt marsh substrates. Conversely, grain sizes (R^2=0.79) are the best estimator for the cliff erosion rates for sediment cores from the mudflat zones that give a positive correlation. Additional, the organic carbon is negatively correlated with erosion rates, which is also a good predictor (R^2=0.40) of the erosion rates from mudflat sediment cores.

Overall, taking all the sediment cores together, the erosion maximum is controlled by the amount of dry belowground biomass and the vegetation density. However, it is difficult to draw any conclusion about the controlling parameter of the erosion rates in salt marsh substrates, whereas it is clear that the erosion rates of mudflat sediment cores are controlled by the median grain size (D_{50}) and organic carbon content.

Table 11: Erodibility properties considering all sediment cores together (Erosion maximum)

Larger erosion maximum	**Medium erosion maximum**	**Smaller erosion maximum**
Mudflats>	Sparsely vegetated>	Densely vegetated
Phragmites australis>	*Scirpus maritimus>*	*Spartina anglica*

Table 12: Erosion maximum & erosion rate for mudflat sediment cores

Larger Erosion maximum & erosion rate	**Smaller erosion maximum & erosion rate**
high D_{50}	Low D_{50}
Low Organic carbon content	High organic carbon content

5.2 Recommendations

Based on the research carried out in this study, some recommendations can be done for the use of salt marshes into coastal zone management. Next, there are also some recommendations following from the present study for future improvements to the measuring techniques.

5.2.1 Salt marshes in coastal zone management

Salt marshes are the common vegetation types found in sheltered shallow intertidal coastal areas of the temperate regions. These salt marshes have proven to serve a protective function against high wave energy experienced in coastal areas. This study revealed the importance of salt marsh vegetation on the reduction of cliff erosion due to wave action. The different species have a different effect on the erodibility. In our study, among the three species, *Spartina anglica* showed minimum erosion. Hence, this type of species is more active in the reduction of erosion from cliff soils. Coarser grain sizes show larger amount of erosion, whereas finer grain sizes show less erosion. Use of the finer soil in the coastal area may give better protection against the erosion in the coastal areas. Therefore, plantation of salt marshes in coastal zones can provide a nature protection in case of coastal zone management. Furthermore, these salt marsh areas will add ecological value as they provide habitat for many species.

5.2.2 Future research and improvement of measuring techniques

More research is required to quantify and better understand the cliff erosion of the salt marshes. At present, not enough research is available on this topic. The results found in this study are very different from the results of the only available preceding study by Feagin et al. (2009). Hence, further studies are required on the quantification of the impact of vegetation characteristics and sediment properties on the cliff erosion of salt marshes. This future research should be an extended study covering a wide range of field conditions (e.g. sites influenced by different water condition, vegetation species).

The hydrodynamic conditions in the tanks are need to be quantified in proper way as the hydrodynamic conditions in the wave tank influence the cliff erosion. Furthermore, the images for the 3D reconstruction of the sediment cores are need to be of good quality. In this study, we had problems with the image quality. Therefore, to improve the quality, it would be better to use additional light sources when taking pictures at night time. Also, the images are need to be taken carefully from 40 different angles. The data processing will be more reliable if these images are taken from fixed positions for each time step and every sediment cores. Additional, variations in hydrodynamic conditions will need to consider to see the effect of wave action on erosion maximum and erosion rate. Field data will need to collect in other season to see the difference of the vegetation characteristics among the season and subsequently the difference in cliff erodibility.

References

Adam, P. (1990). *Salt Marsh Ecology. Cambridge Univ. Press, Cambridge*. Cambridge: Cambridge Univ. Press.

Allen, J. R. L.(2000). Morphodynamics of Holocene salt marshes: a review sketch from the Atlantic and Southern North Sea coasts of Europe. *Quaternary Science Reviews 19*, 1155-1231.

Bakker, Jan P. (2014). Ecology of salt marshes 40 years of research in the Wadden Sea.

Balke, Thorsten. (2013). *Establishment of biogeomorphic ecosystems (A study on mangrove and salt marsh pioneer vegetation)*: ISBN/EAN:9789090278575.

Beeftink, W. G., & Rozema, J. (1988). *The nature and functioning of salt marshes.* (B. B. L. In: Salomons W., Duwsma E. K. and Förstner V. (ed) Ed.). Springer, Berlin.

Borsje, B. W., Vanwesenbeek, B. K., Dekker, F., Paalvast, P., Bouma, T. J., Van Katwijk, M. M., & De Vries, M. M. (2011). How ecological engineering can serve in coastal protection. *Ecological Engineering 37(2)*, 113-122.

Bouma, T. J., Friedrichs, M., Wesenbeeck, van B. K., Temmerman, S., Graf, G., & Herman, P. M. J. (2009). Density-dependent linkage of scale-dependent feedbacks: a flume study on the intertidal macrophyte Spartina anglica. *Oikos 118*, 260–268.

Bouma, T. J., Van Duren, L. A., Temmerman, S., Claverie, T., Blanco-Garcia, A., Ysebaert, T., & Herman, P. M. J. (2005). Trade-offs related to Ecosystem Engineering: A case study on stiffness of Emerging Macrophytes. *Ecology, 86*(2187-2199).

Bouma, T. J., Van Duren, L. A., Temmerman, S., Claverie, T., Blanco-Garcia, A., Ysebaert, T., & Herman, P. M. J. (2007). Spatial flow and sedimentation patterns within pathces of epibenthic structures. *Coastal and Shelf Science, 27 (8)*, 1020-1045.

Brown, S. L., Paterson, D. M., & Cramp, A. (1998). Sedimentation in a Humber salt marsh. *Geological Society*, 69-83.

Bulger, A. J., Hayden, B. P., Monaco, M. E., Nelson, D. M. , & McCorminck-Ray, M. G. . (1993). Biologically-based estuarine salinity zones derived from a multivariate analysis. *Estuaries, 18*, 311-322.

Butler, S. (2010). *Macquarie Concise Dictionary*. Sydney, Australia: Macquarie Dictionary Publishers

Cavazzoni, S., & Gottardo, D. (1983). Processi evolutivi e morfologici nella laguna di Venezia. In: Ministero dei Lavori Pubblici, Atti del Convegno "Laguna, fiumi, lidi: cinque secoli di gestione delle acque nelle Venezie". *Venice*, 2-18.

Christiansena, T., Wiberga, P. L., & Milliganb, T. G. (2000). Flow and Sediment Transport on a Tidal Salt Marsh Surface *Estuarine, Coastal and Shelf Science, 50*, 315-331.

Coops, Hugo, Geilen, N., Verheij, Henk J., Boeters, Rene , & van der Velde, Gerard (1996). Interactions between waves, bank erosion and emergent vegetation: an experimental study in a wave tank. *Aquatic Botany, 53*, 187-198.

Corenblit, D., Tabacchi, E., Steiger, J., & Gurnell, A. (2007). Reciprocal interactions and adjustments between fluvial landforms and vegetation dynamics in river corridors: A review of complementary approaches. *Earth-Sci. Rev. , 84*.

Costanza, R., Pe'rez-Maqueo, O., Martinez, M. L., Sutton, P., Anderson, S. J., & Mulder, K. (2008). The value of coastal wetlands for hurricane protection. *Ambio 37*, 241-248.

Daloffire, J., Lafite, R., Lesueur, P., Verney, R., Lesourd, S., Cuvilliez, A., & Taylor, J. (2006). Controlling factors of rhythmic sedimentation processes on an intertidal estuarine mudflat — Role of the turbidity maximum in the macrotidal Seine estuary. *Fran ce. Mar. Geol. , 235*, 151-164.

Dalrymple, R.A., Kirby, J.T. & Hwang, P.A. . (1984). Wave diffraction due to areas of energy dissipation. *Waterway, Port, Coastal, and Ocean Engineering, 110(1)*, 67-79.

Davies, J. L. (1980). *Geographical Variation in Coastal Development*. London: 2nd ed. Longman.

Day, J. W., Scarton, F., Rismondo, A., & Aret, D. (1998). Rapid Deterioration of a Salt Marsh in Venice Lagoon, Italy. *Journal of Coastal Research, 14*, 583-590.

De Groot, R., Brander, L., VanderPloeg, S, Costanza, R., Bernard, F., Braat, L., . . . Hussain, S. (2012). estimates of the value of ecosystems and their services in monetary units. *Ecosystem services, 1(1)*, 50-61.

Dijkema, K. S. (1984). *Western European salt marshes* (I. D. K. S. e. S. m. i. Europe Ed.).

Dixon, A. M., Leggett, D. J., & Weight, R. C. (1998). Habiatat creation opportunities for landward coastal re-alignment:Essex case study. *Chartered Institution of Water and Environmental Management*, 107-112.

Feagin, R.A., Lozada-Bernard, S.M., Ravens, T.M., Moller, I., Yeager, K.M., & Baird, A.H. (2009). Does vegetation prevent wave erosion of salt marsh edges? *PNAS, 106*, 10109-10113.

Fonseca, M.S. & Cahalan, J.A. (1992). A preliminary evaluation of wave attenuation by four species of seagrass. *Estuarine, Coastal, and Shelf Science, 35(6)*, 565-576.

French, J. R. & Stoddart, D. R. (1992). Hydrodynamics of salt marsh creek systems: implications for marsh morphodynamic development and matter exchange. *Earth Surface Processes and Landforms 17*, 235-252.

Furukawa, K. & Wolnaski, E. (1996). sedimentation in mangrove forests. *Mangrove and salt marshes*, 3-10.
Gedan, K. B., Kirwan, M. L., Wolnaski, E., & Barbier, E. B. (2011). The present and future role of coastal wetland vegetation in protecting shorelines: an answering recent question to the paradigm. *Climate Change 106*, 7-29.
Grabowski, R. C., Droppo, Ian G., & Wharton, G. (2011). Erodibility of cohesive sediment: The importance of sediment properties. *Earth-Science Reviews, 105*, 101-120.
Hampel, Henrietta. (2002). Factors influencing the habitat value of tidal marshes for nekton in the Westerschelde estuary (D. o. Biology, Trans.) *Marine Biology*. Krijgslaan 281, S-89000 Gent, Belgium: University Gent.
Houwing, E. J. (1999). Determination of Ccritical Erosion Threshold of Cohesive Sediments on Intertidal Mudflats Along Dutch Wadden Sea Coast. *Estuarine, Coastal and Shelf Science, 49*, 545-555.
Jadav, R. S., Chen, Q., & Smith, J. M. (2013). Spectral distribution of wave energy dissipation by salt marsh vegetation. *Coastal Engineering 77*, 99-107.
Jones, C. G., Lawton, J. H., & Shachak, M. (1994). Organisms as Ecosystem Engineers. *Oikos 69*.
King, M. . (1995). *Fisheries Biology, Assessment and Management. Fishing News Books*: Oxford, UK.
Koch, E.W., Sanford, L.P., Chen, S-N., Shafer, D.J., & Mckee Smith, J. (2006). Waves in seagrass systems: Review and Technical recommendations. In U. A. C. o. Engineers (Ed.).
Leonard, L., & Luther, M. (1995). Flow hydrodynamics in tidal marsh canopies. *Limnology and Oceanography 40*, 1474–1484.
Lima, S.F., Neves, C.F. , & Rosauro, N.M.L. . (2006). *Damping of gravity waves by fields of flexible vegetation: Proceedings of the 30th International Conference on Coastal Engineering*. Paper presented at the World Scientific.
Lopez, J. A. (2009). The multiple lines of defense strategy to sustain coastal Louisiana. *Journal of Coastal Research*, 186-197.
Lowe, R.J., Falter, J.L., Koseff, J.R., Monismith, S.G. , & Atkinson, M.J. (2007). Spectral wave flow attenuation within submerged canopies: Implications for wave energy dissipation. *Journal of Geophysical Research, 112*.
Magee, D.W. (1981). *A world in our backyard*: U. S. Environmental Protection Agency.
May, R. M. (1973). *Stability and complexity in model ecosystems*. Princeton, NJ: Princeton University Press.
Mayer, Daniel. (2003) *Salt Marsh*.
Méndez, F. J. & Losada, I. J. (2004). An empirical model to estimate the propagation of random breaking and nonbreaking waves over vegetation fields. *Coastal Engineering, 51(2)*103-118.

Méndez, F. J. & Losada, I. J. (1999). Hydrodynamics induced by wind waves in a vegetation field. *Journal of Geophysical Research, 104(C8)*, 18383-18396.
Möller, & Spencer. (2002). Wave dissipation over macro-tidal saltmarshes: effects of marsh edge typology and vegetation change. *J. Coast. Res. S, 136*, 506–521.
Niering, W. A. , & Warren, R. S. (1980). Vegetation patterns and processes in New England salt marshes. *Bioscience, 30*, 301-307.
Paterson, D.M. (1989). Short term changes in the erodibility of intertidal cohesive sediments related to the migratory behaviour of epipelic diatoms. *Limnology and Oceanography, 34 (1)*, 223-234.
Redfield, A. C. (1972). Development of a New England salt marsh. *Ecological Monographs, 42*, 201-237.
Robin, G. D., Davidson, A., Danika, van P., Jeff, O., & Schostak, L. (2002). Hydrodynamics and sedimentation in salt marshes:examples from a macrotidal marsh, Bay of Fundy. *Geomorphology 48*, 209-231.
Scheffer, M., Carpenter, S. , Foley, J. A. , Folke, C. , & Walker, B. (2001). Catastrophic shifts in ecosystems. *Nature 413*, 591–596.
Shi, B. W., Yang, S. L., Bouma, T J., & Zhu, Q. (2012). Relating accretion and erosion at an exposed tidal wetland to the bottom shear stress of combined current–wave action. *Geomorphology, 138*, 380-389.
Shi, B. W., Yang, S. L., Wang, Y. P., Yu, Q., & Li, M. L. (2014). Intratidal erosion and deposition rates inferred from field observations of hydrodynamic and sedimentary processes: A case study of a mudflat–saltmarsh transition at the Yangtze delta front. *Continental Shelf Research, 90*, 109-116.
Sutheland, T. F., Amos, C. L., & Grant, J. . (1998). The erosion threshold of biotic sediments: a comparison of methods. Sedimentary Processes in the Intertidal Zone. *Geological Society, 139*, 135-148.
Tolhurst, T. J., Black, K. S., Shayler, S. A., Mather, S., Black, I., Baker, K., & Paterson, D. M. (1999). Measuring the in situ Erosion Shear Stress of Intertidal Sediments with the Cohesive Strength Meter (CSM). *Coastal and Shelf Science, 49*, 281-294.
Tschirky, P., Hall, K. , & Turcke, D. . (2000). *Wave attenuation by emergent wetland vegetation. Proceedings of the 27th International Conference on Coastal Engineering.* Paper presented at the ASCE.
Van Belzen, Jim, Bouma, T. J., Skov, Martin, Zhang, Liquan, & Yuan, Li (2015). Dynamics, Threats and management of salt marshes. *Marine Biodiversity Wiki*.

Van de Koppel, J., van der Wal, D., Bakker, J. P., & Herman, P. M. J. (2005). Self-Organization and Vegetation Collapse in Salt Marsh Ecosystems. *The American Naturalist 165 (1)*.

Vernberg, F. J. (1993). Salt marsh processes: a review. *Environmental Toxicology and Chemistry, 12*, 2167-2195.

Wang, F., Lu, T. , & Sikora, W. (1993). Intertidal marsh suspended sediment transport processes, Terrebonne Bay, Louisiana, USA. *Journal of Coastal Research 9*, 209–220.

Widdows, J., Brown, S. , Brinsley, M. D. , Salkeld, P. N. , & Elliott, M. (2000). Temporal changes in intertidal sediment erodability: influence of biological and climatic factors. *Continental Shelf Research, 20* 1275-1289.

Zottoli. (2011). A Virtual Field Trip through a Salt Marsh, https://zottoli.wordpress.com/saltmarshes/salt-marsh-pannes-and-pools/

Appendix A

<u>3D image analysis and calculation of sediment volume loss</u>

To be able to process the images and calculation of sediment volume loss, three programmes are needed: Visual SFM (Open source software); Meshlab (Open source software), Matlab (University of Twente licences). The step wise procedure of calculation of sediment volume loss is given below:

- The Photographs taken at ten different time steps of six wave tank runs were organized according to
  - a. Number of wave tank run
  - b. Time step name folder: Timestep-wave tank slot-Site-Core number-Characteristics (without any space between the letters). As an example, folder name format in each wave tank run should looks like

    T0-1A-B-1-LO

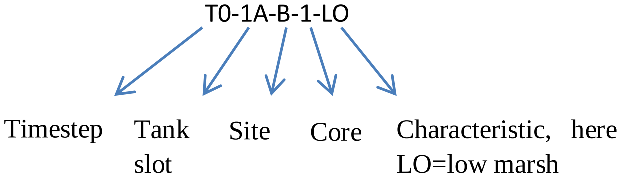

- Use of VisualSFM:
  - a. Open the VisualSFM and load all the photos of one folder by clicking  (i.e. one time step of one core of one wave tank run).

b. The missing matches among the 40 images are computed by clicking 

c. Depending upon the missing matches, the sparse reconstruction was done by clicking  after that this sparse reconstruction is saved to .nvm file extension.

d. Using the saved file after sparse reconstruction, dense reconstruction is done by clicking  the process of dense reconstruction takes almost about 15 minutes.

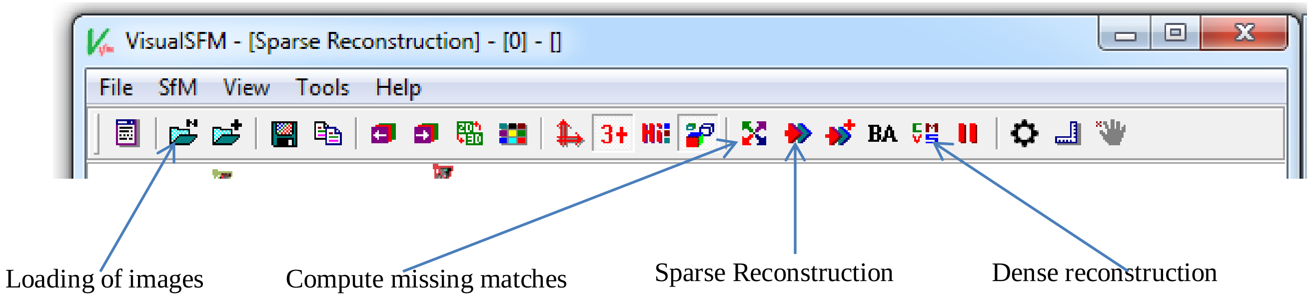

Figure 1: Operation of visual SFM.

e. As to able to analysis these 3D images, points or coordinate needs to add to the 3D images. In each 3D image, three reference points are added by giving x, y, and z coordinates of each point. This is done by clicking 'SfM' then 'more functions' and then 'GCP-based transform'. Addition of three points with x y z coordinates are done by manually using the value in table 1.

Table 1: Wave tank measurements for SFM referencing

	ruler 1	x	y	z	ruler 2	x	y	z	ruler3	x	y	z
1A	10	0	15	0	35	12	15	0	20	0	5	0
1B	60	0	15	0	85	12	15	0	70	0	5	0
1C	110	0	15	0	135	12	15	0	120	0	5	0
2A	15	0	10	0	35	11,9	15	0	20	0	5	0
2B	65	0	10	0	90	12	10	0	70	0	5	0
2C	115	0	10	0	140	12,3	10	0	120	0	5	0
3A	10	0	15	0	35	11,8	15	0	20	0	5	0
3B	65	0	10	0	90	12	10	0	70	0	5	0
3C	110	0	15	0	135	12	15	0	120	0	5	0
4A	10	0	15	0	35	12,1	15	0	15	0	10	0
4B	60	0	15	0	85	11,8	15	0	70	0	5	0
4C	115	0	10	0	140	12	10	0	120	0	5	0

Therefore, each of the 3D images constructed for each tank slots will contain three reference points making triangular mesh by giving the coordinate value of x y z such that the standard error is <0.5mm. During addition of reference points, the corners of rectangle should be visible in order to get the z value right. The resultant file is saved to 'timestep-tank slot.nvm' file format (i.e. T1-1A), (T2-2B)… etc.

- Use of Meshlab:
  a. The resultant nvm file is opened via Meshlab
  b. New mesh is exported by clicking 'Export new mesh'. The opened nvm file is then saved to xyz file format. The nvm file produced through the Visual SFM only contains unstructured triangular mesh. To restructure this triangular unstructured mesh and make it readable to the Matlab, this step needs to carry out.
- Use of Matlab:
  a. The resultant xyz files from all time steps of one tank slots (one tank run) are saved in a folder. i.e. W-3A (contains xyz files of T0 till T9).
  b. In this case, four Matlab script will be used, the Matlab scripts and the folder of xyz file format should be in the same folder directory.
  c. Open four matlab scripts: prepcoredata.m; comparecores.m; Volume loss.m; main_heng.m. Among the four matlab scripts, the 'main_heng' is the main script and others are functions. This script is run by changing the folder name for each wave tank slot. Then two result file is created named Volume.dat', which gives the volume loss in specific time steps and 'Volumeloss.dat' that gives the cumulative volume loss with respect to the initial time step T0. These cumulative sediment volume loss result further used in excel to calculate erosion rates for the sediment cores.

The Matlab scripts were developed by J. van Belzen at the Yerseke-NIOZ. The Matlab scripts are provided in the following section.

Matlab scripts for calculation of eroded sediment volume

Main Matlab script (main_heng.m) for calculation of the cumulative sediment volume eroded

```
%written by J. van Belzen(02042015)
clear;

kmax=9;              %%modify here
type='1B';           %%modify here

%%
for k=0:kmax
    infile=['T' num2str(k) '-' type];
    if ~exist([infile '_z.grid'],'file')
        data=prepcoredata(infile,0.005);
        clear data;
    end
end

%%
fid1=fopen([type '_Volume.dat'],'wt');
for k=1:kmax
   str0=['T'  num2str(k)];
   fprintf(fid1,'%12s',str0);
end
fprintf(fid1,'\n');


fid2=fopen([type '_VolumeLoss.dat'],'wt');
for k=1:kmax
   str0=['T'  num2str(k) '-T0'];
   fprintf(fid2,'%12s',str0);
end
fprintf(fid2,'\n');

%%
for k=1:kmax
    infile=['T' num2str(k) '-' type];
    Volumeloss = comparecores(infile,['T0-' type]);
    V=VolumeCal(infile);

    fprintf(fid1,'%12.4f',V);
    fprintf(fid2,'%12.4f',Volumeloss);

    outfile=['T'  num2str(k) '-T0-' type '.png'];
    print(gcf,'-dpng','-r600',outfile)
    close(Figure(1));

end

fprintf(fid1,'\n');
fprintf(fid2,'\n');
fclose(fid1);
fclose(fid2);
```

Function Matlab script-Prepcoredata.m file

```
function [data] = prepcoredata(filename, resolution)
%PREPCOREDATA prepares the xyz-data from sediment cores for further
% analysis
%
% Version 1.0 (24/04/2014)
% Version 1.1 (17/09/2014)
% Coded and developed by Jim van Belzen
% published under the Creative Commons Attribution Non-Commercial license
% which allows users to read, copy, distribute and make derivative works
% for noncommercial purposes from the material, as long as the author of
% the original work is cited.
% This code comes with no warranties or support
% http://people.zeelandnet.nl/jbelzen/

tic

%%- import data
xyzdata=dlmread([filename,'.xyz']);

%%- define selection frame that becomes gridded
xmin=1;
xmax=11;

ymin=2;
ymax=20;

res=1/resolution;

%%- pre-process xyz-data
xlin=linspace(xmin, xmax, (xmax-xmin)*res);
ylin=linspace(ymin, ymax, (ymax-ymin)*res);
[X Y]=meshgrid(xlin, ylin);
F = TriScatteredInterp(xyzdata(:,1), xyzdata(:,2), xyzdata(:,3),
'nearest');

Z = F(X, Y);

Z1 = medfilt2(Z, [5 5]);

dlmwrite([filename,'_z.grid'], Z);
dlmwrite([filename,'_z_med.grid'], Z1);
dlmwrite('Selected_frame.txt',[xmin xmax ymin ymax res]);

data=Z;

toc
end
```

Function Matlab script-Comparecores.m file

```
function [output] = comparecores(filename1, filename2)
%COMPARECORES compares the 'images' of two sediment cores as prepared by
% the function "prepcoredata.m"
%
% [output] = the volume lost between image1 and image2 (resp. filename2 &
% filename2)
% information about x and y coordinates and resolution is retreaved from
% 'Selected_frame.txt' which is created by 'prepcoredata.m'
%
% Version 1.0 (24/04/2014)
% Version 1.1 (17/09/2014)
% Coded and developed by Jim van Belzen
% published under the Creative Commons Attribution Non-Commercial license
% which allows users to read, copy, distribute and make derivative works
% for noncommercial purposes from the material, as long as the author of
% the original work is cited.
% This code comes with no warranties or support
% http://people.zeelandnet.nl/jbelzen/

on=1;
off=0;

output = [];



%% load data
Z0=dlmread([filename1,'_z.grid']);
Z1=dlmread([filename2,'_z.grid']);
xy_frame=dlmread('Selected_frame.txt');

%%- define selection in images used for comparison
xmin=xy_frame(1);
xmax=xy_frame(2);
ymin=xy_frame(3);
ymax=xy_frame(4);
res=xy_frame(5);

Diff=Z0-Z1;

Diff=Diff.*(Diff>0);

output=sum(Diff(:))*(1/res)^2;
```

Function Matlab script- rest of comparecores.m file

```
%%- Figure output
if on,
    Figure('color','w'),
    subplot(1,3,1)
    imagesc([xmin:xmax],[ymin:ymax],Z0)
    axis image xy
    colorbar
    title('Z0')

    subplot(1,3,2)
    imagesc([xmin:xmax],[ymin:ymax],Z1)
    axis image xy
    colorbar
    title('Z1')

    subplot(1,3,3)
    imagesc([xmin:xmax],[ymin:ymax],Diff)
    axis image xy
    colorbar
    title('Diff.')
end

end
```

Function Matlab script-VolumeCal.m file

```
function V = VolumeCal(filename)
%VOLUMELOSS calculates loss relative to reference plain
%
% V = Volume
%
% information about x and y coordinates and resolution is retreaved from
% 'Selected_frame.txt' which is created by 'prepcoredata.m'
%
% Version 1.0 (24/04/2014)
% Version 1.1 (17/09/2014)
% Coded and developed by Jim van Belzen
% Modified by Heng Wang (07/04/2015)
% published under the Creative Commons Attribution Non-Commercial license
% which allows users to read, copy, distribute and make derivative works
% for noncommercial purposes from the material, as long as the author of
% the original work is cited.
% This code comes with no warranties or support
% http://people.zeelandnet.nl/jbelzen/

on=1;
off=0;

V = [];



%% load data
Z=dlmread([filename,'_z.grid']);
xy_frame=dlmread('Selected_frame.txt');

%%- define selection in images used for comparison
xmin=xy_frame(1);
xmax=xy_frame(2);

ymin=xy_frame(3);
ymax=xy_frame(4);
res=xy_frame(5);

%%- calc volume
V=sum(-Z(:))*(1/res)^2;



end
```

Appendix B

Table 2: Number of stems counted of 33 vegetated sediment cores (Name of the sediment cores was chosen as location (2=vegetated, 3=sparse vegetated, 4=dense vegetated)-Study sites (B=Bath, H=Hellegatpolder, Z=Zuidgors, G=Groot Buitenschoor, D=De Zaag)-Vegetation species (Sc=Scirpus maritimus, Sp=Spartina anglica, Ph=Phragmites australis)-Characteristics vegetation (SV=Sparse vegetated, DV=Dense vegetated, V=Vegetated)-number of replicates (1, 2, 3)).

Name of the sediment cores	Number of stems in cylindrical metal core	no. of stems/m²	Name of the sediment cores	Number of stems in cylindrical metal core	no. of stems/m²
3B_Sc_SV_1	5	313	4H_Sp_DV_1	38	2382
3B_Sc_SV_2	3	188	4H_Sp_DV_2	30	1881
3B_Sc_SV_3	1	63	4H_Sp_DV_3	34	2132
4B_Sc_DV_1	23	1442	2Z_Sp_V_1	32	2006
4B_Sc_DV_2	28	1755	2Z_Sp_V_2	43	2696
4B_Sc_DV_3	17	1066	2Z_Sp_V_3	42	2633
2B_Ph_V_1	14	878	3G_Sc_SV_1	4	251
2B_Ph_V_2	20	1254	3G_Sc_SV_2	2	125
2B_Ph_V_3	12	752	3G_Sc_SV_3	5	313
2B_Sp_V_1	44	2758	4G_Sc_DV_1	12	752
2B_Sp_V_2	52	3260	4G_Sc_DV_2	6	376
2B_Sp_V_3	41	2570	4G_Sc_DV_3	9	564
2H_Sp_V_1	38	2382	2D_Ph_V_1	12	752
2H_Sp_V_2	35	2194	2D_Ph_V_2	14	878
2H_Sp_V_3	32	2006	2D_Ph_V_3	7	439
3H_Sp_SV_1	30	1881			
3H_Sp_SV_2	17	1066			
3H_Sp_SV_3	16	1003			

Table 3: Results of above ground biomass of 33 vegetated sediment cores ((explanation of name of the sediment cores are same as for previous table 2).

Name of the sediment cores	dry above ground biomass [g]	dry above ground biomass [g]/cm²	dry above ground biomass [g]/m²	Name of the sediment cores	dry above ground biomass [g]	dry above ground biomass [g]/cm²	dry above ground biomass [g]/m²
3B_Sc_SV_1	1.83	0.011	114.73	**4H_Sp_DV_1**	15.06	0.094	944.14
3B_Sc_SV_2	1.87	0.012	117.23	**4H_Sp_DV_2**	11.29	0.071	707.79
3B_Sc_SV_3				**4H_Sp_DV_3**	10.44	0.065	654.50
4B_Sc_DV_1	5.11	0.032	320.36	**2Z_Sp_V_1**	15.59	0.098	977.37
4B_Sc_DV_2	6.88	0.043	431.32	**2Z_Sp_V_2**	14.05	0.088	880.82
4B_Sc_DV_3	6.01	0.038	376.78	**2Z_Sp_V_3**	10.81	0.068	677.70
2B_Ph_V_1	60.53	0.379	3794.75	**3G_Sc_SV_1**	8.24	0.052	516.58
2B_Ph_V_2	44.38	0.278	2782.27	**3G_Sc_SV_2**	8.07	0.051	505.92
2B_Ph_V_3	40.36	0.253	2530.25	**3G_Sc_SV_3**	12.44	0.078	779.89
2B_Sp_V_1				**4G_Sc_DV_1**	10.96	0.069	687.10
2B_Sp_V_2	2.59	0.016	162.37	**4G_Sc_DV_2**	8.64	0.054	541.66
2B_Sp_V_3				**4G_Sc_DV_3**	15.36	0.096	962.95
2H_Sp_V_1	12.89	0.081	808.10	**2D_Ph_V_1**	48.73	0.305	3054.98
2H_Sp_V_2	10.73	0.067	672.69	**2D_Ph_V_2**	49.79	0.312	3121.43
2H_Sp_V_3	10.03	0.063	628.80	**2D_Ph_V_3**	25.47	0.160	1596.77
3H_Sp_SV_1	7.79	0.049	488.37				
3H_Sp_SV_2							
3H_Sp_SV_3							

Table 4: Belowground biomass for all the vegetated cores (33 vegetated cores) (explanation of name of the sediment cores are same as for previous table 2).

Name of the sediment cores	Root dry biomass (g)	Root dry biomass (g)/cm²	Root dry biomass (g/m²)	Name of the sediment cores	Root dry biomass (g)	Root dry biomass (g)/cm²	Root dry biomass (g/m²)
3B_Sc_SV_1	73.82	0.46	4627.80	**3H_Sp_SV_3**	41.82	0.26	2621.50
3B_Sc_SV_2	43.56	0.27	2730.99	**4H_Sp_DV_1**	79.91	0.50	5009.72
3B_Sc_SV_3	26.38	0.17	1653.94	**4H_Sp_DV_2**	109.03	0.68	6835.46
4B_Sc_DV_1	159.03	1.00	9969.88	**4H_Sp_DV_3**	102.56	0.64	6429.47
4B_Sc_DV_2	101.10	0.63	6338.23	**2Z_Sp_V_1**	185.50	1.16	11629.57
4B_Sc_DV_3	128.14	0.80	8033.33	**2Z_Sp_V_2**	130.38	0.82	8173.56
2B_Ph_V_1	76.39	0.48	4789.18	**2Z_Sp_V_3**	91.27	0.57	5722.20
2B_Ph_V_2	89.87	0.56	5633.87	**3G_Sc_SV_1**	22.46	0.14	1408.06
2B_Ph_V_3	81.75	0.51	5125.25	**3G_Sc_SV_2**	33.26	0.21	2085.14
2B_Sp_V_1	300.82	1.89	18859.01	**3G_Sc_SV_3**	47.07	0.30	2950.91
2B_Sp_V_2	169.05	1.06	10597.77	**4G_Sc_DV_1**	126.64	0.79	7939.16
2B_Sp_V_3	209.86	1.32	13156.34	**4G_Sc_DV_2**	104.09	0.65	6525.40
2H_Sp_V_1	38.28	0.24	2399.96	**4G_Sc_DV_3**	92.29	0.58	5785.99
2H_Sp_V_2	22.03	0.14	1381.37	**2D_Ph_V_1**	222.76	1.40	13965.35
2H_Sp_V_3	75.64	0.47	4741.76	**2D_Ph_V_2**	160.19	1.00	10042.46
3H_Sp_SV_1	53.29	0.33	3340.77	**2D_Ph_V_3**	97.28	0.61	6098.39
3H_Sp_SV_2	41.82	0.26	2622.02				

Table 5: Sediment sizes (D50) of top, bottom layer and the averaged of the two layers (Name of the sediment samples was chosen as location (1=mudflat/unvegetated, 2=vegetated, 3=sparse vegetated, 4=dense vegetated)-Study sites (B=Bath, H=Hellegatpolder, Z=Zuidgors, G=Groot Buitenschoor, D=De Zaag)-Vegetation species (Sc=Scirpus maritimus, Sp=Spartina anglica, Ph=Phragmites australis)-Characteristics vegetation (Un=unvegetated, SV=Sparse vegetated, DV=Dense vegetated, V=Vegetated)-number of replicates (1, 2, 3)).

Sample name	Sediment sizes (SD50) (µm) top layer (0-10 cm)	Sediment sizes (SD50) (µm) bottom layer (10-20 cm)	Sediment sizes (SD50) average of two layers (µm)	Sample name	Sediment sizes (SD50) (µm) Top layer (0-10 cm)	Sediment sizes (SD50) (µm) bottom layer (10-20 cm)	Sediment sizes (SD50) average of two layers (µm)
1B_Sc_Un_1	93.17	21.42	57.30	**1H_Sp_Un_3**	133.33	135.13	134.23
1B_Sc_Un_2	90.50	22.45	56.48	**3H_Sp_SV_1**	146.66	107.79	127.23
1B_Sc_Un_3	92.25	16.66	54.46	**3H_Sp_SV_2**	123.48	103.46	113.47
3B_Sc_SV_1	95.16	21.83	58.50	**3H_Sp_SV_3**	102.68	107.48	105.08
3B_Sc_SV_2	101.55	109.38	105.47	**4H_Sp_DV_1**	108.63	113.84	111.24
3B_Sc_SV_3	92.85	100.04	96.45	**4H_Sp_DV_2**	123.13	105.13	114.13
4B_Sc_DV_1	69.52	85.67	77.60	**4H_Sp_DV_3**	108.47	109.58	109.03
4B_Sc_DV_2	66.74	89.20	77.97	**1Z_Sp_Un_1**	60.19	55.68	57.94
4B_Sc_DV_3	63.44	91.15	77.30	**1Z_Sp_Un_2**	62.55	55.23	58.89
2B_Ph_V_1	84.09	93.39	88.74	**1Z_Sp_Un_3**	48.95	43.73	46.34
2B_Ph_V_2	86.30	81.06	83.68	**2Z_Sp_V_1**	61.03	67.09	64.06
2B_Ph_V_3	82.54	87.97	85.26	**2Z_Sp_V_2**	40.56	53.25	46.91
1B_Sp_Un_1	91.36	77.94	84.65	**2Z_Sp_V_3**	33.21	57.19	45.20
1B_Sp_Un_2	92.24	82.56	87.40	**1G_Sc_Un_1**	60.00	76.79	68.40
1B_Sp_Un_3	88.73	78.74	83.74	**1G_Sc_Un_2**	57.63	60.87	59.25
2B_Sp_V_1	93.29	84.37	88.83	**1G_Sc_Un_3**	61.31	67.78	64.55
2B_Sp_V_2	89.50	84.46	86.98	**3G_Sc_SV_1**	64.91	136.39	100.65
2B_Sp_V_3	90.50	82.49	86.50	**3G_Sc_SV_2**	44.91	80.64	62.78
1H_Sp_Un_1	32.33	15.23	23.78	**3G_Sc_SV_3**	63.64	98.16	80.90
1H_Sp_Un_2	97.80	14.56	56.18	**4G_Sc_DV_1**	22.16	27.44	24.80
1H_Sp_Un_3				**4G_Sc_DV_2**	19.93	31.35	25.64
2H_Sp_V_1	194.21	16.23	105.22	**4G_Sc_DV_3**	20.28	112.51	66.40
2H_Sp_V_2	106.43	20.10	63.27	**2D_Ph_V_1**	78.30	147.83	113.07
2H_Sp_V_3	173.08	16.10	94.59	**2D_Ph_V_2**	78.82	135.32	107.07
1H_Sp_Un_1	128.75	130.77	129.76	**2D_Ph_V_3**	54.35	156.18	105.27
1H_Sp_Un_2	133.34	124.78	129.06				

Table 6: Organic carbon calculated for top and bottom layers and average organic carbon for the two layers (explanation of name of the sediment cores is same as for table 5).

Sample name	% org C for top layer (0-10) cm	% org. C for bottom layer (10-20) cm	% org C. Average of two layers	Sample name	% org C for top layer (0-10) cm	% org. C for bottom layer (10-20)cm	% org C. Average of two layers
1B_Sc_Un_1	0.22	2.73	1.47	3H_Sp_SV_1	0.45	0.25	0.35
1B_Sc_Un_2	0.53	2.90	1.72	3H_Sp_SV_2	0.33	0.29	0.31
1B_Sc_Un_3	0.26	3.30	1.78	3H_Sp_SV_3	0.54	0.42	0.48
3B_Sc_SV_1	0.25	1.96	1.10	4H_Sp_DV_1	0.35	0.30	0.32
3B_Sc_SV_2	0.23	0.27	0.25	4H_Sp_DV_2	0.25	0.31	0.28
3B_Sc_SV_3	0.19	0.37	0.28	4H_Sp_DV_3	0.34	0.31	0.33
4B_Sc_DV_1	0.47	0.42	0.45	1Z_Sp_Un_1	0.51	0.87	0.69
4B_Sc_DV_2	0.31	0.34	0.32	1Z_Sp_Un_2	0.77	0.95	0.86
4B_Sc_DV_3	0.58	0.54	0.56	1Z_Sp_Un_3	0.48	0.97	0.73
2B_Ph_V_1	0.27	0.20	0.24	2Z_Sp_V_1	0.82	0.61	0.72
2B_Ph_V_2	0.22	0.32	0.27	2Z_Sp_V_2	0.93	1.03	0.98
2B_Ph_V_3	0.31	0.45	0.38	2Z_Sp_V_3	1.00	0.78	0.89
1B_Sp_Un_1	0.30	0.47	0.38	1G_Sc_Un_1	1.06	0.91	0.98
1B_Sp_Un_2	0.23	0.56	0.39	1G_Sc_Un_2	1.08	0.95	1.02
1B_Sp_Un_3	0.26	0.35	0.30	1G_Sc_Un_3	0.99	1.14	1.07
2B_Sp_V_1	0.24	0.29	0.27	3G_Sc_SV_1	1.35	0.30	0.82
2B_Sp_V_2	0.22	0.29	0.25	3G_Sc_SV_2	1.31	0.98	1.14
2B_Sp_V_3	0.29	0.38	0.34	3G_Sc_SV_3	1.09	0.75	0.92
1H_Sp_Un_1	1.04	1.40	1.22	4G_Sc_DV_1	1.87	1.91	1.89
1H_Sp_Un_2	0.51	1.55	1.03	4G_Sc_DV_2	2.07	1.44	1.76
1H_Sp_Un_3				4G_Sc_DV_3	2.24	0.64	1.44
2H_Sp_V_1	0.58	1.76	1.17	2D_Ph_V_1	1.40	0.80	1.10
2H_Sp_V_2	1.40	1.63	1.51	2D_Ph_V_2	1.54	0.71	1.12
2H_Sp_V_3	0.78	2.32	1.55	2D_Ph_V_3	2.40	1.65	2.03
1H_Sp_Un_1	0.19	0.18	0.19				
1H_Sp_Un_2	0.18	0.16	0.17				
1H_Sp_Un_3	0.41	0.13	0.27				

Calculation of relative sediment volume eroded

The sediment volume loss of different types of sediment cores was calculated by using 3D image analysis techniques, as already described in the chapter 2. During the final stage of data analysis process, Matlab was used to calculate cumulative sediment volume loss from the sediment cores with reference to the 'initial time step (T0)'. These were the raw results of the cumulative eroded sediment volumes from the sediment cores.

To make the results suitable for understanding and comparison, these cumulative sediment volume loss data were converted to the 'relative sediment volume eroded' by dividing these cumulative sediment volume loss values with the total sediment volume of the cylindrical metal sediment core. The total sediment volume taken of cylindrical metal sediment core was 1920 cm^3 during the image analysis process considering edge effect. A sample calculation procedure of 'relative sediment volume eroded' calculated for 9 sediment cores of *Scirpus maritimus* species from Rilland Bath study site is given below:

Table 7: Cumulative sediment volume loss (cm^3) of Scirpus maritimus species at the study site Rilland Bath (values obtained from Matlab run of processed images)

Time (hr)	**Bath-Scirpus-mudflat-1 (cm^3)**	**Bath-Scirpus-mudflat-2 (cm^3)**	**Bath-Scirpus-mudflat-3 (cm^3)**	**Bath-Scirpus-Sparse vegetated-1 (cm^3)**	**Bath-Scirpus-Sparse vegetated-2 (cm^3)**	**Bath-Scirpus-Sparse vegetated-3 (cm^3)**	**Bath-Scirpus-Dense vegetated-1 (cm^3)**	**Bath-Scirpus-Dense vegetated-2 (cm^3)**	**Bath-Scirpus-Dense vegetated-3 (cm^3)**
0.00	0.00	0.00	0.00	0.00	0.00	0.00	0.00	0.00	0.00
1.00	113.83	353.13	283.28	46.39	182.69	91.47	43.84	47.54	62.56
2.00	182.61	376.76	308.93	125.14	152.68	112.19	62.86	10.40	137.30
4.00	212.42	398.88	334.63	96.05	139.87	142.75	80.45	59.50	91.63
8.00	416.53	442.65	700.61	214.64	303.82	257.62	67.42	59.10	98.82
16.00	726.99	934.99	1023.75	130.76	367.28	258.39	71.62	16.31	101.28
24.00	667.34	1128.50	877.87	134.49	500.55	578.72	58.56	62.26	107.17
32.00	847.67	1083.98	1008.18	426.84	649.08	737.00	83.71	36.13	120.73
40.00									
48.00	1072.71	1016.44	1132.28	212.70	793.85	157.24	98.37	47.73	121.28

In theory, the cumulative sediment loss values for all the sediment cores should increase in the next time step than previous time step. This was not always in the case as obvious from the table 7. The possible reason behind this, the measurement error such as the taken images from 40 different angles during experiment were not good in quality.

During 40 hrs, the sediment volume loss results were missing due to the measurement complexity during taking images at night.

The total sediment volume of cylindrical metal sediment core was 1920 cm^3 as already calculated in the methodology chapter. Dividing the cumulative sediment loss values of above table by 1920 cm^3 give values of following table 8.

Table 8: Cumulative sediment volume eroded of 9 sediment cores of Scirpus maritimus species from the study site Rilland Bath

Time (hr)	**Bath-Scirpus-mudflat-1 (cm^3)**	**Bath-Scirpus-mudflat-2 (cm^3)**	**Bath-Scirpus-mudflat-3 (cm^3)**	**Bath-Scirpus-Sparse vegetated-1 (cm^3)**	**Bath-Scirpus-Sparse vegetated-2 (cm^3)**	**Bath-Scirpus-Sparse vegetated-3 (cm^3)**	**Bath-Scirpus-Dense vegetated-1 (cm^3)**	**Bath-Scirpus-Dense vegetated-2 (cm^3)**	**Bath-Scirpus-Dense vegetated-3 (cm^3)**
0.00	0.00	0.00	0.00	0.00	0.00	0.00	0.00	0.00	0.00
1.00	0.06	0.18	0.15	0.02	0.10	0.05	0.02	0.02	0.03
2.00	0.10	0.20	0.16	0.07	0.08	0.06	0.03	0.01	0.07
4.00	0.11	0.21	0.17	0.05	0.07	0.07	0.04	0.03	0.05
8.00	0.22	0.23	0.36	0.11	0.16	0.13	0.04	0.03	0.05
16.00	0.38	0.49	0.53	0.07	0.19	0.13	0.04	0.01	0.05
24.00	0.35	0.59	0.46	0.07	0.26	0.30	0.03	0.03	0.06
32.00	0.44	0.56	0.53	0.22	0.34	0.38	0.04	0.02	0.06
40.00									
48.00	0.56	0.53	0.59	0.11	0.41	0.08	0.05	0.02	0.06

<u>Raw data of cumulative sediment volume eroded</u>

The cumulative volume of sediment erosion for all the 51 sediment cores are given in the table 9 till table 14. The table are presented as the carrying of the wave tank experiments (six wave tank run were needed to cover the 51 sediment cores, the arrangements of the wave tank running can be found in table 2 at the main section).

Table 9: Raw Matlab data that gives cumulative sediment volume loss in cm^3 of sediment cores collected from Rilland Bath

	Time	1B_Sc_Un_1	1B_Sc_Un_2	1B_Sc_Un_3	3B_Sc_SpVeg_1	3B_Sc_SpVeg_2	3B_Sc_SpVeg_3	4B_Sc_DeVeg_1	4B_Sc_DeVeg_2	4B_Sc_DeVeg_3	2B_Ph_Veg_1	2B_Ph_Veg_2	2B_Ph_Veg_3
T0-T0	0.00	0.00	0.00	0.00	0.00	0.00	0.00	0.00	0.00	0.00	0.00	0.00	0.00
T1-T0	1.00	113.83	353.13	283.28	46.39	182.69	91.47	43.84	47.54	62.56	55.81	100.70	105.83
T2-T0	2.00	182.61	376.76	308.93	125.14	152.68	112.19	62.86	10.40	137.30	46.87	136.39	91.21
T3-T0	4.00	212.42	398.88	334.63	96.05	139.87	142.75	80.45	59.50	91.63	67.24	139.18	87.54
T4-T0	8.00	416.53	442.65	700.61	214.64	303.82	257.62	67.42	59.10	98.82	78.93	180.24	110.17
T5-T0	16.00	726.99	934.99	1023.75	130.76	367.28	258.39	71.62	16.31	101.28	89.69	222.85	81.24
T6-T0	24.00	667.34	1128.50	877.87	134.49	500.55	578.72	58.56	62.26	107.17	79.17	198.15	81.65
T7-T0	32.00	847.67	1083.98	1008.18	426.84	649.08	737.00	83.71	36.13	120.73	83.69	204.79	90.48
T8-T0													
T9-T0	48.00	1072.71	1016.44	1132.28	212.70	793.85	157.24	98.37	47.73	121.28	74.76	218.90	91.76

Table 10: Raw Matlab data that gives cumulative sediment volume loss in cm^3 of sediment cores collected from Rilland Bath-Spartina dominated areas and Hellegatpolder-Spartina dominated areas.

	Time	1B_Sp_Un_1	1B_Sp_Un_2	1B_Sp_Un_3	2B_Sp_Veg_1	2B_Sp_Veg_2	2B_Sp_Veg_3	1H_Sp_Un_1	1H_Sp_Un_2	1H_Sp_Un_3	2H_Sp_Veg_1	2H_Sp_Veg_2	2H_Sp_Veg_3
T0-T0	0.00	0.00	0.00	0.00	0.00	0.00	0.00	0.00	0.00	0.00	0.00	0.00	0.00
T1-T0	1.00	697.46	460.14	713.11	16.28	2.55	20.64	379.00	498.56	149.66	10.34	27.09	52.26
T2-T0	2.00	1920.00	899.34	1920.00	31.45	2.78	12.43	384.47	572.18	339.17	62.80	29.07	38.88
T3-T0	4.00	1920.00	1367.13	1920.00	10.88	2.27	18.96	828.42	615.57	558.36	37.96	14.71	33.84
T4-T0	8.00	1920.00	1920.00	1920.00	39.80	27.23	28.58	741.74	704.01	710.69	77.85	100.14	41.93
T5-T0	16.00	1920.00	1920.00	1920.00	32.00	5.22	33.35	1048.55	1177.96	679.92	10.02	103.36	49.27
T6-T0	24.00	1920.00	1920.00	1920.00	28.31	27.74	43.03	689.47	1920.00	919.45	90.02	109.00	60.27
T7-T0	32.00	1920.00	1920.00	1920.00	16.50	30.00	40.57	1159.32	1920.00	1030.40	48.09	128.78	56.19
T8-T0													
T9-T0	48.00	1920.00	1920.00	1920.00	28.06	1.65	26.75	1064.26	1920.00	1335.51	43.09	161.97	67.78

Table 11: Raw Matlab data that gives cumulative sediment volume loss in cm^3 of sediment cores collected from Hellegatpolder-salt water influenced area.

	Time	1H_Sp_Un_1	1H_Sp_Un_2	1H_Sp_Un_3	3H_Sp_SpVeg_1	3H_Sp_SpVeg_2	3H_Sp_SpVeg_3	4H_Sp_DeVeg_1	4H_Sp_DeVeg_2	4H_Sp_DeVeg_3
T0-T0	0.00	0.00	0.00	0.00	0.00	0.00	0.00	0.00	0.00	0.00
T1-T0	1.00	1920.00	1920.00	1920.00	218.45	205.33	230.49	27.35	19.47	41.15
T2-T0	2.00	1920.00	1920.00	1920.00	274.39	242.86	170.11	0.01	17.98	38.47
T3-T0	4.00	1920.00	1920.00	1920.00	295.91	166.90	209.86	31.56	36.56	48.96
T4-T0	8.00	1920.00	1920.00	1920.00	225.11	272.29	243.97	50.29	31.46	32.87
T5-T0	16.00	1920.00	1920.00	1920.00	330.05	83.94	253.29	52.73	28.88	53.67
T6-T0	24.00	1920.00	1920.00	1920.00	346.50	400.14	320.12	51.45	48.08	10.16
T7-T0	32.00	1920.00	1920.00	1920.00	522.72	449.70	333.12	49.41	48.95	48.43
T8-T0	40.00	1920.00	1920.00	1920.00	359.42	172.43	229.09	53.48	58.25	56.27
T9-T0	48.00	1920.00	1920.00	1920.00	189.42	631.62	197.52	53.04	51.14	39.61

Table 12: Raw Matlab data that gives cumulative sediment volume loss in cm^3 of sediment cores collected from Zuidgors.

	Time	1Z_Sp_Un_1	1Z_Sp_Un_2	1Z_Sp_Un_3	1Z_Sp_Veg_1	1Z_Sp_Veg_2	1Z_Sp_Veg_3
T0-T0	0.00	0.00	0.00	0.00	0.00	0.00	0.00
T1-T0	1.00	936.84	712.42	656.45	25.42	14.20	16.23
T2-T0	2.00	1920.00	1000.32	551.91	19.53	20.42	21.57
T3-T0	4.00	1920.00	1406.83	1102.72	19.50	24.01	6.62
T4-T0	8.00	1920.00	1452.55	1920.00	32.54	36.38	20.82
T5-T0	16.00	1920.00	1920.00	1920.00	28.68	31.99	21.26
T6-T0	24.00	1920.00	1920.00	1920.00	30.98	25.21	22.07
T7-T0	32.00	1920.00	1920.00	1920.00	34.39	32.64	20.35
T8-T0	40.00	1920.00	1920.00	1920.00	27.15	21.44	17.31
T9-T0	48.00	1920.00	1920.00	1920.00	29.10	64.50	19.19

Table 13: Raw Matlab data that gives cumulative sediment volume loss in cm³ of sediment cores collected from Groot Buitenschoor.

	Time	1G_Sc_Un_1	1G_Sc_Un_2	1G_Sc_Un_3	3G_Sc_SVeg_1	3G_Sc_SVeg_2	3G_Sc_SVeg_3	4G_Sc_DVeg_1	4G_Sc_DVeg_2	4G_Sc_DVeg_3
T0-T0	0.00	0.00	0.00	0.00	0.00	0.00	0.00	0.00	0.00	0.00
T1-T0	1.00	248.61	297.01	353.96	130.32	195.12	126.92	40.36	53.13	39.06
T2-T0	2.00	733.29	477.08	1493.93	670.22	380.57	311.91	50.10	56.39	25.15
T3-T0	4.00	1920.00	768.02	1920.00	804.04	704.06	383.34	48.26	44.85	51.72
T4-T0	8.00	1920.00	1038.33	1920.00	971.79	678.46	1312.24	65.62	48.84	30.26
T5-T0	16.00	1920.00	1920.00	1920.00	1920.00	1920.00	1920.00	44.12	63.22	26.63
T6-T0	24.00	1920.00	1920.00	1920.00	1920.00	1920.00	1920.00	66.50	72.66	61.03
T7-T0	32.00	1920.00	1920.00	1920.00	1920.00	1920.00	1920.00	68.46	63.59	57.83
T8-T0	40.00	1920.00	1920.00	1920.00	1920.00	1920.00	1920.00	40.90	66.80	68.98
T9-T0	48.00	1920.00	1920.00	1920.00	1920.00	1920.00	1920.00	73.53	70.38	61.89

Table 14: Raw Matlab data that gives cumulative sediment volume loss in cm³ of sediment cores collected from De Zaag.

	Time	1D_Ph_Veg_1	1D_Ph_Veg_2	1D_Ph_Veg_3
T0-T0	0.00	0.00	0.00	0.00
T1-T0	1.00	44.57	45.12	46.47
T2-T0	2.00	34.44	58.09	69.01
T3-T0	4.00	36.01	37.24	84.61
T4-T0	8.00	20.81	57.19	71.72
T5-T0	16.00	28.22	44.94	94.85
T6-T0	24.00	42.97	48.17	85.35
T7-T0	32.00	64.38	47.16	130.59
T8-T0	40.00	60.68	36.48	88.63
T9-T0	48.00	0.45	51.02	173.85

Table 15: Bulk density values calculated for all sediment cores

Sediment core name	bulk density	Sediment core name	bulk density	Sediment core name	bulk density	Sediment core name	bulk density
1B_Sc_Un_1	1.01	1B_Sp_Un_3	1.48	3H_Sp_SV_1	1.37	1G_Sc_Un_2	1.26
1B_Sc_Un_2	1.10	2B_Sp_V_1	1.13	3H_Sp_SV_2	1.36	1G_Sc_Un_3	1.30
1B_Sc_Un_3	1.03	2B_Sp_V_2	1.28	3H_Sp_SV_3	0.93	3G_Sc_SV_1	0.98
3B_Sc_SV_1	1.19	2B_Sp_V_3	0.99	4H_Sp_DV_1	1.30	3G_Sc_SV_2	1.03
3B_Sc_SV_2	1.28	1H_Sp_Un_1	1.11	4H_Sp_DV_2	1.40	3G_Sc_SV_3	1.18
3B_Sc_SV_3	1.31	1H_Sp_Un_2	1.13	4H_Sp_DV_3	1.21	4G_Sc_DV_1	0.83
4B_Sc_DV_1	1.11	1H_Sp_Un_3		1Z_Sp_Un_1	1.33	4G_Sc_DV_2	0.87
4B_Sc_DV_2	1.03	2H_Sp_V_1	0.95	1Z_Sp_Un_2	1.38	4G_Sc_DV_3	0.89
4B_Sc_DV_3	1.13	2H_Sp_V_2	0.87	1Z_Sp_Un_3	1.37	2D_Ph_V_1	1.29
2B_Ph_V_1	1.36	2H_Sp_V_3	0.94	2Z_Sp_V_1	1.08	2D_Ph_V_2	1.15
2B_Ph_V_2	1.46	1H_Sp_Un_1	1.56	2Z_Sp_V_2	0.95	2D_Ph_V_3	1.13
2B_Ph_V_3	1.33	1H_Sp_Un_2	1.68	2Z_Sp_V_3	0.98		
1B_Sp_Un_1	1.35	1H_Sp_Un_3	1.54	1G_Sc_Un_1	1.28		
1B_Sp_Un_2	1.50						

Results of relative sediment volume eroded for different study sites and vegetation species

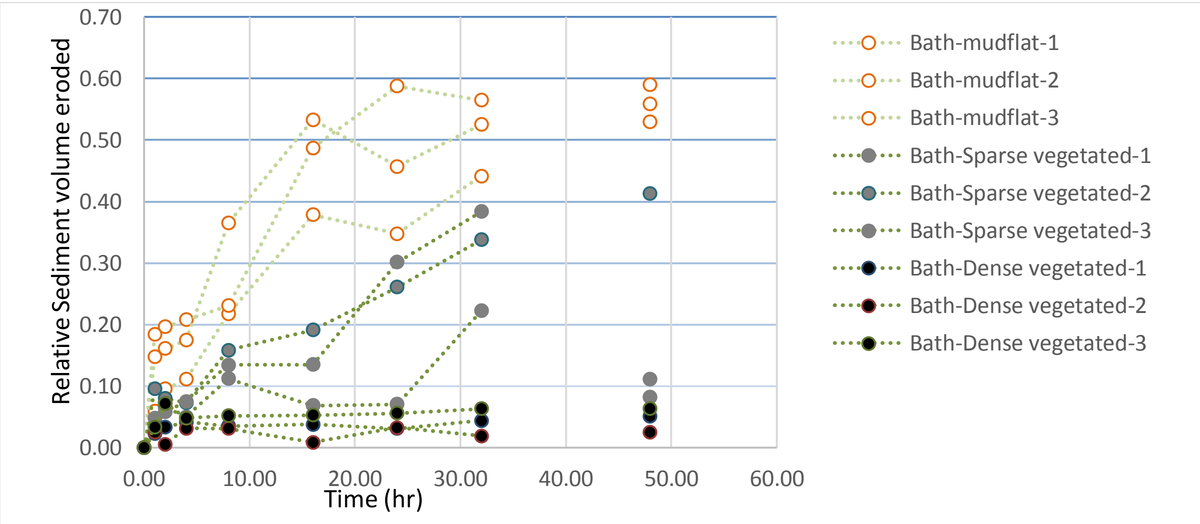

Figure 2: Relative sediment volume eroded for 9 sediment cores of Scirpus maritimus from study site Rilland Bath (black marker=sediment cores from dense vegetated zone, grey marker=sediment cores from sparse vegetated zone, white marker=sediment cores from the mudflat zone).

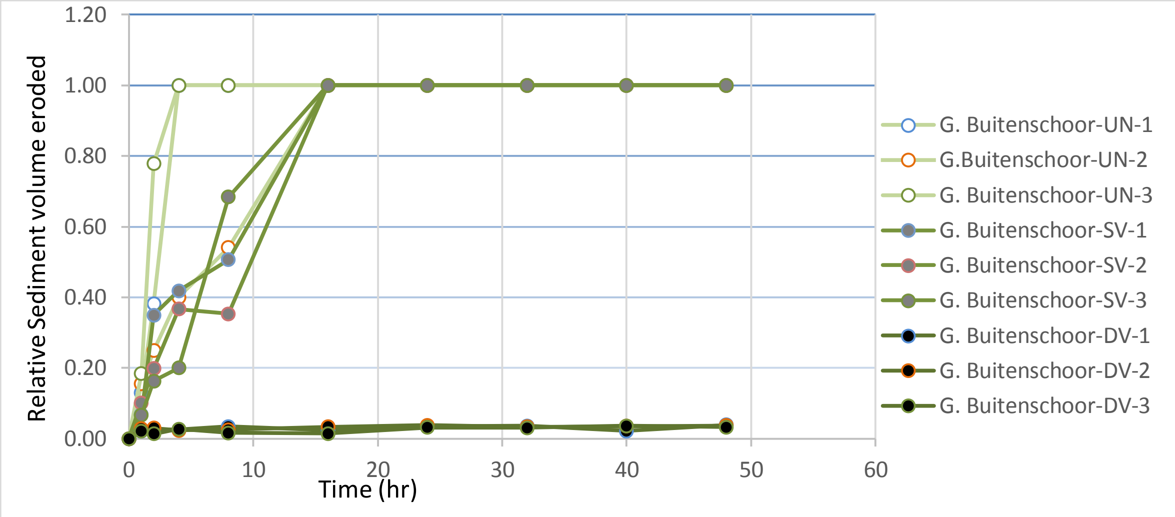

Figure 3: Relative sediment volume eroded for 9 sediment cores of Scirpus maritimus from study site Groot Buitenschoor (black marker=sediment cores from dense vegetated zone, grey marker=sediment cores from sparse vegetated zone, white marker=sediment cores from the mudflat zone).

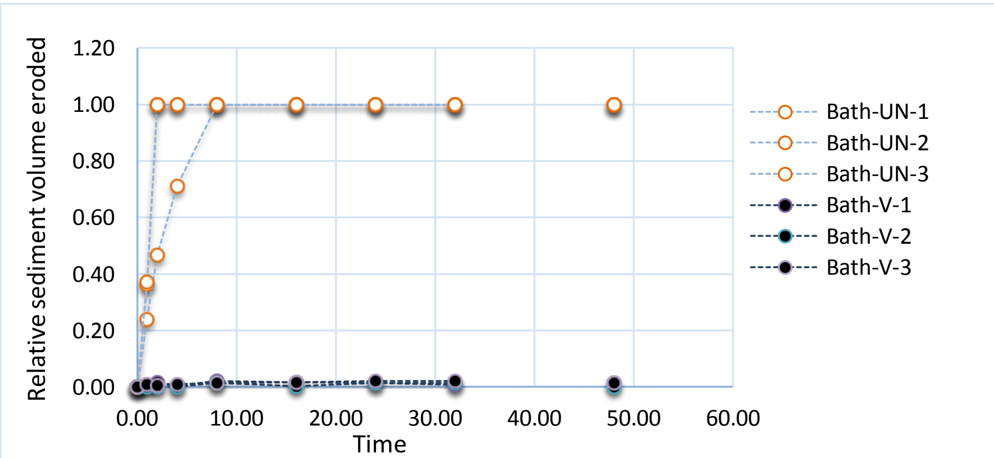

Figure 4: Relative sediment volume eroded of 6 sediment cores of Spartina anglica from study site Rilland Bath (black marker=sediment cores from dense vegetated zone, white marker=sediment cores from the mudflat zone. In legend, name is selected as study site (Bath)-location of sediment cores taken (UN=mudflat, DV=Dense vegetated)-replicates number (1, 2, 3)).

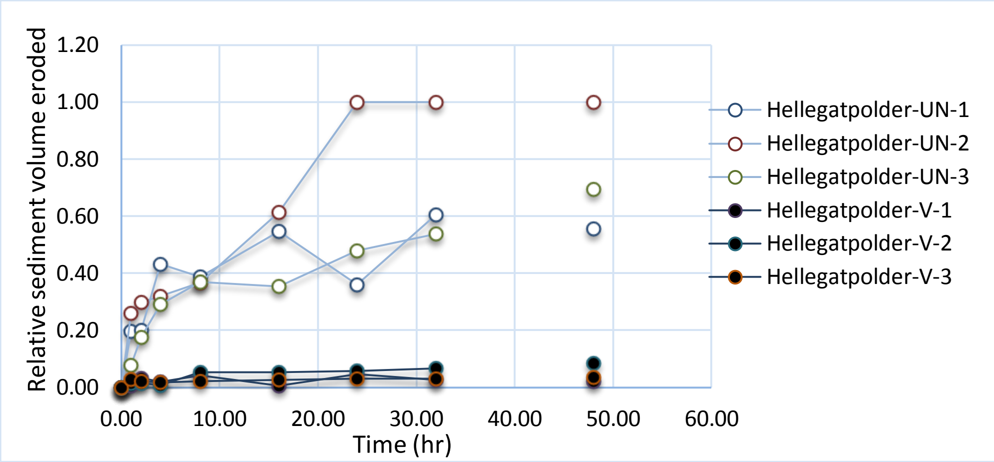

Figure 5: Relative sediment volume eroded of 6 sediment cores of Spartina anglica from study site Hellegatpolder with very brackish water dominated area (black marker=sediment cores from dense vegetated zone, white marker=sediment cores from the mudflat zone. In legend, name is selected as study site (Hellegatpolder)-location of sediment cores taken (UN=mudflat, V=Marsh zone)-replicates number (1, 2, 3)).

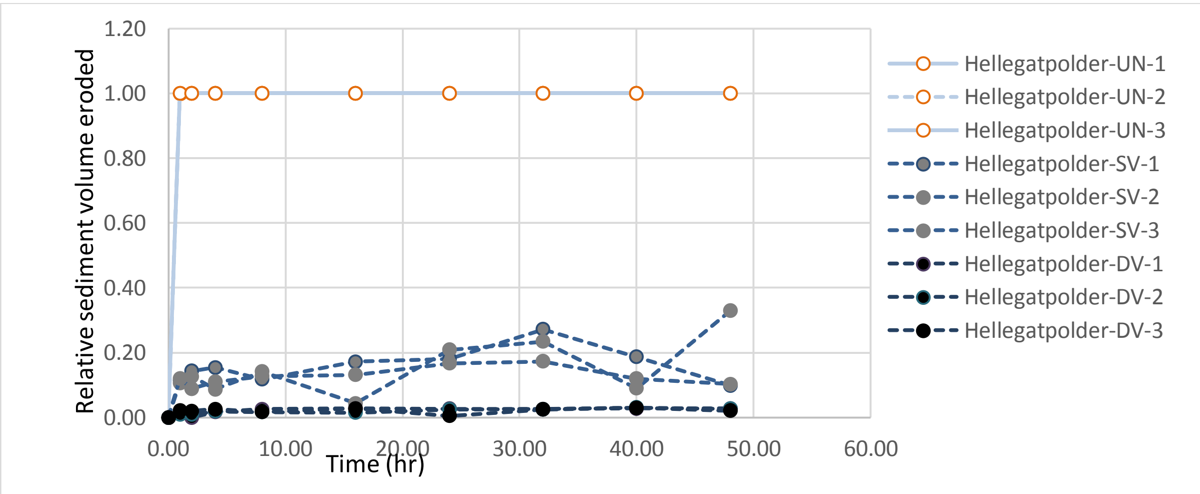

Figure 6: Relative sediment volume eroded for 9 sediment cores of Spartina anglica from study site Hellegatpolder with salt water dominated area (black marker=sediment cores from dense vegetated zone, grey marker=sediment cores from sparse vegetated zone, white marker=sediment cores from the mudflat zone. In legend, name is selected as study site (Hellegatpolder)-location of sediment cores taken (UN=mudflat, SV=sparse vegetated, DV=Dense vegetated)-replicates number (1, 2, 3)).

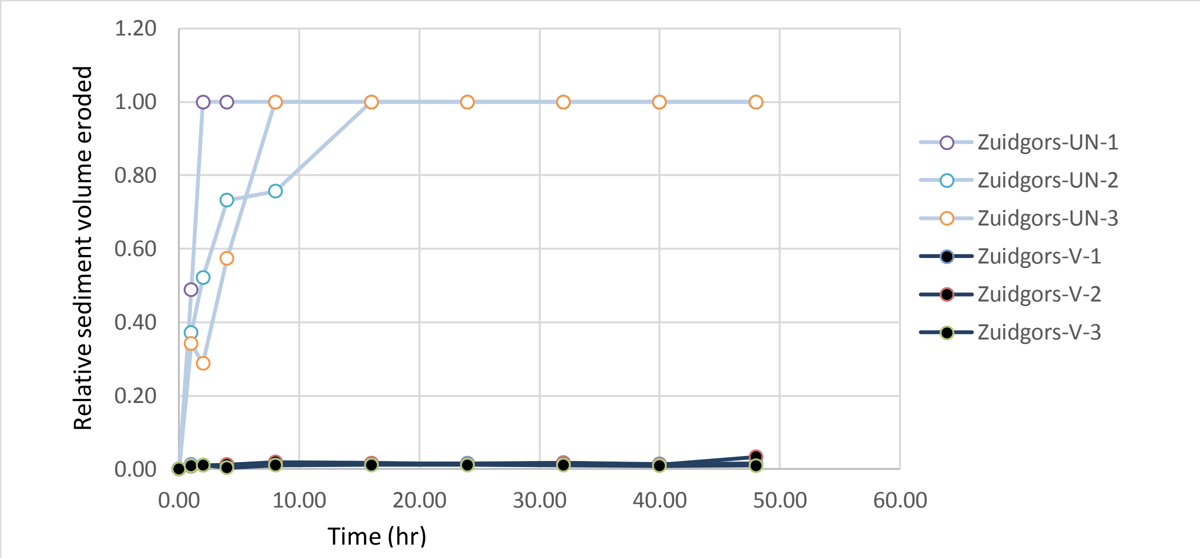

Figure 7: Relative sediment volume eroded of 6 sediment cores of Spartina anglica from study site Zuidgors with salt water dominated area (black marker=sediment cores from dense vegetated zone, white marker=sediment cores from the mudflat zone. In legend, name is selected as study site (Zuidgors)-location of sediment cores taken (UN=mudflat, DV=Dense vegetated)-replicates number (1, 2, 3)).

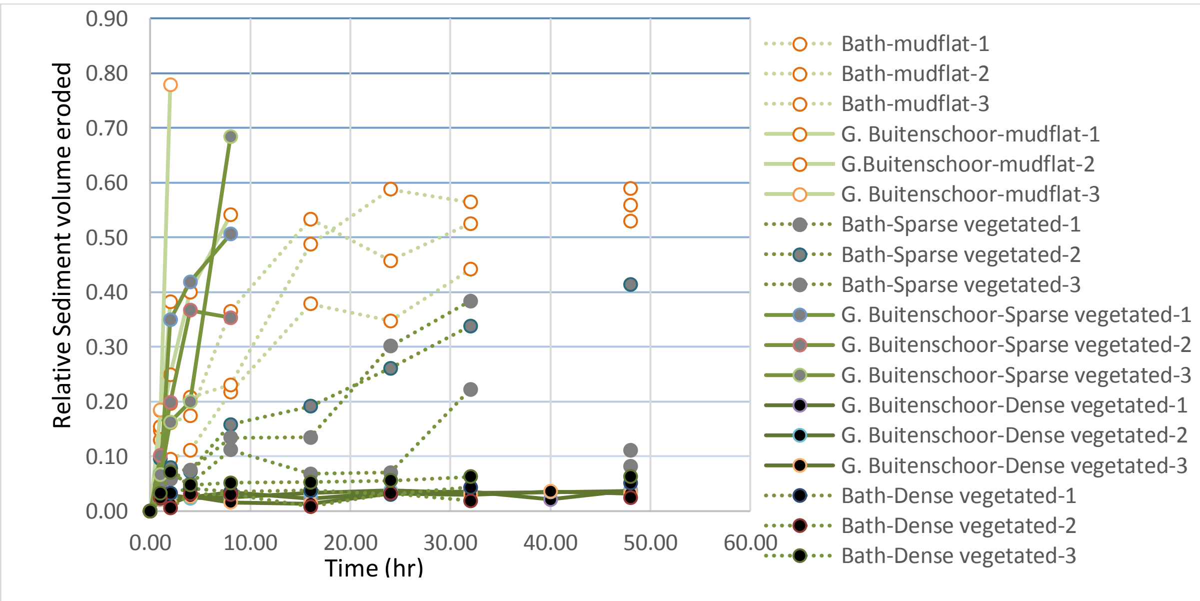

Figure 8: Relative sediment volume eroded for 18 sediment cores of Scirpus maritimus collected from two study sites: Bath (dotted lines) and Groot Buitenschoor (full lines) (black marker=sediment cores from dense vegetated zone, grey marker=sediment cores from sparse vegetated zone, white marker=sediment cores from the mudflat zone).

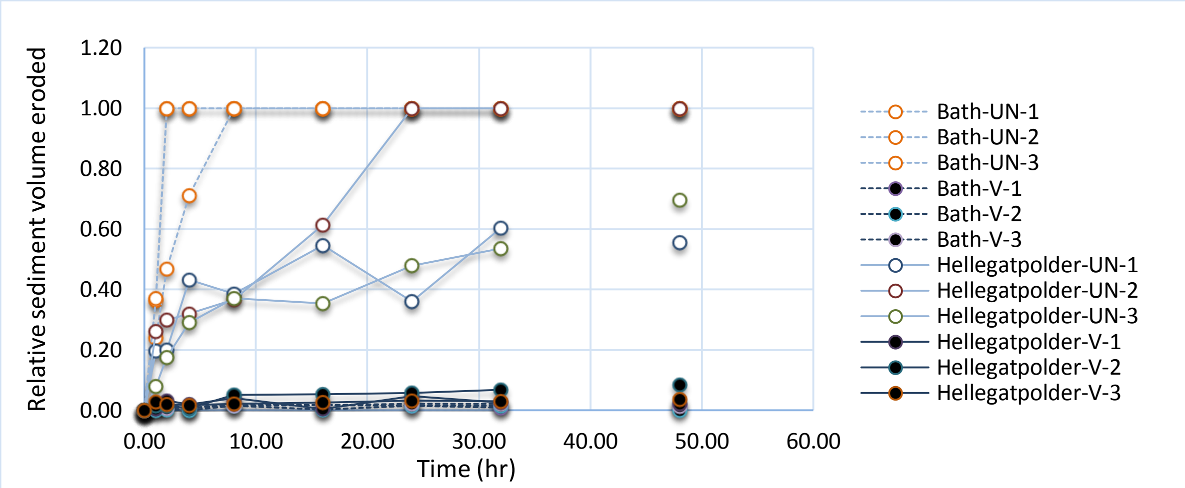

Figure 9: Relative sediment volume eroded for Spartina anglica from study site Bath (dotted lines) and Hellegatpolder (full lines) with very brackish water dominated area (black marker=sediment cores from dense vegetated zone, grey marker=sediment cores from sparse vegetated zone, white marker=sediment cores from the mudflat zone. In legend, name is selected as study site (Hellegatpolder/Bath)-location of sediment cores taken (UN=mudflat, V=Marsh zone)-replicates number (1, 2, 3)).

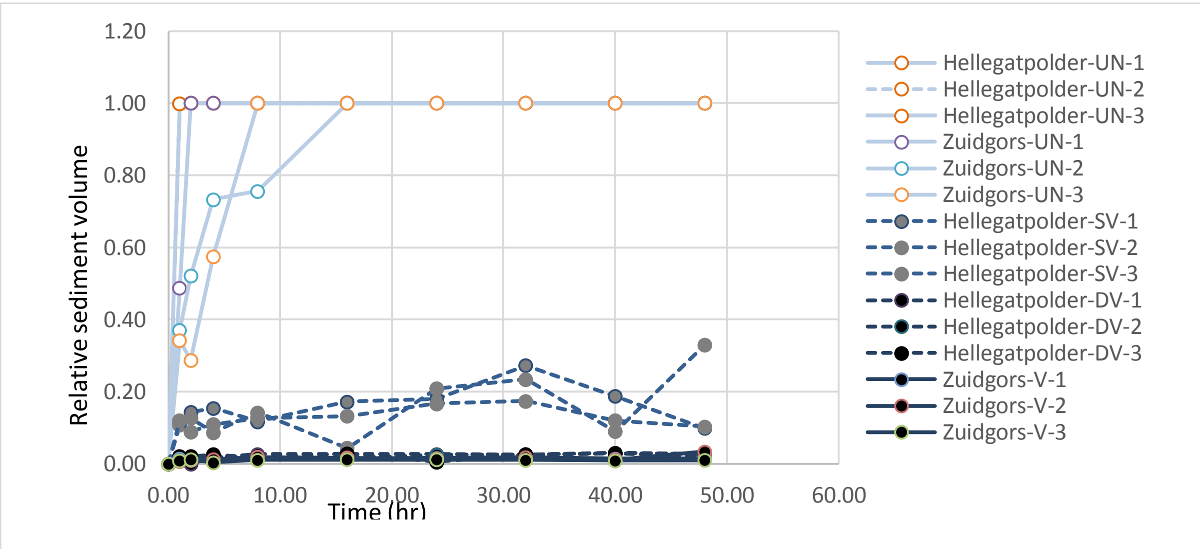

Figure 10: Relative sediment volume eroded for Spartina anglica from study site Hellegatpolder (dotted lines) and Zuidgors (full lines) with salt water dominated area (black marker=sediment cores from dense vegetated zone, grey marker=sediment cores from sparse vegetated zone, white marker=sediment cores from the mudflat zone. In legend, name is selected as study site (Hellegatpolder/Zuidgors)-location of sediment cores taken (UN=mudflat, SV=Sparse vegetated, DV=Dense vegetated)-replicates number (1, 2, 3)).

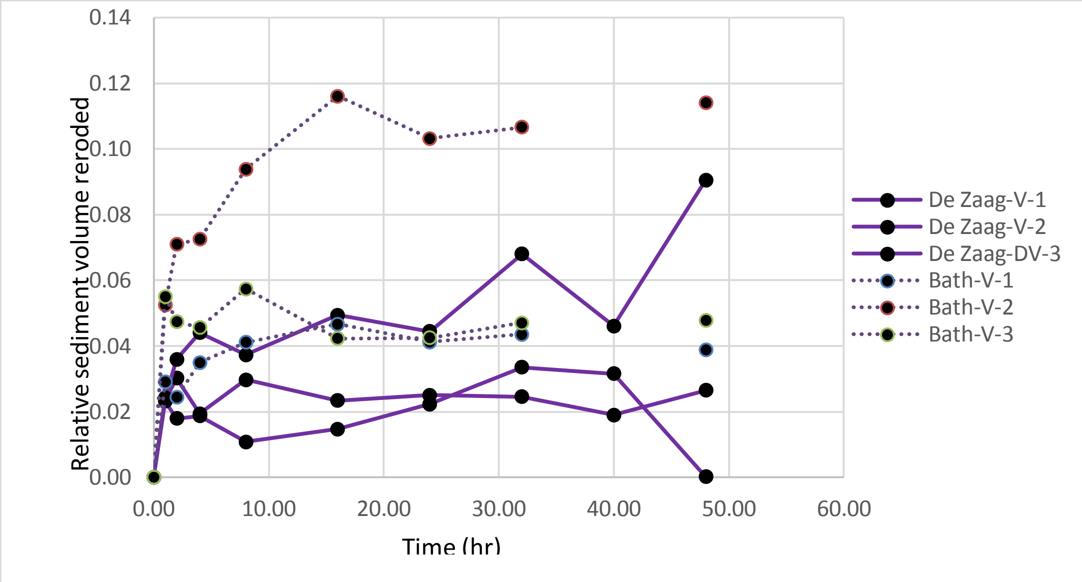

Figure 11: Relative sediment volume eroded for Phragmites australis from study site Bath (dotted lines) and De Zaag (full lines) In legend, name is selected as study site (De Zaag/Bath)-location of sediment cores taken (DV=Marsh zone)-replicates number (1, 2, 3)).